

**Eco-Evolutionary Dynamics of Predators and Prey**

By

SAMUEL R. FLEISCHER  
DISSERTATION

Submitted in partial satisfaction of the requirements for the degree of

DOCTOR OF PHILOSOPHY

in

APPLIED MATHEMATICS

in the

OFFICE OF GRADUATE STUDIES

of the

UNIVERSITY OF CALIFORNIA

DAVIS

Approved:

---

Marissa Baskett

---

Tim Lewis

---

Sebastian Schreiber

Committee in Charge

2020

To my wife Kelly, my sunflower, who gives me unyielding love and support, and who inspires me to reach for the stars.

To my parents, Paula and Neil, who provide me with an unbreakable foundation of unconditional love, self-confidence, and compassion for all people.

To my sisters, Anna and Emily, who enjoy life to the fullest, and who inspire me to be a better person.

## Acknowledgments

Thank you to my advisor, Sebastian Schreiber. You have pushed me to become a more precise thinker and writer, and a better mathematician. Your patience and guidance, especially during the last year, has been incredible. Thank you for our years of illuminating conversation and research.

Thank you to my dissertation committee, Sebastian Schreiber, Marissa Baskett, and Tim Lewis. You have provided me timely feedback on each of my chapters and continue to help me achieve my academic and career goals. You have all been true mentors to me, and guided me to make thoughtful career decisions.

Thank you to my faculty collaborators, Sebastian Schreiber, Dan Bolnick, Jing Li, and Casey terHorst. You each have been so patient with me as I learn to write like a scientist and mathematician. I am so proud of the work we did together, and so lucky to have learned from each of you.

Thank you to my past and present comrades in the Schreiber lab, William Cuello, Michael Culshaw-Maurer, Kelsey Lyberger, Nicholas Roberts, Dale Clement, Swati Patel, Jacob Moore, and Matthew Osmond. You all made lab meetings fun and I enjoyed the opportunities we had to collaborate. You are all brilliant and I am lucky to have worked with you.

Thank you to my comrades engaged in labor and social justice organizing within the Mathematics department and across campus. You inspire me by consistently putting others before yourselves, and by spending valuable time and effort fighting alongside those of us who are most oppressed and discriminated against.

Thank you to my friends and fellow graduate students in the math department, Katy Jarvis, Carter Johnson, Emily Meyer, Esha Datta, Lily Silverstein, Alvin Moon, Dmitry Shemetov, Ryan Chris Moreno-Vasquez, Jorge Arroyo, and many others. In different ways, you've all helped me get through graduate school. From getting through the core courses, to studying for the preliminary exam, to quizzing each other for our respective qualifying exams, to the political battles we've fought against the powers that be within the Math department, you've all been by my side.

Thank you to my trusted staff and faculty confidants in MSB, Sarah Driver, Tina Denena, Matthew Silver, Korana Burke, Becca Thomases, and Mariel Vazquez. You have all supported me and my fellow graduate students when we needed it the most. Knowing that you all care enough about our well-being to take action means the world to me.

Thank you to my friends in the UC Davis teaching community, Sergio Sanchez, Alice Martinic, Chris Miller, Derek Rury, Sarah Silverman, Tori White, Kem Saichai, Cara Theisen, Monica Esqueda, and many others. Together we pushed ourselves to become better collaborators and communicators to improve undergraduate education on campus. You taught me to seek out and value criticism, to listen and create space for others, and to trust my peers and my students. Working with you all was the highlight of my graduate school experience, and I will never forget the professional and life lessons I learned from each and every one of you.

Thank you to my friends, coworkers, and supervisors, at NASA Jet Propulsion Laboratory, Jonathan Castello, Diane Conner, Jairus Hihn, Mike DiNicola, Zac McLaughlin, and many others. Each of you have helped me grow as a professional and guided me as I find my niche at JPL. I am so excited to continue my work there as a full time employee and contribute to an amazing environment where we help each other learn.

Thank you to all my students, past and present. You inspire me to become a better communicator and an empathetic leader. Your drive to learn mathematics and your interest in its satisfying simplicity and frustrating complexity keeps me sane and consistently reminds me of why I choose to study this beautiful subject.

Thank you to all my teachers, Cyndi Lingua from Valencia Valley, Paul Kass from Placerita, Kerry Strothe and Steve Whelan from Valencia, Leigh Dillon and Akil Davis at SUNY Purchase, Katherine Stevenson and Jing Li at CSU Northridge, and many others. Each of you have made a lasting impact in the way I learn and the way I teach. You inspire me to be a better communicator and to stay focused.

Thank you to my friends from so many other contexts, Jack Geier, Lindsay Clark, Austin Gould, Jamison Gilmore, Maxx Tepper, Sattik Ghosh, Ema Miille, Neil Yazma, Paris Gravely, Robbie Linden, Jose Torres, Angelica Ruiz, Joshua White, Ian Lee, Matt DeSanctis, Sophia Zukoski, Delano Montgomery, and so many others. I hold you all near and dear as I navigate through my life. I learn so much from how you care for the ones you love and how you stay true to yourself. I am truly lucky to have such friends as you.

Thank you to my mother, Paula, my father, Neil, my sisters, Anna and Emily, my grandparents, Ruben, Cathy, Mort, and Doris, my aunts and uncles, Allie, Drew, Kari, David, and Marla, my cousins, Molly, Sophie, Lily, Joey, and Beckett, and my in-laws, Terri, Wade, and Taylor. When I am with you, I am surrounded with love. I am so lucky to have family who are invested in my success. You assure me that when all else goes wrong, my family has my back.

Lastly, thank you to my wife, Kelly. Thank you for keeping me focused. Thank you for being my cheerleader. Thank you for believing in me. Thank you for supporting me. Thank you for loving my family and friends and for welcoming me into your family and groups of friends. Thank you for being proud of me. Thank you for caring about our place in the world. Thank you for challenging me and for your patience. Thank you for those days when we just need to chill, and thank you for those days when we need to have an adventure. Nothing in this world means anything to me if I can't share it with you. I am so proud to call myself your husband, and I love you more than words can express.

## Abstract

In this dissertation I formulate and analyze multispecies eco-evolutionary differential equation models to understand the effects of evolution on ecological processes, and vice versa. In each chapter, I fuse different Lotka-Volterra models of ecological dynamics with population genetic models of one or more evolving traits.

The first chapter is a study on the effects of different types of prey evolution on coevolutionary predator-prey dynamics. Here, the predator maximizes its fitness if its trait matches the prey in some way. For example, predators with larger or smaller mouths are better suited to consume larger or smaller prey, respectively. Prey fitness depends on its trait in two ways. First, evolution of its trait away from the predator's trait reduces the predation rate, increasing prey fitness. Second, evolution away from some optimal trait reduces either its intrinsic growth rate or carrying capacity, decreasing prey fitness. Predator-prey dynamics are affected by the tradeoff between defense against predation and these two other components of prey fitness in different ways. In particular, evolution of the prey's intrinsic growth rate is more likely to result in coexistence than evolution of its carrying capacity is. Predator-prey oscillations are also qualitatively different under these different tradeoffs.

The second chapter is a study on the coevolution of predator morphology and immunity when its prey are infected with parasites that use the predator as a secondary host. Here, predator morphological evolution shifts the consumption rate of each of the two prey. This evolution also results in greater exposure to the multitrophic parasites residing in the prey. Predator immunity evolves in response to this increased exposure. The analytical results provide support for a Stutz et al. [2014] hypothesis: negative correlations between parasite intake and parasite infection across stickleback populations are caused by dual evolution of morphology and immunity. Furthermore, these correlations only exist if evolutionary tradeoffs are weak, which suggests that selection pressure on stickleback morphology and immunity is weak.

The third chapter is a study on the effect of predator evolution on coexistence of its competing prey. In the absence of the predator, Lotka-Volterra competitors either exhibit asymptotically stable equilibrium coexistence, dominance (in which one prey always excludes the other), or bistability (in which neither prey can invade an environment already established by the other). While a non-evolving Lotka-Volterra predator can facilitate permanence between a dominant and inferior prey,

it cannot facilitate permanence for bistable prey; any coexistence between a non-evolving predator and bistable prey is initial condition dependent. I derive conditions for permanence between a predator with an evolving quantitative trait and its two prey. I find conditions which guarantee permanence even when the prey are bistable. I also describe various forms of permanence observed in the model, including eco-evolutionary cycles when evolution is sufficiently slow, and stable equilibrium coexistence to an otherwise unstable equilibrium when evolution is sufficiently fast. This is the second study to show that evolution can mediate permanence between bistable prey, and the first to show that predator evolution can do so.

## Contents

Introduction	1
Chapter 1. Pick your trade-offs wisely: predator-prey eco-evo dynamics are qualitatively different under different trade-offs	4
Chapter 2. Sick of Eating: eco-evo-immuno dynamics of predators and their trophically acquired parasites	29
Chapter 3. Predator evolution mediates permanence among competing prey	51
Appendix A. Chapter 1 (Pick Your Tradeoffs Wisely) Appendices	75
Appendix B. Chapter 2 (Sick of Eating) Appendices	93
Appendix C. Chapter 3 (Predator Evolution-Mediated Permanence) Appendices	103
Bibliography	118

## Introduction

The perception that ecological and evolutionary shifts occur on vastly different timescales, and thus that theoreticians can effectively model ecological processes without considering evolution, first began to conflict with empirical studies in the 1960s (e.g. the evolution of house mice [Berry, 1964] or fruit flies [Bush, 1969]). By the 1980s, many more studies provided examples of evolution and ecological shifts occurring on commensurate timescales, and by the 1990s, rapid evolution had been accepted as common [see Carroll et al., 2007, for a review]. In the words of Hendry and Kinnison [1999], “the fundamental conclusion that must be drawn is that evolution as hitherto considered ‘rapid’ may often be the norm and not the exception.”

Evolution and ecological shifts are not simply contemporary; they can drive each other. There is genetic and phenotypic variation in natural populations, and phenotype often correlates to reproductive fitness in a given environment [Darwin, 1859, Grant and Grant, 2002, Reznick and Ghalambor, 2001]. Thus, when an environment shifts, individuals relatively more fit in the new environment produce relatively more offspring, which drives evolution [Hendry, 2017]. Conversely, phenotypic change in a population can greatly affect its population dynamics [e.g. Gomulkiewicz and Holt, 1995]. Because shifts in population density can directly affect community structure, this gives rise to an “eco-evo feedback” in which evolutionary trajectories determined in part by their ecological context changes the context itself [see Schoener, 2011, for a review].

Empirical studies have driven the work of theoreticians, who help to formalize conceptual frameworks and delineate possibilities that arise from certain assumptions [Hendry, 2017]. Many theoreticians have incorporated evolution into predator-prey models in an attempt to explain predator-prey dynamics seen in laboratory microcosm or natural experiments. Some incorporated prey evolution [e.g. Abrams and Matsuda, 1997a, Yoshida et al., 2003, 2007], and others incorporated predator-prey coevolution [e.g. Bengfort et al., 2017, Cortez and Weitz, 2014, Mougi, 2012, Mougi and Iwasa, 2010, 2011, Saloniemi, 1993, Tien and Ellner, 2012, Tirok et al., 2011, van Velzen and

Gaedke, 2017]. Eco-evo feedbacks also play a fundamental role in competitive communities [e.g. Vasseur et al., 2011] or in communities of more than just two species [e.g. Klauschies et al., 2016, Schreiber et al., 2011]. Each chapter in this dissertation addresses gaps in the literature regarding the nature of eco-evo feedbacks in a variety of ecological and evolutionary contexts.

In the first chapter, I formulated and analyzed two coevolutionary predator-prey models. Predators and prey often serve as important selective agents on each other [Brodie III., 1992, Endler, 1991, Walsh and Reznick, 2008, Lill, 2001, Motychak et al., 1999, West et al., 1991, Strauss et al., 2006]. Predator evolution in response to prey should increase consumption rates, while prey evolution of increased escape ability or avoidance in response to predation should decrease consumption rates [Strauss et al., 2006]. Examples of traits which often affect consumption rates are the mouth or jaw size in predators [e.g. Stutz et al., 2014], and visual cues or chemical defenses in prey [e.g. Brodie III., 1992, Clark et al., 2005]. However, evolution comes at some cost; prey evolution of increased defense can reduce its fecundity or resource use or increase intraspecific competition [DeLong, 2017]. I therefore asked how these various types of tradeoffs affect predator-prey coevolutionary dynamics. In both models, each population contains a trait which affects the predator attack rate on the prey, but the prey trait is ecologically pleiotropic. In the first model, the prey trait also affects its intrinsic growth rate, and in the second model, the prey trait also affects its carrying capacity in the absence of predation. In particular, I was interested in the conditions under which coexistence among species is more likely, but also the dynamic nature of this coexistence - how are predator-prey eco-evolutionary cycles different under these distinct prey tradeoffs?

In the second chapter, I formulated and analyzed an apparent-competition model [Holt, 1977] based on the aquatic threespine stickleback system. Stickleback consume benthic or limnetic prey, which are intermediate hosts for distinct species of parasites (*Eustrongylides* nematodes in benthic oligocheates and *Schistocephalus solidus* cestodes in limnetic copepods) [Snowberg et al., 2015]. Stutz et al. [2014] found that within a particular lake, individual stickleback who consume more benthic or limnetic prey are proportionally more infected with the benthic or limnetic parasites residing in those prey, respectively. They also found that across a variety of lakes, stickleback populations which consume more benthic or limnetic prey are proportionally *less* infected with the benthic or limnetic parasites residing in those prey, respectively. They hypothesized that this

negative correlation is caused by the dual evolution of predator morphology (as in chapter 1) and immunity against these multitrophic parasites. To test this hypothesis, I addressed three main questions. First, *under what conditions is there a reciprocal feedback between morphological and immunological evolution?* Morphology (and hence parasite exposure risk) will evolve in response to prey availability, but changes in parasite exposure will drive evolution of immunity, which can reduce the harmful effects of parasites, potentially enabling niche expansion onto a formerly hazardous prey. When can these feedbacks arise? And, if they do not, when does the evolution of morphology determine the evolution of immunity, and *vice versa*? Second, *how are morphological and immune traits correlated?* Even if traits are genetically independent, correlated selection pressure may result in correlated evolutionary outcomes. Third, *how does the joint evolution of morphology and immunity obscure the relationship between parasite exposure risk and infection rates?* As Stutz et al. [2014] hypothesized, evolution of predator immunity may negate or even reverse an expected positive correlation between intake of, and infection by, parasites.

In the third chapter, I formulated and analyzed an eco-evolutionary model in which a predator consumes two competing prey. As in the previous chapters, the predator has a trait which alters its morphology and thus its attack rates on the two prey. I was interested in how an evolving predator can facilitate coexistence between competitors. In the absence of a predator, Lotka-Volterra prey have three qualitatively different outcomes. Either (i) they can coexist in an asymptotically stable equilibrium, (ii) one can dominate the other, or (iii) neither can invade an environment in which the other has established. Because I was interested in predator-mediated coexistence, I only considered cases (ii) and (iii). A non-evolving predator can mediate some form of coexistence in both cases. If one prey is dominant, a Lotka-Volterra non-evolving predator can mediate permanence among the competitors, but if the prey are bistable, this is not possible. Non-evolving predators of bistable prey can mediate locally stable coexistence, but it is always bistable with a state in which the predator and one of the prey are excluded [Hutson and Vickers, 1983]. I explored how predator evolution can facilitate permanence [see e.g. Schreiber, 2006] among bistable prey. I also described the nature of permanence dynamics when evolution is very slow or occurs on a commensurate timescale with ecological shifts.

## CHAPTER 1

# **Pick your trade-offs wisely: predator-prey eco-evo dynamics are qualitatively different under different trade-offs**

Published on November 7, 2018 in the *Journal of Theoretical Biology*

Joint work with:

**Casey P. terHorst**

*Department of Biological Sciences, California State University Northridge, Northridge, 91330,  
California*

**Jing Li**

*Department of Mathematics, California State University Northridge, Northridge, 91330,  
California*

### **1.1. Abstract**

In recent decades, myriad studies have explored the population dynamics of coevolving populations of predator and prey. A variety of choices are made in these models: exponential or logistic prey growth in the absence of a predator, various forms of predator functional response, and uni- or bi-directional trait axes. In addition, some form of trade-offs are assumed in order to prevent run-away evolution of the prey and predator traits. While there is a considerable amount of theory regarding various forms of prey growth rates and predator functional responses, only a few studies have explored how different types of trade-offs affect predator-prey dynamics. Here, we compared two ditrophic coevolution models incorporating different trade-offs via dual effects of the prey trait on attack rate and either prey carrying capacity or intrinsic growth rate. We employed a standard dynamical systems approach to analyze the equilibrium conditions of each model and find conditions for non-equilibrium oscillatory coexistence. The exact effect of various parameters on the outcome of predator-prey interactions depends on whether the trade-offs affect the intrinsic

growth rate or carrying capacity. In particular, coexistence is more likely when prey growth rate is affected by the evolving trait. In addition, in parameter regimes where cycles occur in both models, oscillations typically have larger periods and amplitudes when prey growth rate is affected by the evolving trait.

## 1.2. Introduction

Interactions between predators and their prey are among the most frequently studied ecological interactions in nature. Classic ecological theory led to hundreds of experiments that have documented the relative importance of these interactions [Englund et al., 1999, Gurevitch et al., 2000a] and their cascading effects on other trophic levels [Schmitz et al., 2000, Shurin et al., 2002]. Classic theory predicts various outcomes in terms of coexistence of predator and prey, but a common prediction is that predator and prey coexist in oscillations [Lotka, 1925, Volterra and Brelot, 1931, Beddington et al., 1975, Berryman, 1992]. In these cases, predator abundances increase with increasing prey density until a threshold level where predators overexploit prey, resulting in a decrease in prey abundance, followed by a decrease in predator abundance, which ultimately allows the prey population to recover. Theoretically, predator population cycles should lag behind prey population cycles by a quarter of a cycle phase [Case and Roughgarden, 2000]. These dynamics are well supported in some systems (Lynx-hare [Krebs et al., 2001], rotifer-algae [Yoshida et al., 2003]), but in other systems, stable coexistence between predator and prey have proved unlikely [Huffaker, 1958, Fujii, 1999], or predator-prey cycles do not match those predicted by theory [Hiltunen et al., 2014, Yoshida et al., 2003, 2007].

One reason that dynamics in natural systems may not match theoretical predictions is the context-dependency of species interactions. The strength of interactions between species may depend on the environment in which those interactions occur [Bertness and Callaway, 1994]. Moreover, we could broadly define environmental context to include the genetic environment of the predator and prey populations. Intraspecific trait variation plays an important role in the strength of interactions between predator and prey [Litchman and Klausmeier, 2008, Gross et al., 2009, Bolnick et al., 2011]. For example, different individuals of three-spined sticklebacks differ in morphology, depending on whether they come from benthic or limnetic habitats, which affects what

they eat, or by whom they are eaten [Reimchen, 1980, Reimchen and Nosil, 2001]. In addition to such spatial variation in traits, temporal trait variability over evolutionary time may also affect predator-prey interactions.

Recent evidence suggests that evolution can occur on contemporary time scales that affect ecological interactions, particularly when selection pressure is very strong, or when generation times are very short [Thompson, 1999, Hairston Jr. et al., 2005, Schoener, 2011]. DeLong et al. [2016] recently quantified that rates of change of phenotypes are on average  $\frac{1}{4}$  of the concurrent rates of change of population sizes. In many cases, predators serve as important selective agents on prey populations [Endler, 1991, Brodie III., 1992, Walsh and Reznick, 2008] and, conversely, prey can serve as important selective agents on predator populations [West et al., 1991, Motychak et al., 1999, Lill, 2001]. When predators evolve in response to prey, attack rates or consumption of prey should increase, thus increasing the strength of ecological interactions between predator and prey (Strauss et al. 2006). Conversely, prey that evolve increased escape ability or avoidance of predators should decrease the strength of the ecological interaction [Strauss et al., 2006].

Evolution can have important consequences for predator-prey cycles [Hiltunen et al., 2014]. Previous models have shown that incorporating prey evolution can shift predator-prey population dynamics between equilibrium, stable cycles, and chaotic coexistence [Saloniemi, 1993, Abrams and Matsuda, 1997b]. Yoshida et al. [2007] modeled prey that evolve on ecological time scales and found that prey evolution largely masked the predator-prey cycles that occurred in the absence of predation. These results were supported by experiments in laboratory microcosms, in which algal evolution in response to rotifer predation eliminated the oscillating cycles that occurred when algal population lacked sufficient genetic variation to evolve [Yoshida et al., 2003, 2007]. Becks et al. [2010] extended this work and found that in the presence of sufficient genetic variation, populations underwent ecological predator-prey oscillations, as defended prey were favored when predators were abundant and undefended prey were favored when predators were rare; without initial genetic variation, populations quickly converged on a steady state equilibrium.

Because both predator and prey species may be important selective agents on each other, coevolution between predator and prey might be important for determining the stability of the system. Early models found that an evolutionary arms race leads to Red Queen dynamics, in which

both predator and prey evolve in response to fluctuating selection that maintains their ecological interaction over time [Van Valen, 1973, Brodie III and Brodie Jr., 1999]. However, coevolution need not lead to a stable ecological equilibrium [Saloniemi, 1993, Abrams and Matsuda, 1997b, Mougi and Iwasa, 2011, Tirok et al., 2011, Mougi, 2012, Tien and Ellner, 2012, Cortez and Weitz, 2014, Klauschies et al., 2016, Bengfort et al., 2017, van Velzen and Gaedke, 2017]. Small adaptive trait changes in predator or prey can result in changes in attack rates that lead to antiphase oscillations [Bengfort et al., 2017]. Similarly, Mougi [2012] suggested that antiphase cycles or cryptic cycles could occur in systems in which both predator and prey evolve, but not when only a single species evolves. Mougi's results seemingly contradict those of Yoshida et al. [2007], who find cryptic cycles in models with on prey evolution. However, their modeling approaches vary in a critical way: Yoshida et al. [2007] assume a unidirectional axis in the prey trait, while Mougi assumes bidirectional axes in both predator and prey. Predator and prey often have dramatically different generation times, which could lead to differences in rates of evolution in each species. Even if generation times are similar, selection on prey may be stronger because a single interaction between predator and prey individuals has a huge effect on prey fitness, but often less effect on predator fitness (life vs. lunch; [Brodie III and Brodie Jr., 1999]). Furthermore, traits in one species may be more heritable than traits in another, resulting in different rates of evolution even under equivalent selection pressure.

Coevolutionary models can result in unrealistic runaway evolution, unless models incorporate some form of trade-off. For example, some models assume an increase in predator or prey traits on a uni-directional axis linearly also decreases the growth rate of that species. (e.g. Tien and Ellner [2012]. Other models assume that increases in predator traits along a uni-directional axis result in reductions in conversion efficiency (Mougi and Iwasa [2011], Tirok et al. [2011], Klauschies et al. [2016], van Velzen and Gaedke [2017] or death rate [Tien and Ellner, 2012, Mougi, 2012, Cortez and Weitz, 2014, van Velzen and Gaedke, 2017]. Few studies have explored how the natures of different trade-offs affect ecological dynamics [Tien and Ellner, 2012].

Because of the variety of results which have arisen out of recent eco-evolutionary models of coevolving predator and prey, it is crucial that we gain a deeper understanding of how modeling choices surrounding trade-offs affect the outcomes of population dynamics. Here we analyze and

compare two simple models of predator and prey which contain different trade-offs for the prey population. We assume bi-directional trait axes for both predator and prey traits (e.g. body size), where attack rates of predator on prey are maximized if trait matching occurs. Run-away evolution of the prey is prevented by the tethering of the prey trait to an optimal value via some form of trade-off, while runaway evolution of the predator is prevented via the trait matching requirement for attack rate. For this reason, we do not include additional trade-offs in the predator. Our goal in this study is to understand how predator-prey eco-evolutionary dynamics differ under two different trade-offs in prey.

### 1.3. Model Formulation

Consider predator and prey species with densities  $P = P(t)$  and  $N = N(t)$  at time  $t$ , respectively. Assume the predator and prey populations have mean quantitative traits  $\bar{p} = \bar{p}(t)$  and  $\bar{n} = \bar{n}(t)$ , respectively, and that these traits can be measured in the same unit, or can be transformed into the same unit. Also assume these traits are normally distributed through the populations with constant phenotypic variances  $\sigma^2$  and  $\beta^2$ , respectively [Schreiber et al., 2011]. In other words, their trait distributions are given by

$$q_p(p, \bar{p}) = \frac{1}{\sqrt{2\pi\sigma^2}} \exp\left[-\frac{(p - \bar{p})^2}{2\sigma^2}\right], \quad q_n(n, \bar{n}) = \frac{1}{\sqrt{2\pi\beta^2}} \exp\left[-\frac{(n - \bar{n})^2}{2\beta^2}\right],$$

where phenotypic variances  $\sigma^2$  and  $\beta^2$  have additive genetic (subscript  $G$ ) and environmental (subscript  $E$ ) components (i.e.,  $\sigma^2 = \sigma_G^2 + \sigma_E^2$  and  $\beta^2 = \beta_G^2 + \beta_E^2$ ).

Assume predator individuals with trait value  $p$  attack prey individuals with trait value  $n$  with attack rate  $a = a(p, n)$ . Also assume predators have a linear functional response and convert consumed prey in to offspring with efficiency  $e$  and have a constant death rate  $d$ . Then the fitness of predators with trait value  $p$  and consuming prey individuals with trait value  $n$  is

$$W(N, n, p) = ea(p, n)N - d,$$

and the per-capita mean fitness of the predator population is

$$(1.1) \quad \overline{W}(N, \bar{n}, \bar{p}) = \int_{\mathbb{R}^2} W(N, n, p) q_p(p, \bar{p}) q_n(n, \bar{n}) dp dn.$$

Assume prey with trait value  $n$  experience density-dependent logistic-type growth with growth rate  $r = r(n)$  and carrying capacity  $K = K(n)$  in the absence of predation. Since the prey trait  $n$  affects the predator-prey interaction  $a$  in addition to ecological variables in the absence of predation, we consider the prey trait to be ecologically pleiotropic. Thus the fitness of prey with trait value  $n$  interacting only with predators with trait value  $p$  is

$$Y(N, P, n, p) = r(n) \left( 1 - \frac{N}{K(n)} \right) - a(p, n)P,$$

and the per-capita mean fitness of the prey population is

$$(1.2) \quad \overline{Y}(N, P, \bar{n}, \bar{p}) = \int_{\mathbb{R}^2} Y(N, P, n, p) q_n(n, \bar{n}) q_p(p, \bar{p}) dn dp.$$

Thus, the ecological dynamics are given by

$$(1.3) \quad \frac{dP}{dt} = P \overline{W}(N, \bar{n}, \bar{p}), \quad \frac{dN}{dt} = N \overline{Y}(N, P, \bar{n}, \bar{p}).$$

Assuming each evolutionary variable stays normally distributed with unchanging variance, then the change of each evolutionary variable is proportional to the partial derivative of their mean fitness function with respect to that variable. In other words, evolution is always in the direction which immediately increases the mean fitness of the population [Lande, 1976]. Specifically, the constant of proportionality is the genetic component of the phenotypic variances. This gives rise to the evolutionary components of this model:

$$\frac{d\bar{p}}{dt} = \sigma_G^2 \frac{\partial \overline{W}}{\partial \bar{p}}, \quad \frac{d\bar{n}}{dt} = \beta_G^2 \frac{\partial \overline{Y}}{\partial \bar{n}}.$$

If there is no evolution, i.e., all of the ecological parameters are constant ( $\sigma_G = \beta_G = 0$ ), the dynamics of the resulting purely-ecological system (1.4) are well known.

$$(1.4) \quad \frac{dP}{dt} = P[eaN - d], \quad \frac{dN}{dt} = N \left[ r \left( 1 - \frac{N}{K} \right) - aP \right]$$

As a review, the three equilibria of this simplified model are extinction  $(P^*, N^*) = (0, 0)$ , (unstable), exclusion  $(P^*, N^*) = (0, K)$  (locally asymptotically stable if  $d > Kea$ ), and coexistence  $(P^*, N^*) = \left( \frac{r}{a} \left( 1 - \frac{N^*}{K} \right), \frac{d}{ea} \right)$ , (biologically feasible and locally asymptotically stable if  $d < Kea$ ). Since the exclusion and coexistence stability conditions are equal and opposite, there is no non-equilibrium dynamic. In other words, either the predator becomes extinct and the prey population asymptotically approaches its carrying capacity, or the predator and prey asymptotically approach a stable coexistence state.

However, ecological interactions are often dependent on which genetic variants are involved in the interactions. Evolutionary changes in traits may shift the strength of ecological interactions, which may in turn cause feedback by shifting the evolutionary variables via selection by ecological interactions. This eco-evolutionary feedback loop can affect both ecological and evolutionary outcomes. Since the purely-ecological model (1.4) is completely asymptotically stable, incorporating evolution here can only serve to destabilize the ecological equilibria.

**Model 0 – No Stabilizing Selection.** First we define the attack rate of a predator individual with phenotype  $p$  on a prey individual with phenotype  $n$  as a Gaussian function of their difference. For this study, we assume prey have a bidirectional axis of vulnerability to predation, which means they can reduce the successful predation rate by having a phenotype either greater or less than the matching predator phenotype. Examples of foraging traits on bidirectional axes are relative body sizes of predator and prey, and number and size of gill rakers in predatory freshwater fish (i.e. threespine stickleback) compared to body size of insect larvae or zooplanktonic prey [Saloniemi, 1993]. Similar to Schreiber et al. [2011], the attack rate is maximized when  $p - n$  is equal to some optimal difference  $\theta_a$  and decreases hyperexponentially as  $|p - n|$  diverges from  $\theta_a$ :

$$a(p, n) = \alpha \exp \left[ -\frac{((p - n) - \theta_a)^2}{2\tau_a^2} \right],$$

where  $\alpha$  is the maximal attack rate and  $\tau_a$  determines how steeply the attack rate declines with distance from the optimal trait difference  $\theta_a$ . In effect,  $\tau_a$  determines how phenotypically specialized the predator must be to consume the prey [Schreiber et al., 2011]. In other words, for large  $\tau_a$  only large deviations from the optimal trait difference will result in large reductions in the attack rate, while for small  $\tau_a$  even small deviations from the optimal trait difference have large fitness consequences. Under these assumptions, the average attack rate of the predator species on the prey species is

$$\bar{a}(\bar{p}, \bar{n}) = \int_{\mathbb{R}^2} a(p, n) q_p(p, \bar{p}) q_n(n, \bar{n}) dp dn = \frac{\alpha \tau_a}{\sqrt{A}} \exp \left[ -\frac{((\bar{p} - \bar{n}) - \theta_a)^2}{2A} \right],$$

where  $A := \tau_a^2 + \sigma^2 + \beta^2$ . If all other ecological parameters ( $r$ ,  $K$ ,  $d$ , and  $e$ ) are constant, this model may result in asymptotically stable ecological equilibrium, but runaway evolution, i.e., an evolutionary arms race where the population densities are constant but trait values are unbounded in time (Appendix A.4). This is not realistic because all characters have some constraints on their evolution [Saloniemi, 1993]. Below we introduce two expanded models which tether the prey character  $\bar{n}$  to an optimal value via decreases of vital ecological functions.

**Model 1 – Stabilizing Selection via Prey Intrinsic Growth Rate.** It may be the case that there is an optimal prey body size which maximizes prey intrinsic growth rate [Werner et al., 1984]. If trait matching must occur for the prey species and their resource, then it is appropriate to model prey growth rate  $r$  as a Gaussian function of its trait value  $n$ , given by

$$r(n) = \rho \exp \left[ -\frac{(n - \theta_r)^2}{2\tau_r^2} \right],$$

where  $\rho$  is the maximal growth rate of the prey species and  $\tau_r$  determines how steeply the growth rate declines with distance from the optimal trait value  $\theta_r$ . In effect,  $\tau_r$  determines how far the prey trait value can deviate from the optimal trait value while still maintaining an adequate growth rate. In other words, for large  $\tau_r$  only large deviations from the optimal trait value  $\theta_r$  can result in large reductions in prey growth rate, while for small  $\tau_r$  even small deviations from  $\theta_r$  can result in large reductions in prey growth rate. Under these assumptions, the average growth rate of the prey species is

$$\bar{r}(\bar{n}) = \int_{\mathbb{R}} r(n)q_n(n, \bar{n})dn = \frac{\rho\tau_r}{\sqrt{B}} \exp\left[-\frac{(\bar{n} - \theta_r)^2}{2B}\right]$$

where  $B := \tau_r^2 + \beta^2$ . For this first model, we assume the prey trait does not affect its resource use, i.e., the prey population carrying capacity  $K$  is constant. Thus the ecological and evolutionary dynamics of Model 1 are:

$$(1.5a) \quad \frac{dP}{dt} = P[e\bar{a}(\bar{p}, \bar{n})N - d],$$

$$(1.5b) \quad \frac{dN}{dt} = N\left[\bar{r}(\bar{n})\left(1 - \frac{N}{K}\right) - \bar{a}(\bar{p}, \bar{n})P\right],$$

$$(1.5c) \quad \frac{d\bar{p}}{dt} = \sigma_G^2 \left[ \frac{eN(\theta_a - (\bar{p} - \bar{n}))}{A} \bar{a}(\bar{p}, \bar{n}) \right],$$

$$(1.5d) \quad \frac{d\bar{n}}{dt} = \beta_G^2 \left[ \bar{r}(\bar{n})\left(1 - \frac{N}{K}\right) \frac{\theta_r - \bar{n}}{B} + \frac{P(\theta_a - (\bar{p} - \bar{n}))}{A} \bar{a}(\bar{p}, \bar{n}) \right].$$

**Model 2 – Stabilizing Selection via Prey Carrying Capacity.** It may be the case that suboptimal investment in prey body size can result in reduced ability to process resources, which causes an uptake in prey foraging effort and an increase in intraspecific competition. A reduction in the carrying capacity  $K$  is synonymous with an increase in intraspecific competition. Thus, for the second model, we assume the prey trait does not affect its intrinsic growth rate, i.e.,  $r$  is constant. Rather, the prey population carrying capacity  $K$  is a Gaussian function of its trait value  $n$ .

$$K(n) = \kappa \exp\left[-\frac{(n - \theta_K)^2}{2\tau_K^2}\right]$$

where  $\kappa$  is the maximal carrying capacity of the prey species and  $\tau_K$  determines how steeply the carrying capacity declines with distance from the optimal trait value  $\theta_K$ . In effect,  $1/K(n)$  gives the strength of competition of a prey individual with trait value  $n$ , and  $K(n)$  gives the carrying capacity of a population consisting entirely of individuals with trait value  $n$ . Thus the ecological and evolutionary dynamics of Model 2 are:

$$(1.6a) \quad \frac{dP}{dt} = P[e\bar{a}(\bar{p}, \bar{n})N - d],$$

$$(1.6b) \quad \frac{dN}{dt} = N \left[ r \left( 1 - \frac{N}{\bar{K}(\bar{n})} \right) - \bar{a}(\bar{p}, \bar{n})P \right],$$

$$(1.6c) \quad \frac{d\bar{p}}{dt} = \sigma_G^2 \left[ \frac{eN(\theta_a - (\bar{p} - \bar{n}))}{A} \bar{a}(\bar{p}, \bar{n}) \right],$$

$$(1.6d) \quad \frac{d\bar{n}}{dt} = \beta_G^2 \left[ -\frac{rN(\bar{n} - \theta_K)}{\bar{K}(\bar{n})C} + \frac{P(\theta_a - (\bar{p} - \bar{n}))}{A} \bar{a}(\bar{p}, \bar{n}) \right],$$

where the harmonic mean of prey carrying capacity is given by

$$\bar{K}(\bar{n}) = \left( \int_{\mathbb{R}} \frac{1}{K(n)} q_K(n, \bar{n}) dn \right)^{-1} = \frac{\kappa\sqrt{C}}{\tau_K} \exp \left[ -\frac{(n - \theta_K)^2}{2C} \right],$$

and  $C := \tau_K^2 - \beta^2$  (note that our use of the harmonic mean here is a result of the calculation of mean prey fitness (equations 1.2, 1.3)). This formulation requires  $\tau_K > \beta$ . If  $\tau_K$  approaches  $\beta$  from above, then  $\bar{K}$  decreases to 0, which causes immediate extinction of the prey and thus extinction of the predator. If  $\tau_K \leq \beta$ , a significant portion of the prey population has extremely low resource use ability (low carrying capacity), which also causes immediate extinction of the prey and thus extinction of the predator. This is mathematically intuitive since the harmonic mean is highly sensitive to small numbers. All parameters and their descriptions are listed in Table 1.1. See Appendix A.1 for model derivation details.

## 1.4. Results

**Equilibria and Stability Analysis.** In addition to using standard numerical techniques to simulate the model (figures 1.1 and 1.2), we analyze both models by employing a standard dynamical systems approach, which includes solving for equilibrium points and determining conditions for local linear stability. Both models have three types of equilibria ( $N^*, P^*, \bar{n}^*, \bar{p}^*$ ): extinction (of both species), exclusion (of the predator species), and coexistence. The extinction equilibria are given by

$$(1.7) \quad (N^*, P^*, \bar{n}^*, \bar{p}^*) = (0, 0, *, *),$$

Parameter	Description
$r, K$	Prey intrinsic growth rate and carrying capacity
$d, e$	Predator death rate and efficiency
$\sigma^2$	Predator trait distribution variance; $\sigma^2 = \sigma_G^2 + \sigma_E^2$
$\beta^2$	Prey trait distribution variance; $\beta^2 = \beta_G^2 + \beta_E^2$
$\alpha, \tau_a, \theta_a$	Maximum value, width, and location of optimal trait difference of the Gaussian attack rate function $a(p, n)$
$\rho, \tau_r, \theta_r$	Maximum value, width, and location of optimal trait of the Gaussian intrinsic growth rate function $r(n)$
$\kappa, \tau_K, \theta_K$	Maximum value, width, and location of optimal trait of the Gaussian carrying capacity function $K(n)$
$A$	$\tau_a^2 + \sigma^2 + \beta^2$
$B$	$\tau_r^2 + \beta^2$
$C$	$\tau_K^2 - \beta^2$

TABLE 1.1. All model parameters and their biological meaning.

and are unstable for all biologically relevant parameters (\* represents an arbitrary quantity). The exclusion equilibria are given by

$$(1.8) \quad (N^*, P^*, \bar{n}^*, \bar{p}^*) = (K^*, 0, \theta_{\text{excl}}, \theta_{\text{excl}} + \theta_a),$$

where

$$\theta_{\text{excl}} = \begin{cases} *, & \text{for Model 1,} \\ \theta_K, & \text{for Model 2,} \end{cases} \quad \text{and} \quad K^* = \begin{cases} K, & \text{for Model 1,} \\ \frac{\kappa\sqrt{C}}{\tau_K}, & \text{for Model 2,} \end{cases}$$

and are stable if

$$(1.9) \quad d > \frac{K^* e \alpha \tau_a}{\sqrt{A}}.$$

The coexistence equilibrium is given by

$$(1.10) \quad (N^*, P^*, \bar{n}^*, \bar{p}^*) = \left( \frac{d\sqrt{A}}{e\alpha\tau_a}, \frac{r^*\sqrt{A}}{\alpha\tau_a} \left( 1 - \frac{N^*}{K^*} \right), \theta_{\text{coex}}, \theta_{\text{coex}} + \theta_a \right),$$

where

$$\theta_{\text{coex}} = \begin{cases} \theta_r, & \text{for Model 1,} \\ \theta_K, & \text{for Model 2,} \end{cases} \quad \text{and} \quad r^* = \begin{cases} \frac{\rho\tau_r}{\sqrt{B}}, & \text{for Model 1,} \\ r, & \text{for Model 2,} \end{cases}$$

and is stable if

$$(1.11) \quad \frac{\sigma_G^2}{\beta_G^2} > \frac{r_{\text{stab}}}{d} \left( 1 - \frac{d\sqrt{A}}{K_{\text{stab}}e\alpha\tau_a} \right),$$

where

$$r_{\text{stab}} = \begin{cases} \frac{\rho\tau_r}{\sqrt{B}} \left( 1 - \frac{A}{B} \right), & \text{for Model 1,} \\ r, & \text{for Model 2,} \end{cases} \quad \text{and} \quad K_{\text{stab}} = \begin{cases} K, & \text{for Model 1,} \\ \frac{\kappa\sqrt{C}}{\tau_K(1+\frac{A}{C})}, & \text{for Model 2,} \end{cases}.$$

See Appendices A.2 and A.3 for details of equilibria stability analysis.

In both models, the prey face a trade off between evolution of anti-predator traits and optimization of growth rate or carrying capacity. The size of this trade off  $|\bar{n} - \theta_{\text{coex}}|$  is irrelevant when determining stability of the coexistence equilibrium (1.11). This is because Models 1 and 2 do not reduce to Model 0 when  $\theta_{\text{coex}} = \theta_a$ ; rather, Model 1 and Model 2 reduce to Model 0 when growth rate and carrying capacity are constant, respectively. This happens when  $\tau_r \rightarrow \infty$  and  $\tau_K \rightarrow \infty$  because  $\tau_r$  and  $\tau_K$  describe the variation of prey growth rate and carrying capacity caused by variation in prey genotype. As  $\tau_r \rightarrow \infty$  or  $\tau_K \rightarrow \infty$ , growth rate or carrying capacity approaches a constant value for the population because there are few individuals with extreme genotypes. Therefore coexistence stability is independent of the relative values of  $\theta_a$  and  $\theta_{\text{coex}}$  and dependent on the variance terms  $\tau_r$  and  $\tau_K$ .

Note that if both populations are extinct, their trait values can be arbitrary because the populations are in ecological equilibrium for any values of  $\bar{p}^*$  and  $\bar{n}^*$ . Since  $\theta_{\text{excl}}$  is arbitrary for Model 1, there are an infinite number of exclusion equilibria for Model 1. Thus, when (1.9) holds, the evolutionary dynamics will approach an equilibrium based on initial conditions. The prey trait at carrying capacity is arbitrary since selection on traits which affect intrinsic growth rate is weak when the prey population is near its carrying capacity. On the other hand, Model 2 has a unique

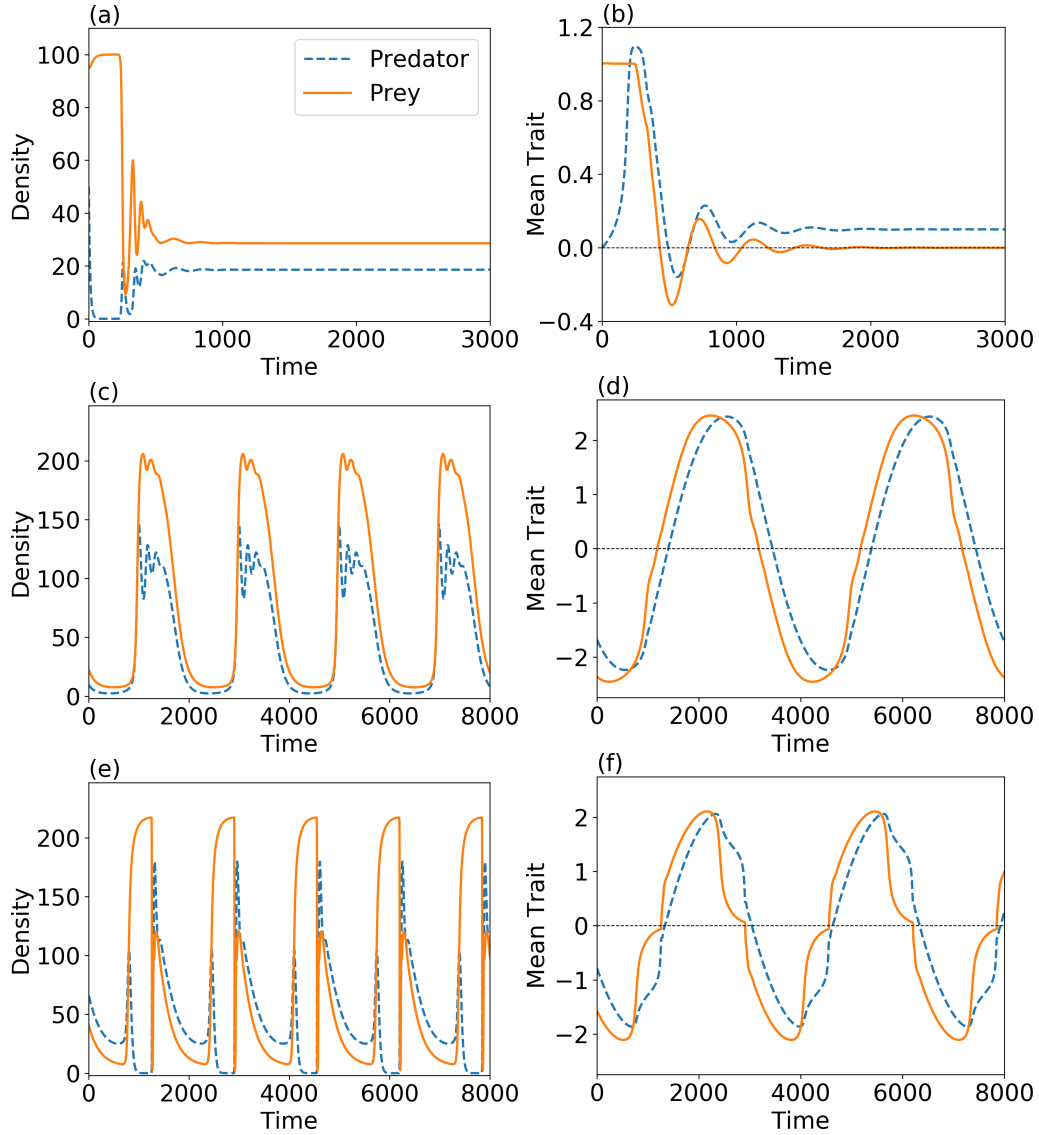


FIGURE 1.1. **Timeseries.** The left panels (a,c,e) depict predator and prey population densities. The right panels (b,d,f) depict predator and prey mean trait values. Panels (a,b) show stable coexistence equilibrium dynamics in Model 1. Panels (c,d) show cyclic coexistence dynamics in Model 1. Panels (e,f) show cyclic coexistence dynamics in Model 2. Parameter values:  $e = 0.5$ ,  $\alpha = 0.05$ ,  $\sigma = \beta = 0.25$ ,  $\theta_a = 0.1$ ,  $\theta_r = \theta_K = 0$ . Panels (a,b) parameter values:  $d = 0.1$ ,  $\tau_a = 0.05$ ,  $\tau_r = 0.55$ ,  $\sigma_G = 0.18$ ,  $\beta_G = 0.17$ ,  $\rho = 0.2$ ,  $K = 100$ . Panels (c,d,e,f) parameter values:  $d = 0.05$ ,  $\tau_a = 0.1$ ,  $\tau_r = \tau_K = 1.0$ ,  $\sigma_G = 0.106$ ,  $\beta_G = 0.1$ ,  $\rho = r = 0.5$ ,  $\kappa = K = 225$ .

exclusion equilibrium since selection on traits which affect prey population carrying capacity is strong when the population is near its carrying capacity. This is intuitive since increasing prey carrying capacity always increases average prey fitness. The predator population will be excluded if its death rate is sufficiently high. Also, higher prey carrying capacity, predator efficiency, and

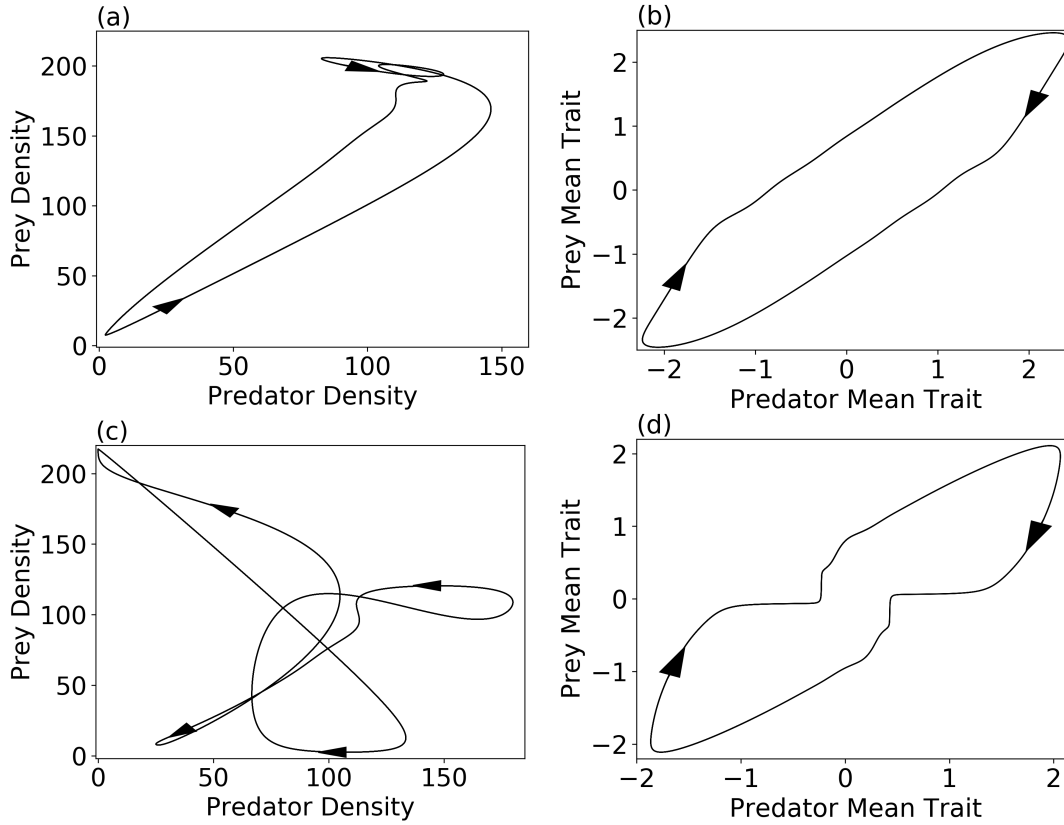


FIGURE 1.2. **Cycle Phaseplanes for Model 1 (a,b) and Model 2 (c,d).** The left panels (a,c) depict phaseplanes of predator and prey population densities. The right panels (b,d) depict phaseplanes of predator and prey mean trait values. Panels (a,b) are the phaseplanes of the cyclic dynamics of Model 1 shown in Figures 1.1(c,d). Panels (c,d) are the phaseplanes of the cyclic dynamics of Model 2 shown in Figures 1.1(e,f).

predator maximum attack rate can destabilize the exclusion equilibrium in favor of the internal coexistence equilibrium, which is unique for each model. When (1.11) holds, the prey character  $\bar{n}$  reaches its optimal value for the trait undergoing stabilizing selection, and the predator character  $\bar{p}$  reaches the optimal difference to maximize attack rate.

In (1.11),  $\sigma_G/\beta_G$  is the ratio of predator and prey speeds of evolution given equivalent selection pressure. This means the coexistence equilibrium (1.10) is stable if predator evolution can be fast enough in comparison to prey evolution. More precisely, stable equilibrium coexistence is more likely if the predator's trait is more heritable than the prey's trait. If this happens, the predator trait value “catches up” to the prey trait value, which increases the attack rate, hence decreasing

prey density, and decreasing  $|d\bar{n}/dt|$ . The trait dynamics stabilize, resulting in decaying ecological oscillations.

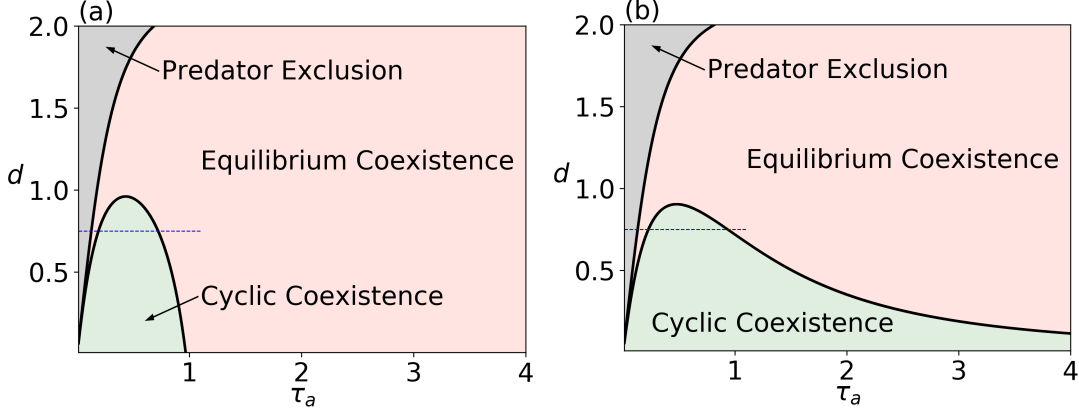


FIGURE 1.3. **Bifurcation diagrams for model 1 (Panel a) and model 2 (Panel b), with predator death rate ( $d$ ) vs. predator specialization ( $\tau_a$ ).** In (a), the coexistence stability boundary crosses the  $\tau_a$  axis, while in (b), the coexistence stability boundary approaches the  $\tau_a$  axis as  $\tau_a \rightarrow \infty$ . There is a much larger region in parameter space that results in cyclic behavior in Model 2 than in Model 1. Parameter values:  $\sigma = \beta = 0.25$ ,  $e = \alpha = 0.1$ ,  $\tau_r = \tau_K = 1$ ,  $\sigma_G/\beta_G = 0.4$ ,  $\rho = r = 0.5$ ,  $K = \kappa = 225$ . Figure 1.6(c) shows cycle maxima, minima, and periods for the parameter values indicated by the blue dotted line ( $d = 0.75$ ,  $0 \leq \tau_a \leq 1.1$ ).

In Model 1, if  $\tau_a^2 > \tau_r^2 - \sigma^2$ , then  $r_{\text{stab}} < 0$ . This always results in stable coexistence provided that (1.10) is biologically feasible. The biological feasibility condition for coexistence is the opposite condition as the exclusion stability condition (1.9). That is, provided  $d < \frac{K e \alpha \tau_a}{\sqrt{A}}$ , then stable coexistence is inevitable if the variance of the attack rate curve  $\tau_a$  is high enough. Biologically, this means that if the attack rate does not require high predator specificity, then stable equilibrium coexistence is more likely.

In Model 2, however, the coexistence stability condition boundary can be arranged so that only  $d$  is on the left hand side:

$$d = \frac{r \kappa e \alpha \tau_a \sqrt{C}}{\frac{\sigma_G^2}{\beta_G^2} \kappa e \alpha \tau_a \sqrt{C} + r \sqrt{A} \tau_K \left(1 + \frac{A}{C}\right)}$$

and we find that  $d$  decreases to 0 as  $\tau_a$  grows without bound to  $\infty$  (since all terms are positive, the numerator is  $\mathcal{O}(\tau_a)$  and the denominator is  $\mathcal{O}(\tau_a^3)$ ). This means that for any value of  $\tau_a$ , there is always a value of  $d$  such that (1.9) is not satisfied (Figure 1.3). This is a key difference between the models: in Model 1, high values of  $\tau_a$  never result in cyclic coexistence, whereas in Model 2, high

values of  $\tau_a$  may result in cycles for sufficiently low  $d$ . For fixed  $d$  in Model 2, however, the stable coexistence condition (1.11) will hold for sufficiently high  $\tau_a$ . The notation  $\mathcal{O}(\tau_a)$  and  $\mathcal{O}(\tau_a^3)$  here mean that as  $\tau_a$  grows indefinitely, the expression grows proportionally to  $\tau_a$  or  $\tau_a^3$ , respectively. The notation  $\mathcal{O}(1)$  means an expression approaches a constant value in a given limit.

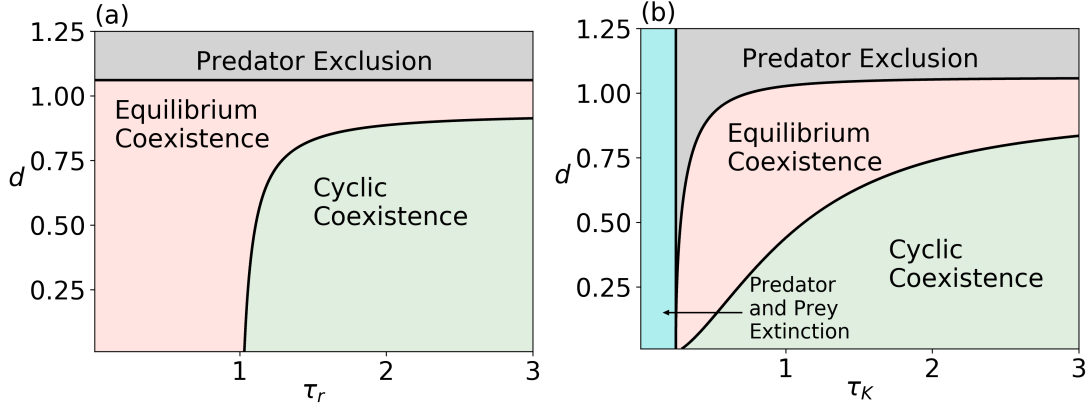


FIGURE 1.4. Bifurcation diagrams for model 1 (Panel a) and model 2 (Panel b), with predator death rate ( $d$ ) vs. prey trade-off strength ( $\tau_r$  or  $\tau_K$ ). Parameter values:  $e = 0.1$ ,  $\alpha = 0.05$ ,  $\tau_a = 1$ ,  $\sigma_G/\beta_G = 0.2$ ,  $\rho = r = 0.3$ ,  $K = \kappa = 225$ ,  $\sigma = \beta = 0.25$ .

Note that  $B = \mathcal{O}(\tau_r^2)$  as  $\tau_r$  increases, and thus  $\frac{\rho\tau_r}{\sqrt{B}} = \mathcal{O}(1)$ . This means  $r_{\text{stab}}$  (for Model 1) is eventually an increasing function of  $\tau_r$ . Since the right hand side of the coexistence stability condition (1.11) is an increasing function of  $r_{\text{stab}}$ , then increasing  $\tau_r$  can destabilize the coexistence equilibrium. Similarly, note that  $C = \mathcal{O}(\tau_K^2)$  as  $\tau_K$  increases, and thus  $\frac{\kappa\sqrt{C}}{\tau_K} = \mathcal{O}(1)$ . This means  $K_{\text{stab}}$  is eventually an increasing function of  $\tau_K$ . Since the right hand side of (1.11) is an increasing function of  $K_{\text{stab}}$ , then increasing  $\tau_K$  can also destabilize the coexistence equilibrium. Biologically, these results mean that if prey are not required to be particularly close to the optimal trait value in order to have adequate growth rate or carrying capacity, then cyclic coexistence is more likely. More precisely, the coexistence stability condition boundaries are

$$(1.12a) \quad d = \begin{cases} \frac{\rho\tau_R K e \alpha \tau_a (\tau_r^2 - \tau_a^2 - \sigma^2)}{\frac{\sigma_G^2}{\beta_G^2} K e \alpha \tau_a (\tau_r^2 + \beta^2)^{3/2} + \rho\tau_r (\tau_r^2 - \tau_a^2 - \sigma^2) \sqrt{\tau_a^2 + \sigma^2 + \beta^2}} & \text{for Model 1,} \\ \frac{r\kappa e \alpha \tau_a (\tau_K^2 - \beta^2)^{3/2}}{\frac{\sigma_G^2}{\beta_G^2} \kappa e \alpha \tau_a (\tau_K^2 - \beta^2)^{3/2} + r\tau_K (\tau_K^2 + \tau_a^2 + \sigma^2) \sqrt{\tau_a^2 + \sigma^2 + \beta^2}} & \text{for Model 2.} \end{cases}$$

In Model 1,  $d \rightarrow \frac{\tau K e \alpha \tau_a}{\frac{\sigma_G^2}{\beta_G} K e \alpha \tau_a + \rho \sqrt{A}}$  as  $\tau_r \rightarrow \infty$ , and in Model 2  $d \rightarrow \frac{\tau K e \alpha \tau_a}{\frac{\sigma_G^2}{\beta_G} \kappa e \alpha \tau_a + r \sqrt{A}}$  as  $\tau_K \rightarrow \infty$ . These limiting values of  $d$  are less than the predator exclusion boundary, so as  $\tau_r$  or  $\tau_K \rightarrow \infty$ , there is an intermediate range of  $d$  values which results in stable coexistence, while low  $d$  values will result in cyclic coexistence and high  $d$  values result in predator exclusion (Figure 1.4). The models differ, however, as  $\tau_r$  or  $\tau_K$  decrease. First, Model 2 predicts both predator and prey go extinct for  $\tau_K < \beta$ , while coexistence is possible for arbitrarily small  $\tau_r$  in Model 1. In addition, while the denominator of (1.12b) is positive for  $\tau_K > \beta$  in Model 2, the denominator of (1.12a) is negative for sufficiently small  $\tau_r$  in Model 1.

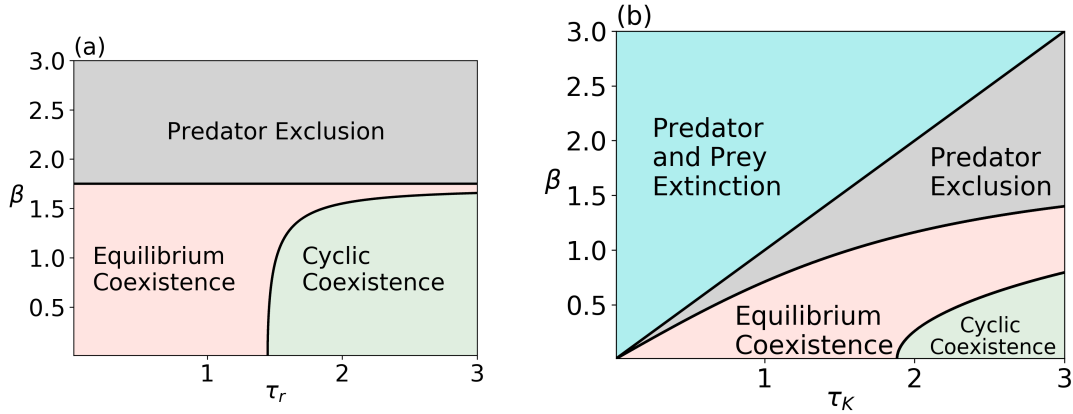


FIGURE 1.5. Bifurcation diagrams for model 1 (Panel a) and model 2 (Panel b), with prey trait distribution variance ( $\beta$ ) vs. prey trade-off strength ( $\tau_r$  or  $\tau_K$ ). Parameter values:  $e = 0.1$ ,  $\alpha = 0.05$ ,  $d = 0.5$ ,  $\tau_a = 1$ ,  $\sigma = 1$ ,  $\sigma_G/\beta_G = 0.1$ ,  $\rho = r = 0.3$ ,  $K = \kappa = 225$

Figure 1.5 shows similar distinctions between the models. The predator exclusion stability condition (1.9) is independent of  $\tau_r$ , and thus the boundary between the “Predator Exclusion” and “Equilibrium Coexistence” regions is flat for Model 1. However, (1.9) is dependent on  $\tau_K$  which accounts for the different shape for Model 2. We also see a larger region of coexistence in Model 1 than in Model 2.

**Qualitative Differences in the Models’ Cycles.** Figures 1.1(a,b) display a stable coexistence dynamic from Model 1. In this simulation, the initial prey and predator mean trait values,  $\bar{n}_0$  and  $\bar{p}_0$ , respectively, are far enough apart that the predator is not a threat. Their initial difference is  $\bar{p}_0 - \bar{n}_0 = 1$ , which is large in comparison to the variance of the attack rate curve  $\tau_a = 0.05$ . This means that only a very small percentage of predators are initially well suited to attack the prey,

resulting in very strong selective pressure on the predators. In contrast, the prey population is not initially threatened by the predator, resulting in very weak selective pressure on the prey. Once the predator mean trait value is close enough to the optimal difference  $\theta_a$ , the predator becomes a viable threat to the prey, increasing predator density and decreasing prey density. The predator and prey then undergo dampening oscillations to coexistence equilibrium as their mean trait values stabilize. Model 2 simulations resulting in stable equilibrium coexistence show similar dynamics.

In contrast to the purely ecological system (1.4), both models' exclusion and coexistence stability conditions are not equal or opposite, which implies there is at least one type of non-equilibrium dynamic. Figures 1.1(c,d) depict long-term stable oscillatory behavior in Model 1, and figures 1.1(e,f) depict long-term stable oscillatory behavior in Model 2. In order to achieve a good comparison between Models 1 and 2, we matched the parameters as closely as possible. In particular, we set the constant carrying capacity  $K$  from Model 1 equal to the maximum carrying capacity  $\kappa$  from Model 2, the constant intrinsic growth rate  $r$  from Model 2 equal to the maximum intrinsic growth rate  $\rho$  from Model 1, and the growth rate variance  $\tau_r$  from Model 1 equal to the carrying capacity variance  $\tau_K$  from Model 2.

The oscillations seen in Figures 1.1(c,d,e,f) are similar in many ways, and we can intuitively understand them by considering the inverse effects that the evolution of the prey mean trait value sometimes has on its own fitness. In particular, consider the periods of time in which the prey mean trait value is undergoing selection *away* from the optimal value ( $\theta_r$  for Model 1;  $\theta_K$  for Model 2). Since the predator is a threat, the prey evolves away from the predator, decreasing attack rate  $\bar{a}$ , and hence increasing its fitness. However, as the prey evolves away from its optimal value, the trade off  $|\bar{n} - \theta_{\text{coex}}|$  increases, reducing the average growth rate  $\bar{r}$  (Model 1) or carrying capacity  $\bar{K}$  (Model 2), and thus reducing prey fitness. These two inverse effects nullify each other whenever the prey mean trait value reaches a minimum or maximum. At these extrema, both populations are suppressed to low levels (due to either low growth rate in Model 1 or low carrying capacity in Model 2), and thus the selection pressure toward the optimal trait value outweighs the selection pressure of predation. The prey trait value then reverses direction and evolves *toward* its optimal value. During this time, prey mean fitness increases for two reasons: a negative effect on attack

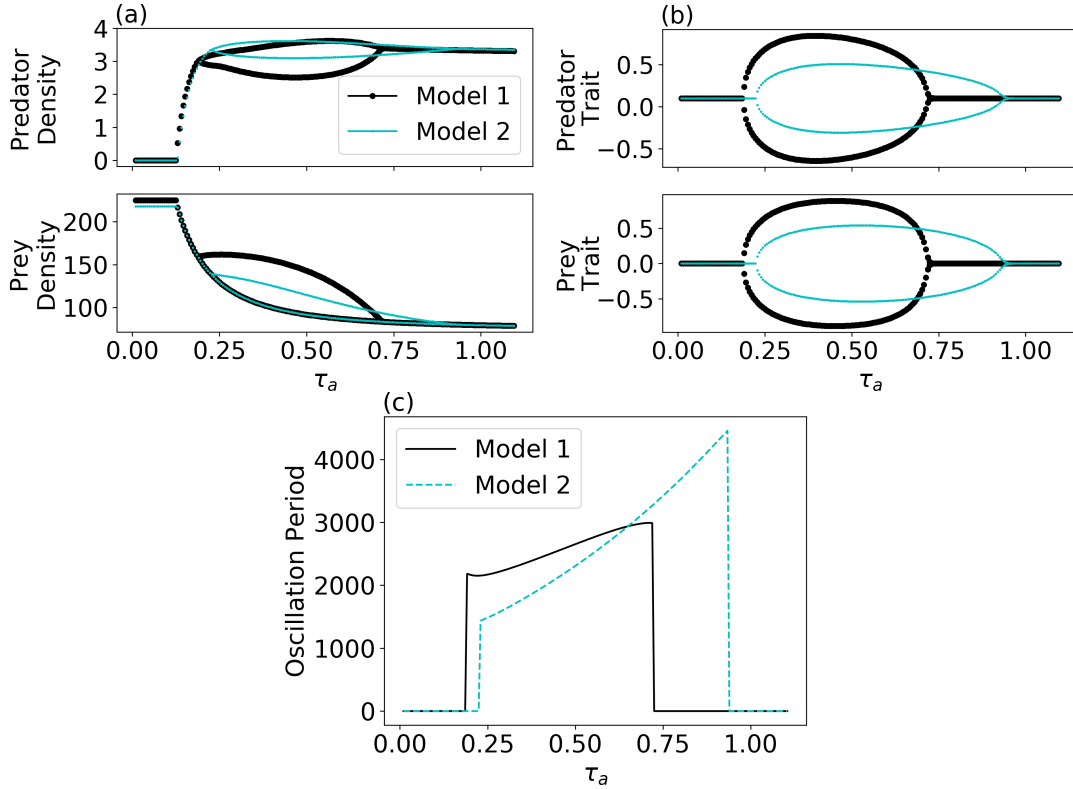


FIGURE 1.6. **Models 1 and 2 Bifurcation Diagrams (Panels a,b) and oscillation periods (Panel c).** Parameter values match Figure 1.3 for predator death rate  $d = 0.75$ . Also,  $\theta_a = 0.1$ ,  $\theta_r = \theta_K = 0$ ,  $\sigma_G = 0.04$ , and  $\beta_G = 0.1$ . As  $\tau_a$  increases the population moves from predator exclusion, to coexistence equilibrium, to cyclic coexistence, and back to coexistence equilibrium. There is a small region of  $\tau_a$  where Model 1 exhibits oscillatory coexistence and Model 2 exhibits coexistence equilibrium ( $\tau_a$  between 0.18 and 0.2, approximately) and a larger region of  $\tau_a$  where Model 2 exhibits oscillatory coexistence and Model 1 exhibits coexistence equilibrium ( $\tau_a$  between 0.71 and 0.93, approximately). In (c), oscillation periods of 0 indicate non-oscillatory behavior.

rate and a positive effect on the prey trait undergoing selection. Immediately after passing through the optimal value, however, the inverse effects take hold and the cycle begins again.

Predator and prey density cycles can be in phase in the larger evolutionary time scale, and out of phase in the smaller ecological time scale (Figure 1.2). Note the density phase trajectory of Model 1 is generally positively sloped, which means prey and predator densities reach their minima and maxima at around the same time (Figures 1.2(a,c)). However, when prey and predator densities are near their relative maxima, their cycles are temporarily out of phase, as indicated in Figure 1.2(a) by the negative slope of the top part of the density phase trajectory. In other words, as the genetic environment changes to favor a high-density equilibrium, predator and prey densities

diverge from the low-density equilibrium together, but on the ecological time scale predator and prey densities undergo out-of-phase, dampening oscillations toward this high-density equilibrium.

There are qualitative differences between the cycles in these two models, however, which may be attributed to the decrease in  $|\frac{d\bar{n}}{dt}|$  (1.5d) as growth rate decreases, as opposed to the increase in  $|\frac{d\bar{n}}{dt}|$  (1.6d) as carrying capacity decreases. This results in more rapid prey evolution when the prey mean trait is at an extrema in Model 2, and less rapid prey evolution when the prey mean trait is at an extrema in Model 1. In addition, prey growth rate in Model 2 is never as low as the mean prey growth rate in Model 1. Higher prey growth rate causes an increased predator equilibrium density, which increases selective pressure on the prey, causing bouts of more rapid prey evolution. On the other hand, the predators in Model 2 cannot adequately respond to this rapid evolution, resulting in a lag time where predator density is exponentially decreasing and the rate of predator evolution is diminished. In the simulations shown in Figures 1.1(c,d,e,f), the increase in the Model 2 period due to the lag time is outweighed by its decrease due to the increase in  $|\frac{d\bar{n}}{dt}|$  as carrying capacity decreases, and thus we see longer oscillatory periods in Model 1 ( $T \approx 4000$  in Figures 1.1(c,d) and 1.2(a,b)) than in Model 2 ( $T \approx 3300$  in Figures 1.1(e,f) and 1.2(c,d)). In Figure 1.6 we see that the oscillation periods in Model 1 are greater than that in Model 2 for intermediate values of  $\tau_a$ . This is intuitive since generalist predators are more able to respond to bouts of rapid prey evolution than specialist predators, thus removing the period of the exponentially decaying predator population. However, at larger values of  $\tau_a$ , the oscillation periods in Model 2 are greater than that of Model 1. This may seem counterintuitive, but an increased ability to respond decreases the overall selective pressure on predators, ultimately resulting in slower evolution and greater oscillatory periods.

Finally, we proved the existence of Hopf bifurcations [Hale and Koçak, 1991] as parameters are shifted from satisfying the coexistence equilibrium stability condition of either model to not satisfying them. Hopf bifurcations occur when a shifting parameter causes a stable equilibrium to become unstable, while also creating cyclic behavior around the equilibrium. The existence of Hopf Bifurcations in both models suggests the existence of asymptotically stable limit cycles, which we conjecture are globally stable given positive density initial conditions. In this study we have shown the models exhibit stable cyclic behavior using simulations, but we stop short of rigorously proving the asymptotic stability of the attractors.

## 1.5. Summary and Discussion

We formulated two coevolutionary predator-prey models which differ only in the form of an evolutionary trade-off. For both models, we found all equilibria and their local stability conditions. We showed the existence of Hopf bifurcations in both models, which suggests the existence of stable limit cycles (and which we conjecture are globally stable provided positive density initial conditions). While predator-prey cycles are possible without evolution if the predator has a saturating functional response, our models show that coevolution can cause ecological cycles even under the assumption of a linear functional response. This is important because the predator-prey model with logistic growth and linear functional response is well-known to not produce stable cycles.

In the first model, prey evolution to avoid predation is halted by a trade-off due to reductions in growth rate. This is a very common form of trade-off incorporated into models and is a reasonable choice in many systems [Abrams and Matsuda, 1997a, Mougi and Iwasa, 2011, Mougi, 2012, Klauschies et al., 2016, van Velzen and Gaedke, 2017]. In the second model, prey evolution is halted by a trade-off due to reductions in carrying capacity. This is a less common choice but can be reasonable if shifting a continuous trait (i.e. body size) affects how prey are able to consume resources, altering their effective carrying capacity.

Previous models of coevolution in exploiter-victim systems have incorporated evolutionary trade-offs in various ways. Iwasa et al. [1991] modeled mate preference as a fitness cost, and in later analyses, Mougi and Iwasa [2010, 2011] found that the coexistence equilibrium is stable if the evolutionary adaptation of the prey is faster than that of the predator. These studies assumed unidirectional trait axes and trade-offs in prey and predator basal per-capita growth rates. Later, Mougi [2012] analyzed a coevolutionary model with bidirectional traits with trade-offs in prey growth rate and predator death rate. In contrast to their earlier studies, they found that the coexistence equilibrium is stable if the predator can adapt faster than the prey. These conflicting results may have been a result of choosing unidirectional or bidirectional trait axes, but they also may have been a result of choosing different forms of evolutionary trade-offs.

While many modeling choices can be justified by various biological examples, relatively few studies have explored how these choices affect results. Tien and Ellner [2012] compared two models

with unidirectional trait axes and density independent and density dependent trade-offs. Interestingly, they found that stable coexistence is more likely if both predator *and* prey have fast adaptation in the density independent trade-off model, while stable coexistence is more likely if predator has faster adaptation than the prey in the density dependent trade-off model. In our study, both models resulted in stable coexistence if the ratio of predator to prey speeds of adaptation is sufficiently high. These conflicting results highlight the need for theoreticians to consider how the forms of trade-offs can affect model analyses. It is surprising this has not been a larger area of research given that trade-offs are so widely accepted as a necessary component of eco-evo models.

While this study follows the work of Mougi and Iwasa [2010, 2011], Mougi [2012], Tien and Ellner [2012], who used a quantitative genetics framework to model trait evolution, others have utilized adaptive dynamics frameworks [Nuismer et al., 2005] and/or individual-based frameworks [Calcagno et al., 2010, DeLong and Gibert, 2016]. Quantitative genetics eco-evo models typically assume that traits stay normally distributed with constant variance and that selection pressure is proportional to that variance [Lande, 1976, Abrams and Matsuda, 1997b]. This is a reasonable assumption according to studies by Gaylord [1953], Van Valen [1969], who have noted that variance of morphological traits in a lineage often remains roughly constant [Lande, 1976]. Others have assumed variance is constant but there is some other evolutionary force which decreases selective pressure as the mean trait approaches one or more boundary values [Saloniemi, 1993, Tien and Ellner, 2012, Cortez and Weitz, 2014, Bengfort et al., 2017, van Velzen and Gaedke, 2017, Klauschies et al., 2016]. Nuismer et al. [2005] used an adaptive dynamics framework to model the evolution of trait variance for normally distributed traits, and Tirok et al. [2011] used a quantitative genetics framework to derive differential equations to model the evolution of trait mean and variance for normally distributed traits.

Any of the above evolutionary modeling choices also greatly affect analytical results. When using the framework of Tirok et al. [2011] to incorporate the dynamics of the trait variance  $\sigma_G^2$  and  $\beta_G^2$ , we obtain results different from the main text, as seen in the comparison between Figures 1.1 and 1.7. The shorter periods seen in the oscillating solutions is a result of increased and evolving trait variances. We also see coexistence is threatened if prey variance can increase without bound

in Model 1. This is because reductions in growth rates are of little consequence to prey when their population is at its carrying capacity. Calcagno et al. [2010] utilized an individual-based framework to model the full distribution of traits and found that rapid predator evolution resulted in prey and/or predator speciation and fewer interactions between predator and prey. They also found that the predator went extinct if its adaptation speed was too slow, suggesting that predators are more successful if the ratio of speeds of adaptation of predators and prey is at some optimal level. We expect that comparing models with different evolutionary trade-offs and full trait distributions will yield similar results to Calcagno et al. [2010]. and future work will entail modeling the evolution of the full trait distribution of both predator and prey.

Our study shows that analytical outcomes are affected greatly by the choice of trade-off in prey species; the specific traits under consideration matter. We investigated the qualitative differences between cycles produced by the two models using simulations. Since the prey rate of evolution  $|\overline{d\bar{n}}/dt|$  generally decreases as prey growth rate decreases but increases as carrying capacity decreases, there are bouts of more rapid prey evolution in Model 2 that are not present in Model 1 (Figures 1.1(d,f)) These bouts of rapid evolution present an evolutionary challenge to the predators, who are suddenly unequipped to deal with the changing genetic landscape. This results in periods of time in which the predator population decays exponentially and would go extinct if evolution were to cease (Figure 1.1(e)). At these low densities, the predator population is able to quickly respond evolutionarily, making them a threat to the prey, enabling them to recover ecologically. Since generalist predators (higher  $\tau_a$ ) are more able to respond to rapid prey evolution than specialist predators, they spend less time at extremely low densities. This decrease in selective pressure results in cycles of longer periods (Figure 1.6(c)).

Our models produce cycles with generally in-phase ecological dynamics over the longer evolutionary time scale, and out-of-phase fluctuations on an ecological time scale immediately following bouts of more rapid evolution. These ecological fluctuations are not offset by a quarter cycle, as predicted by classical ecological models, but rather resemble dynamics seen in Khibnik and Kondrashov [1997], Mougi [2012] and supported by studies incorporating rapid prey evolution [Yoshida et al., 2003, Cortez and Ellner, 2010].

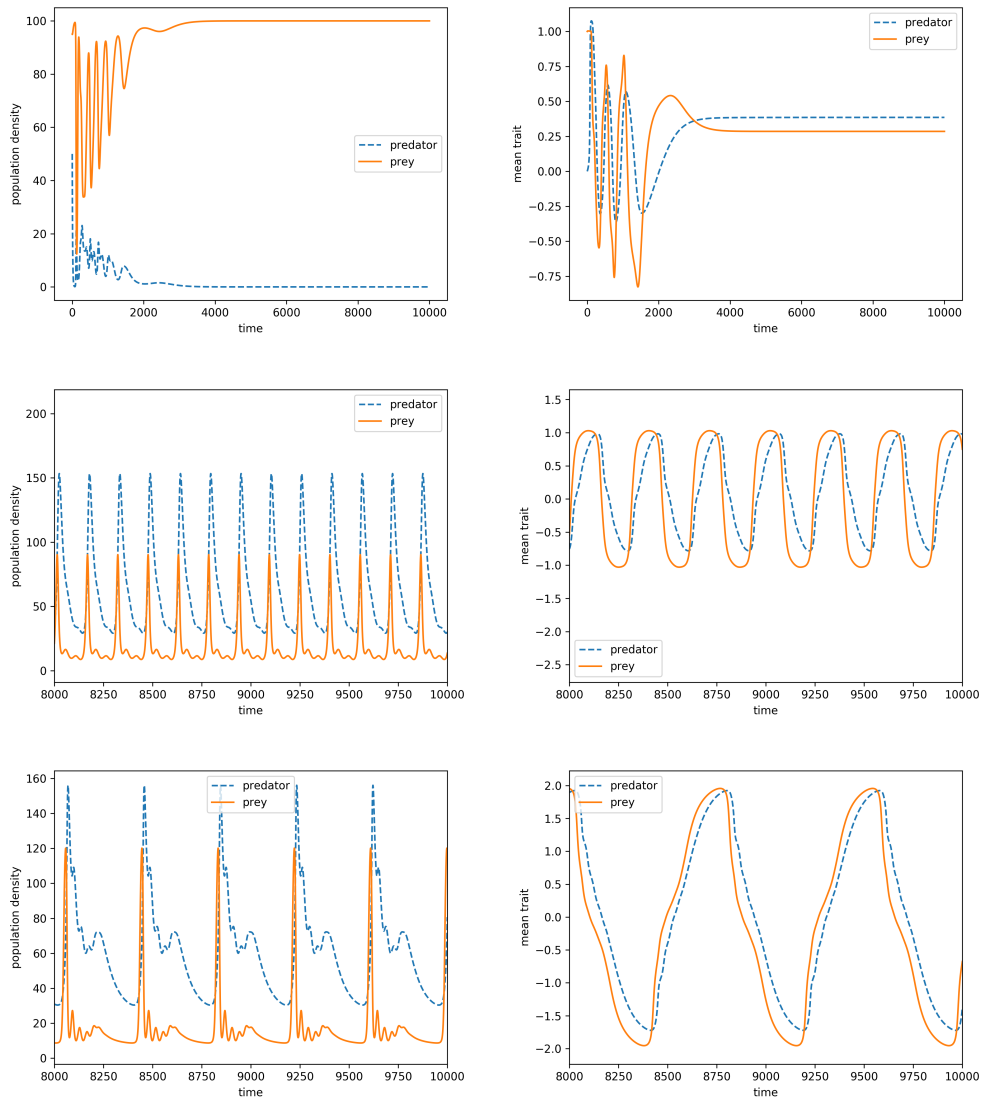


FIGURE 1.7. **Timeseries.** Parameters are identical to those from 1.1, but results were obtained by running the model with evolving variance according to the framework of Tirok et al. [2011].

This study expands our theoretical understanding of predator-prey eco-evolutionary dynamics. In particular, we explored the effects of two types of trait linkage on ecological dynamics and concluded that one must be mindful of the type of stabilizing selection included in theoretical models. In reality, many groups of traits which affect ecological interactions are correlated with varying strengths, and predator and prey species interact in the context of a larger food web. Future studies can potentially expand on this model by considering more complex trait linkage

in the context of multiple prey species, multiple predator species, intraguild predation, or more general multitrophic food webs.

### **1.6. Acknowledgements**

We thank Pablo Chavarria for his assistance, the Pacific Mathematics Alliance and PUMP Program for partially supporting this research (National Science Foundation grant DMS-1247679), and Sebastian Schreiber for his helpful feedback.

## CHAPTER 2

# Sick of Eating: eco-evo-immuno dynamics of predators and their trophically acquired parasites

Posted to *bioRxiv* on May 30, 2020

Joint work with:

**Daniel I. Bolnick**

*Department of Ecology and Evolutionary Biology, University of Connecticut, Mansfield, 06269, Connecticut*

**Sebastian Schreiber**

*Department of Evolution and Ecology, University of California Davis, Davis, 95616, California*

### 2.1. Abstract

When predators consume prey, they risk becoming infected with their prey's parasites, which can then establish the predator as a secondary host. For example, stickleback in northern temperate lakes consume benthic or limnetic prey, which are intermediate hosts for distinct species of parasites (e.g. *Eustrongylides* nematodes in benthic oligochaetes and *Schistocephalus solidus* copepods in limnetic copepods). These worms then establish the stickleback as a secondary host and can cause behavioral changes linked to increased predation by birds. In this study, we use a quantitative genetics framework to consider the simultaneous eco-evolutionary dynamics of predator ecomorphology and predator immunity when alternative prey may confer different parasite exposures. When evolutionary tradeoffs are sufficiently weak, predator ecomorphology and immunity are correlated among populations, potentially generating a negative correlation between parasite intake and infection.

## 2.2. Introduction

Many predators acquire parasites by consuming infected prey [Rogawa et al., 2018, Iritani and Sato, 2018], and community ecologists are increasingly interested in the impact of parasites on communities [Sukhdeo, 2012, Wood and Johnson, 2015, Anderson and Sukhdeo, 2011]. For example, parasites have been shown to alter both food web dynamics and structure [Lafferty et al., 2006, van Velzen and Gaedke, 2017, Cortez and Weitz, 2014]. Conversely, a host’s position within the food web may affect parasite infection rates. After a parasite passes through this ‘encounter filter,’ it must then pass through a ‘compatibility filter’ by establishing an infection despite the host’s immune response. Therefore, to understand the role of parasitism within an ecological community we must consider both the host diet (encounters) and host immunity (compatibility).

Trait evolution modifies predator-prey interactions in ways that can change their population dynamics, coexistence, and food web structure. For instance, Yoshida et al. [2003] found that prey evolution can affect the period and phase difference in predator-prey cycles, and Becks et al. [2010] found that the amount of heritable variation in a prey defense trait can shift dynamics between equilibrium and oscillatory states. These changes in predator diet or foraging rates will entail consequent changes in exposure rates to trophically-transmitted parasites.

Parasite exposure risk can differ between ecologically divergent consumer individuals or populations. A well-known example is the threespine stickleback (*Gasterosteus aculeatus*), a small fish found in north temperate coastal habitats. Stickleback populations in different lakes typically specialize on eating the local abundant prey and evolve functional morphology to suit this niche [Lavin and McPhail, 1985, 1986]. In lakes with multiple abundant prey, the population as a whole is a generalist but individual stickleback differ in trophic morphology (e.g. jaw shape, gill rake length) and use correspondingly different subsets of the available resources [Snowberg et al., 2015]. Because of the complex lifecycle of the trophically-transmitted cestodes and nematodes that infect stickleback, only individuals who consume particular prey are at risk of infection by those parasites. The cestode *Schistocephalus solidus* uses cyclopoid copepods as a first host, which are eaten by stickleback in open water (limnetic habitat). In contrast, the nematode *Eustrongylides sp.* uses benthic-dwelling oligochaete worms as their primary host. As a result, stickleback morphology and diet should be correlated with parasite intake rates: individuals consuming more limnetic copepods

should have higher *S. solidus* infection rates. This expectation has been confirmed within each of many populations showing correlations between individuals' ecomorphology and infection status [Stutz et al., 2014]. These associations between ecomorphology, diet, and infection risk have also been found in coastal California sea otters [Johnson et al., 2009, Estes et al., 2003, Tinker et al., 2008], cichlids [Hayward et al., 2017], and barbs [Sibbing et al., 1998].

One might expect this correlation between stickleback ecomorphology and infection risk to hold not only within populations, but also among populations. However, Stutz et al. [2014] found that nematode prevalence was lowest in populations where we would a priori expect it to be highest (where fish consume more benthic prey). Stutz et al. [2014] suggested that correlated evolution of diet and immunity might be the cause of this negative correlation. And, since these cestodes and nematodes come from different prey and are phylogenetically distant parasites, it seems possible that immunity to infection might need to be specialized to one or the other. Motivated by this unexpected negative correlation, we seek to address three questions.

*First, under what conditions is there a reciprocal feedback between niche and immune evolution? If these conditions do not hold, when does the evolution of the predator's trophic niche determine the evolution of its immune system, or vice versa?* Environmental conditions may dictate the relative availability of alternative prey, which in turn generates selection on the predator's foraging morphology. The subsequent eco-evolutionary feedbacks involve coupled changes in species abundances and predator traits. Changes in both prey availability and predator efficiency will alter the predator's diet and thus change its exposure to parasites, which will likely drive evolution of the predator's immune system to resist whichever parasites represent the greatest risk. On the other hand, the evolution of a predator's immune trait can reduce the harmful effects of parasites, enabling niche expansion or a niche shift onto a formerly hazardous prey. Trophic traits may then subsequently evolve to optimize attack efficiency on this new diet. When do these effects create a feedback loop and cause multivariate-trait evolutionary cycles?

*Second, how are trophic and immune trait values correlated?* Even if traits are genetically independent, their selection pressures may not be. The predator's immune trait may affect the

selection pressure on morphology, and vice versa. The joint evolution of traits may lead to correlations between diet and immunity either because habitat differences favor bivariate outcomes or because populations are at different phases of some cyclical dynamic.

*Third, when does the joint evolution of niche and immune traits, along with predator-prey dynamics, obscure the relationship between parasite exposure risk and actual infection rates?* As hypothesized by Stutz et al. [2014], evolution of predator immune traits may negate or even reverse an expected positive correlation between intake of, and infection by, a particular parasite. Thus, populations frequently exposed to particular parasites may have lower infection rates than populations that are rarely exposed (and hence susceptible) to the few parasites they do encounter.

### 2.3. Models

Let  $P = P(t)$  be the density of a predator population and  $N_i = N_i(t)$  be the densities of prey populations  $i$  for  $i = 1, 2$ . Each prey species experiences logistic growth in the absence of the predator, with intrinsic growth rates  $r_i$  and carrying capacities  $K_i$ . The predator species has a per-capita death rate  $d$ , attacks prey species  $i$  with attack rate  $a_i$ , and converts food into offspring with efficiency  $b_i$ .

A percentage  $c_i$  of prey  $i$  individuals are infected with parasite  $i$  that decreases predator fecundity by  $m_i S_i$ , where  $m_i$  is the maximal negative effect of parasite  $i$  and  $S_i \leq 1$  is a measure of predator susceptibility to parasite  $i$ . Low  $S_i$  corresponds to a strong immunity to parasite  $i$ . Then the ecological dynamics are given by

$$\begin{aligned} \frac{dP}{dt} &= P \left[ (b_1 - c_1 m_1 S_1) a_1 N_1 + (b_2 - c_2 m_2 S_2) a_2 N_2 - d \right], \\ \frac{dN_i}{dt} &= N_i \left[ r_i \left( 1 - \frac{N_i}{K_i} \right) - a_i P \right], \quad i = 1, 2 \end{aligned}$$

The attack rate of the predator on prey  $i$  is determined by a quantitative trait  $x$ . Attack rate of prey species  $i$  is maximal when  $x = \theta_i$ , where  $\theta_i$  is the optimum trait to consume prey  $i$ , and decreases in a Gaussian manner as  $|x - \theta_i|$  increases (as in Schreiber et al. [2011]). Specifically, the attack rate  $a_i(x)$  on prey  $i$  equals

$$a_i(x) = \alpha_i \exp \left[ -\frac{(x - \theta_i)^2}{2\zeta_i^2} \right]$$

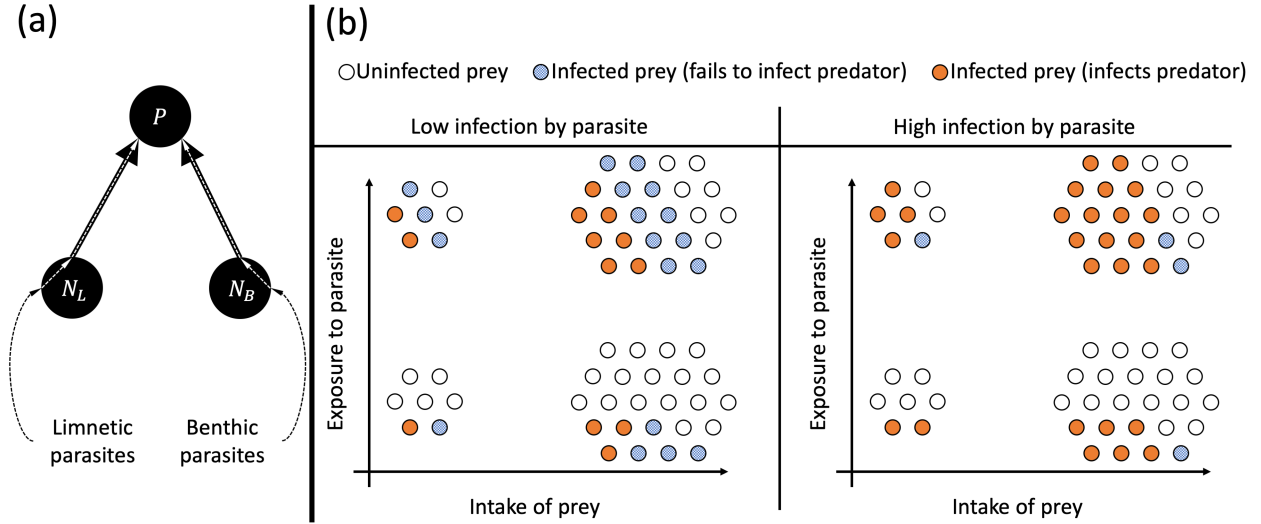


FIGURE 2.1. (a) Schematic of the model. The predator is exposed to limnetic and benthic parasites via intake of limnetic and benthic prey. The proportion of prey infected by parasites stays constant. The predator average morphology  $\bar{x}$  and average immune response  $\bar{y}$  evolves in response to selection pressures caused by prey availability and parasite infection. (b) Intake of prey  $i$  ( $\bar{a}_i(\bar{x})N_i$ ) describes total intake of both infected and uninfected prey. Exposure to parasite  $i$  ( $\bar{a}_iN_ic_i$ ) describes total intake of parasites (a constant proportion  $c_i$  of prey  $i$  are infected with parasites). Infection by parasite  $i$  ( $\bar{a}_iN_ic_i\bar{S}_i(\bar{y})$ ) describes the total number of ingested parasites which successfully infect the predator (a proportion  $\bar{S}_i(\bar{y})$  of ingested parasites infect the predator).

where  $\alpha_i$  is the maximal successful attack rate on prey  $i$ , and  $\zeta_i$  is the width of the attack rate function. The smaller  $\zeta_i$ , the more phenotypically specialized a predator must be to use prey  $i$ . Thus, predator populations with greater  $\zeta_i$  values experience less pressure to evolve morphological specialization.

The susceptibility of the predator to infection by parasite  $i$  is determined by a quantitative trait  $y$ . Susceptibility is minimized when  $y = \phi_i$ , where  $\phi_i$  is the optimum trait to resist parasite  $i$ , and increases in a Gaussian manner as  $|y - \phi_i|$  increases. Specifically, the susceptibility  $S_i(y)$  to parasite  $i$  equals

$$S_i(y) = \beta_i - (\beta_i - \gamma_i) \exp \left[ -\frac{(y - \phi_i)^2}{2\tau_i^2} \right]$$

where  $\beta_i \leq 1$  and  $\gamma_i < \beta_i$  are the maximum and minimum susceptibility to parasite  $i$ , respectively, and  $\tau_i$  is the width of the immunity function. The smaller  $\tau_i$ , the more immunologically specialized

a predator must be to significantly reduce susceptibility to infection by parasite  $i$ . Thus, predator populations with greater  $\tau_i$  values experience less pressure to evolve immunological specialization. We have in mind a model of constitutively expressed innate immunity rather than adaptive immunity that is induced and grows following initial exposure.

The per-capita growth rate  $W$  (fitness) of a predator with ecomorphology  $x$  and immunity  $y$  is given by

$$W(x, y, P, N_1, N_2) = (b_1 - c_1 m_1 S_1(y)) a_1(x) N_1 + (b_2 - c_2 m_2 S_2(y)) a_2(x) N_2 - d$$

and the per-capita growth rate  $Y_i$  of prey interacting with predators with ecomorphology  $x$  is given by

$$Y_i(x, P, N_1, N_2) = r_i \left( 1 - \frac{N_i}{K_i} \right) - a_i(x) P, \quad i = 1, 2.$$

We assume the predator traits  $x$  and  $y$  are genetically independent and normally distributed over the population with means  $\bar{x}$  and  $\bar{y}$ , respectively. Let  $p_x(x, \bar{x})$  and  $p_y(y, \bar{y})$  denote these distributions:

$$p_x(x, \bar{x}) = \frac{1}{\sqrt{2\pi\sigma_x^2}} \exp \left[ -\frac{(x - \bar{x})^2}{2\sigma_x^2} \right], \quad p_y(y, \bar{y}) = \frac{1}{\sqrt{2\pi\sigma_y^2}} \exp \left[ -\frac{(y - \bar{y})^2}{2\sigma_y^2} \right],$$

where  $\sigma_x^2$  and  $\sigma_y^2$  are the total phenotypic variances of traits  $x$  and  $y$ , respectively. Let  $\sigma_x^2 = \sigma_{x,G}^2 + \sigma_{x,E}^2$ , where  $\sigma_{x,G}^2$  is the phenotypic variation of trait  $x$  due to genotype and  $\sigma_{x,E}^2$  is the phenotypic variation of trait  $x$  due to environmental conditions. Similarly, let  $\sigma_y^2 = \sigma_{y,G}^2 + \sigma_{y,E}^2$ . Here, we omit genetic-by-environmental interactions for mathematical simplicity, though these are common for both trophic and immunological traits. Note that the environmental variance component is not adaptive plasticity (e.g. not directionally dictated by prey availability or parasite exposure experience).

Integrating across the predator distribution of phenotypes, the average per-capita growth rate of the predator population  $\bar{W}$  equals

$$\begin{aligned} \bar{W}(\bar{x}, \bar{y}, P, N_1, N_2) &= \iint W(x, y, P, N_1, N_2) p_x(x, \bar{x}) p_y(y, \bar{y}) dx dy \\ &= (b_1 - c_1 m_1 \bar{S}_1(\bar{y})) \bar{a}_1(\bar{x}) N_1 + (b_2 - c_2 m_2 \bar{S}_2(\bar{y})) \bar{a}_2(\bar{x}) N_2 - d, \end{aligned}$$

where  $\bar{a}_i$  and  $\bar{S}_i$  are the averaged attack rate and susceptibility:

$$\bar{a}_i(\bar{x}) = \int a_i(x)p_x(x, \bar{x})dx = \frac{\alpha_i \zeta_i}{\sqrt{\sigma_x^2 + \zeta_i^2}} \exp \left[ -\frac{(\bar{x} - \theta_i)^2}{2(\sigma_x^2 + \zeta_i^2)} \right], \quad i = 1, 2,$$

$$\bar{S}_i(\bar{y}) = \int S_i(y)p_y(y, \bar{y})dy = \beta_i - (\beta_i - \gamma_i) \frac{\tau_i}{\sqrt{\sigma_y^2 + \tau_i^2}} \exp \left[ -\frac{(\bar{y} - \phi_i)^2}{2(\sigma_y^2 + \tau_i^2)} \right], \quad i = 1, 2.$$

The average per-capita growth rate  $\bar{Y}_i$  of the prey  $i$  population is given by

$$\bar{Y}_i(\bar{x}, P, N_1, N_2) = \int Y_i(x, P, N_1, N_2)p_x(x, \bar{x})dx = r_i \left( 1 - \frac{N_i}{K_i} \right) - \bar{a}_i(\bar{x})N_i, \quad i = 1, 2.$$

These functions describe the ecological dynamics:

$$(3.1a) \quad \begin{aligned} \frac{dP}{dt} &= P\bar{W}(\bar{x}, \bar{y}, P, N_1, N_2), \\ \frac{dN_i}{dt} &= N_i\bar{Y}_i(\bar{x}, P, N_1, N_2), \quad i = 1, 2. \end{aligned}$$

See Appendix B.1 for additional details regarding the model formulation.

Provided the predator trait distributions  $p_x$  and  $p_y$  stay normal with constant variance over time, Lande [1976] showed that the rates of change of the average traits are proportional to the derivative of the average fitness  $\bar{W}$  with respect to that trait. The constants of proportionality are the portions of phenotypic variance due to genetic variation. We assume the morphological and immunological traits are genetically independent, and thus the evolutionary dynamics of  $\bar{x}$  and  $\bar{y}$  are given by:

$$(3.1b) \quad \begin{aligned} \frac{d\bar{x}}{dt} &= \sigma_{x,G}^2 \frac{\partial \bar{W}}{\partial \bar{x}} \\ \frac{d\bar{y}}{dt} &= \sigma_{y,G}^2 \frac{\partial \bar{W}}{\partial \bar{y}} \end{aligned}$$

where

$$\begin{aligned} \frac{\partial \bar{W}}{\partial \bar{x}} &= (b_1 - m_1 c_1 \bar{S}_1(\bar{y})) \bar{a}_1(\bar{x}) N_1 \frac{\theta_1 - \bar{x}}{\sigma_x^2 + \zeta_1^2} + (b_2 - m_2 c_2 \bar{S}_2(\bar{y})) \bar{a}_2(\bar{x}) N_2 \frac{\theta_2 - \bar{x}}{\sigma_x^2 + \zeta_2^2}, \\ \frac{\partial \bar{W}}{\partial \bar{y}} &= m_1 c_1 \bar{a}_1(\bar{x}) N_1 (\beta_1 - \bar{S}_1(\bar{y})) \frac{\phi_1 - \bar{y}}{\sigma_y^2 + \tau_1^2} + m_2 c_2 \bar{a}_2(\bar{x}) N_2 (\beta_2 - \bar{S}_2(\bar{y})) \frac{\phi_2 - \bar{y}}{\sigma_y^2 + \tau_2^2}. \end{aligned}$$

## 2.4. Methods

We use four numerical and analytical approaches to explore the three questions posed in the introduction: (i) numerical simulations of population and evolutionary dynamics, (ii) analytical results obtained in the limit of slow evolution (low heritability) and timescale differences between the evolution of the two traits, (iii) Latin hypercube sampling across parameter space to analyze the effect of model parameters on simulation outcomes, and (iv) numerical approximations of Lyapunov exponents to determine conditions for stable or chaotic dynamical behavior.

**Numerical Simulations.** We used standard numerical integration techniques (Runge-Kutta 4(5) with adaptive step size using Python’s `scipy.integrate.odeint` [Jones et al., 2001–]) to simulate the models (3.1a,3.1b) and (2.2). Parameters are given in Appendix B.2.

Lyapunov exponents describe how nearby trajectories behave in relation to a reference trajectory [Sprott, 2003]. Given an initial condition, a positive (negative) Lyapunov exponent means that nearby trajectories on average move away from (towards) the reference trajectory, indicating chaos (stability) (Appendix B.3). We calculated Lyapunov exponents for full-model simulations over a two-dimensional subset of parameter space ( $\sigma_{y,G}$  vs.  $\tau$ ) to determine how the evolution of the immune trait  $\bar{y}$  affects the eco-evolutionary dynamics.

**Analytic Reductions for Slow Evolution Dynamics.** When the trait dynamics evolve at a sufficiently slower time scale than ecological dynamics, we can reduce the five-dimensional system to a two-dimensional system. This occurs, for example, if ecomorphological and immunity traits are only marginally heritable (small  $\sigma_{x,G}^2/\sigma_x^2$  and  $\sigma_{y,G}^2/\sigma_y^2$ ). Then  $\bar{x}$  and  $\bar{y}$  are effectively constant with respect to the changing population densities  $P$  and  $N_i$ ,  $i = 1, 2$ . In which case, the population dynamics of the fast ecological system converges to a unique globally stable attractor with a time-averaged ecological state  $(P^*(\bar{x}, \bar{y}), N_1^*(\bar{x}, \bar{y}), N_2^*(\bar{x}, \bar{y}))$  equal to the coexistence equilibrium  $P^*(\bar{x}, \bar{y}) > 0, N_1^*(\bar{x}, \bar{y}) > 0, N_2^*(\bar{x}, \bar{y}) > 0$  (Appendix B.4). Thus, on the evolutionary timescale, the

trait dynamics are

$$(2.2) \quad \begin{aligned} \frac{d\bar{x}}{dt} &= \sigma_{x,G}^2 \left[ (b_1 - m_1 c_1 \bar{S}_1(\bar{y})) \bar{a}_1(\bar{x}) N_1^*(\bar{x}, \bar{y}) \frac{\theta_1 - \bar{x}}{\sigma_x^2 + \zeta_1^2} \right. \\ &\quad \left. + (b_2 - m_2 c_2 \bar{S}_2(\bar{y})) \bar{a}_2(\bar{x}) N_2^*(\bar{x}, \bar{y}) \frac{\theta_2 - \bar{x}}{\sigma_x^2 + \zeta_2^2} \right], \\ \frac{d\bar{y}}{dt} &= \sigma_{y,G}^2 \left[ m_1 c_1 \bar{a}_1(\bar{x}) N_1^*(\bar{x}, \bar{y}) (\beta_1 - \bar{S}_1(\bar{y})) \frac{\phi_1 - \bar{y}}{\sigma_y^2 + \tau_1^2} \right. \\ &\quad \left. + m_2 c_2 \bar{a}_2(\bar{x}) N_2^*(\bar{x}, \bar{y}) (\beta_2 - \bar{S}_2(\bar{y})) \frac{\phi_2 - \bar{y}}{\sigma_y^2 + \tau_2^2} \right]. \end{aligned}$$

For the reduced system (2.2), we calculate nullclines, stable and unstable equilibria, and separatrices across a range of foraging trade-offs.

Beyond the separation of timescale between ecological and evolutionary dynamics, the niche and immune traits can themselves evolve on different timescales. As the two traits are genetically independent, one trait may evolve on a slower timescale than the other if the two traits differ significantly in their genotypic variance or their selection pressure. These differences can arise in three ways, as discussed in the Results section.

**Latin Hypercube Sampling.** Using the equilibria of the slow-evolution model (2.2), we calculated the relative intake rates of the two prey types  $\bar{a}_i(\bar{x})N_i / \sum_{k=1}^2 \bar{a}_k(\bar{x})N_k$ , ( $i = 1, 2$ ), the relative exposure rates to the two parasite types  $\bar{a}_i(\bar{x})N_i c_i / \sum_{k=1}^2 \bar{a}_k(\bar{x})N_k c_k$ , ( $i = 1, 2$ ), as well as the relative parasite infection rates (Figure 2.1b) of the two parasite types  $\bar{a}_i(\bar{x})N_i c_i \bar{S}_i(\bar{y}) / \sum_{k=1}^2 \bar{a}_k(\bar{x})N_k c_k \bar{S}_k(\bar{y})$ , ( $i = 1, 2$ ) over a two-dimensional range of foraging tradeoffs ( $\zeta_i$ ) and immune tradeoffs ( $\tau_i$ ). For each tradeoff pair, we ran 4,000 simulations using Latin hypercube sampling, varying lake size (e.g.  $K_1/K_2$ ), maximal attack rates ( $\alpha_1, \alpha_2$ ), parasite frequency in prey ( $c_1, c_2$ ), parasitic effects on stickleback ( $m_1, m_2$ ), prey growth rates ( $r_1, r_2$ ), and initial stickleback ecomorphology and immunity ( $\bar{x}_0, \bar{y}_0$ ). For each set of parameter values, we ran the two-timescale model (2.2) until  $\bar{x}$  and  $\bar{y}$  reached an evolutionary equilibrium and calculated the relative intake, exposure, and infection rates. We then plotted the results to gain insight about the joint evolution of niche and immune traits and how their evolution affects the relationship between diet, parasite exposure, and infection.

## 2.5. Results

We first present results of the slow-evolution models to address how the evolution of niche affects the evolution of immunity and vice versa. We then present the Latin hypercube sampling results to address how the two traits are correlated across populations, as well as how that correlation affects the relationship between diet and infection across populations. We conclude with a “within populations” perspective by using the full single-timescale five-dimensional model to examine temporal correlations in traits and diet and infection rates for systems with cyclic or chaotic dynamics.

**Three-timescale dynamics.** For a given immune state  $\bar{y}$ , the average predator fitness  $\bar{W}$  is unimodal with respect to the foraging trait  $\bar{x}$  if

$$(2.3) \quad |\theta_1 - \theta_2| < 2\sqrt{\sigma_x^2 + \zeta^2},$$

where  $\zeta := \zeta_1 = \zeta_2$  [Schreiber et al., 2011, Schreiber and Patel, 2015]. Namely, if foraging tradeoffs are weak relative to the phenotypic variation in foraging, then there is a single fitness maximum with respect to  $\bar{x}$ . When the contributions of the two prey populations to predator fitness are equal (i.e.  $(b_1 - c_1 m_1 \bar{S}_1(\bar{y})) \bar{a}_1 N_1 = (b_2 - c_2 m_2 \bar{S}_2(\bar{y})) \bar{a}_2 N_2$ ), condition (2.3) is necessary and sufficient, but when prey contributions to predator fitness are unequal, predator fitness may be unimodal with respect to  $\bar{x}$  even if (2.3) does not hold.

Similarly, for a given foraging trait  $\bar{x}$ ,  $\bar{W}$  is unimodal with respect to the immune trait  $\bar{y}$  if the immune tradeoff is weak relative to the phenotypic variance in immunity, i.e.

$$(2.4) \quad |\phi_1 - \phi_2| < 2\sqrt{\sigma_y^2 + \tau^2},$$

where  $\tau := \tau_1 = \tau_2$  (Appendix B.5). This condition is necessary and sufficient only when the difference between the effects of parasites infecting predators maximally and minimally susceptible to those parasites is symmetric (i.e.  $m_1 c_1 (\beta_1 - \gamma_1) \bar{a}_1(\bar{x}) N_1 = m_2 c_2 (\beta_2 - \gamma_2) \bar{a}_2(\bar{x}) N_2$ ). Again, if these differences are unequal,  $\bar{W}$  may still be unimodal with respect to  $\bar{y}$  even if (2.4) does not hold.

There are three ways in which the predator traits may evolve at different timescales. First, all else being equal, the trait with a higher genotypic variance evolves more quickly than the other (Figure 2.2a,b,d,e,g,h,j,k). Second, if the parasite is rare or has a weak effect on the predator,

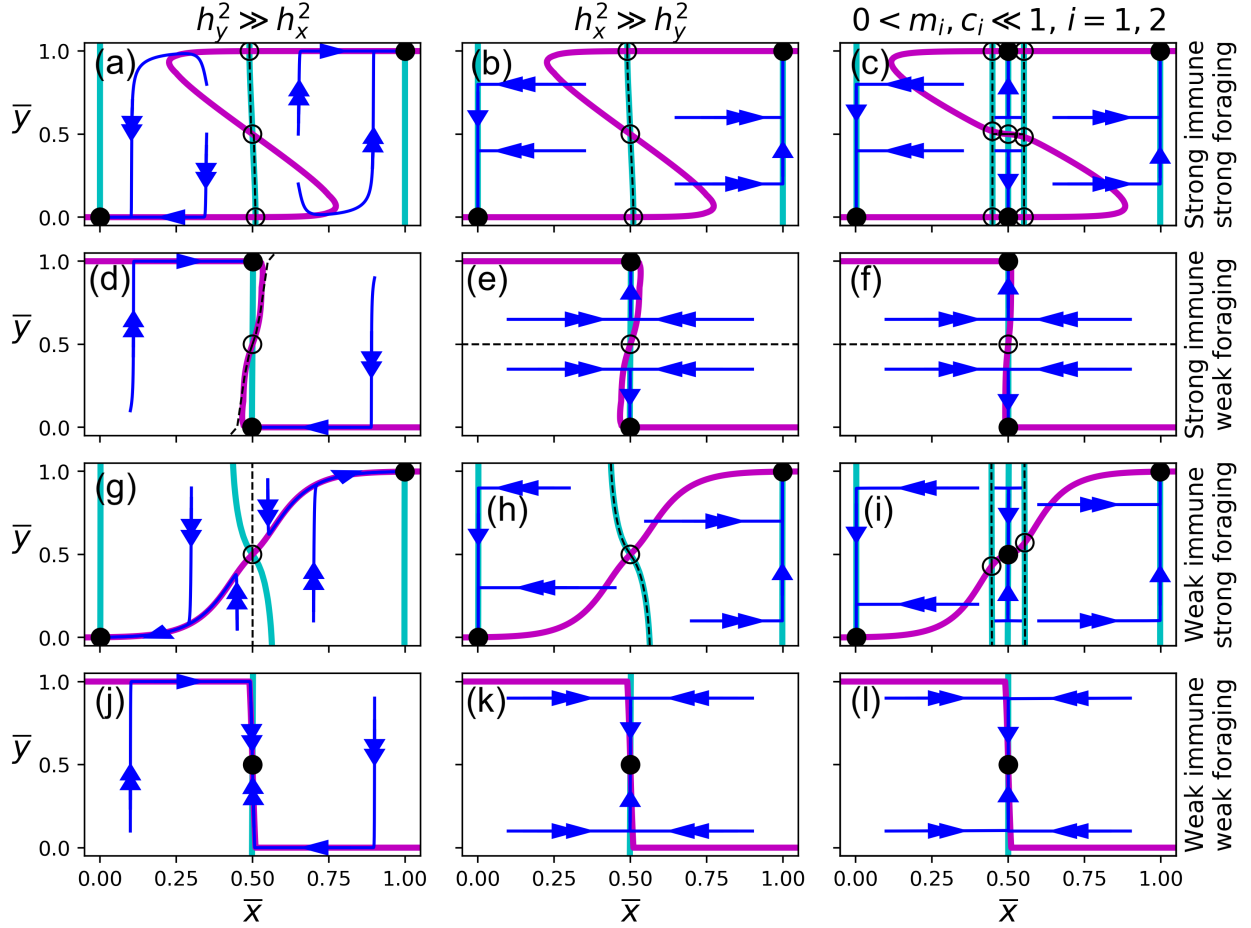


FIGURE 2.2. Nullclines, stable and unstable equilibria, separatrices, and evolutionary dynamics of (2.2). The cyan and pink curves denote the  $\bar{x}$ - and  $\bar{y}$ -nullclines, respectively. Filled-in and hollow circles indicate stable and unstable evolutionary equilibria, respectively. Blue lines are sample trajectories, and dashed lines indicate separatrices between stable equilibria (as well as the stable manifolds of the saddles). In (a), (d), (g), and (j),  $\sigma_{x,G} = 0.005$  and  $\sigma_{y,G} = 0.25$ . In (b), (e), (h), and (k),  $\sigma_{x,G} = 0.25$  and  $\sigma_{y,G} = 0.005$ . In (c), (f), (i), and (l),  $m_i = c_i = 0.1$  for  $i = 1, 2$ . In (a)-(f) immune tradeoffs are strong ( $\tau_i = 0.01$ ), and in (g)-(l) immune tradeoffs are weak ( $\tau_i = 1$ ). In the (a)-(c) and (g)-(i) foraging tradeoffs are strong ( $\zeta_i = 0.01$ ) and in (d)-(f) and (j)-(l) foraging tradeoffs are weak ( $\zeta_i = 1$ ).

then selection pressure on the immune trait  $\bar{y}$  is weak and therefore evolves much slower than the foraging trait  $\bar{x}$  (Figure 2.2c,f,i,l). Third, weak tradeoffs in either trait result in weak selection pressure on that trait. In particular, large  $\zeta_i$  corresponds to slower  $\bar{x}$  evolution (Figure 2.2d-f,j-l), and large  $\tau_i$  corresponds to slower  $\bar{y}$  evolution (Figure 2.2a-c,g-i).

Figure 2.2 shows the evolutionary dynamics of (2.2) for a variety of scenarios. It also highlights three major asymmetries of the foraging and immune traits in the context of three-timescale dynamics: (i) the relationship between trait tradeoff and equilibrium location, (ii) the relationship between initial and final evolutionary state, and (iii) the directionality of trait evolution.

Predators evolve generalist foraging strategies if the foraging tradeoff is weak, regardless of the immune tradeoff (Figure 2.2d-f,j-l). In contrast, predators evolve generalist immune strategies if the immune tradeoff is weak, but only when the predator already has a generalist foraging strategy (Figure 2.2i-l). The immune tradeoff needs to be very weak (in relation to the foraging tradeoff) in order to have the same effect as the foraging tradeoff.

The final foraging state is generally determined by the initial foraging state, regardless of the strengths of trait tradeoffs. In contrast, the final immune state depends on both initial foraging and immune states, the strength of the trait tradeoffs, and ecological parameters such as parasite prevalence and lethality. Graphically, the  $\bar{x}$ -nullclines in Figure (2.2) remain relatively vertical regardless of the strength of the foraging and immune tradeoffs, in contrast to the  $\bar{y}$ -nullclines, which are never only horizontal. Consider for example a specialist predator (in both foraging and immune state) in an environment in which foraging and immune tradeoffs are strong (Figure 2.2a-c). The stabilizing selection at this evolutionary state is strong enough to withstand weakening immune tradeoffs, but not weakening foraging tradeoffs. In fact, if the foraging tradeoff becomes sufficiently weak, the predator will evolve a generalist foraging strategy, and an immune strategy dependent on the environment and the relative heritabilities of the two traits.

As a result of the extreme nature of the  $\bar{x}$ -nullclines, the foraging trait always evolves unidirectionally. On the other hand, because the  $\bar{y}$ -nullclines are not strictly horizontal, the immune state may reverse its evolution when immune heritability is high relative to foraging heritability (Figure 2.2a,g,j). In these scenarios, the immune state evolves quickly toward a stable branch of the  $\bar{y}$ -nullcline, and then both traits evolve along the  $\bar{y}$ -nullcline toward a stable evolutionary equilibrium.

**Two-timescale dynamics.** We used Latin hypercube sampling over a subset of parameter space to understand how the locations of the stable equilibria change as parameters vary (Figure

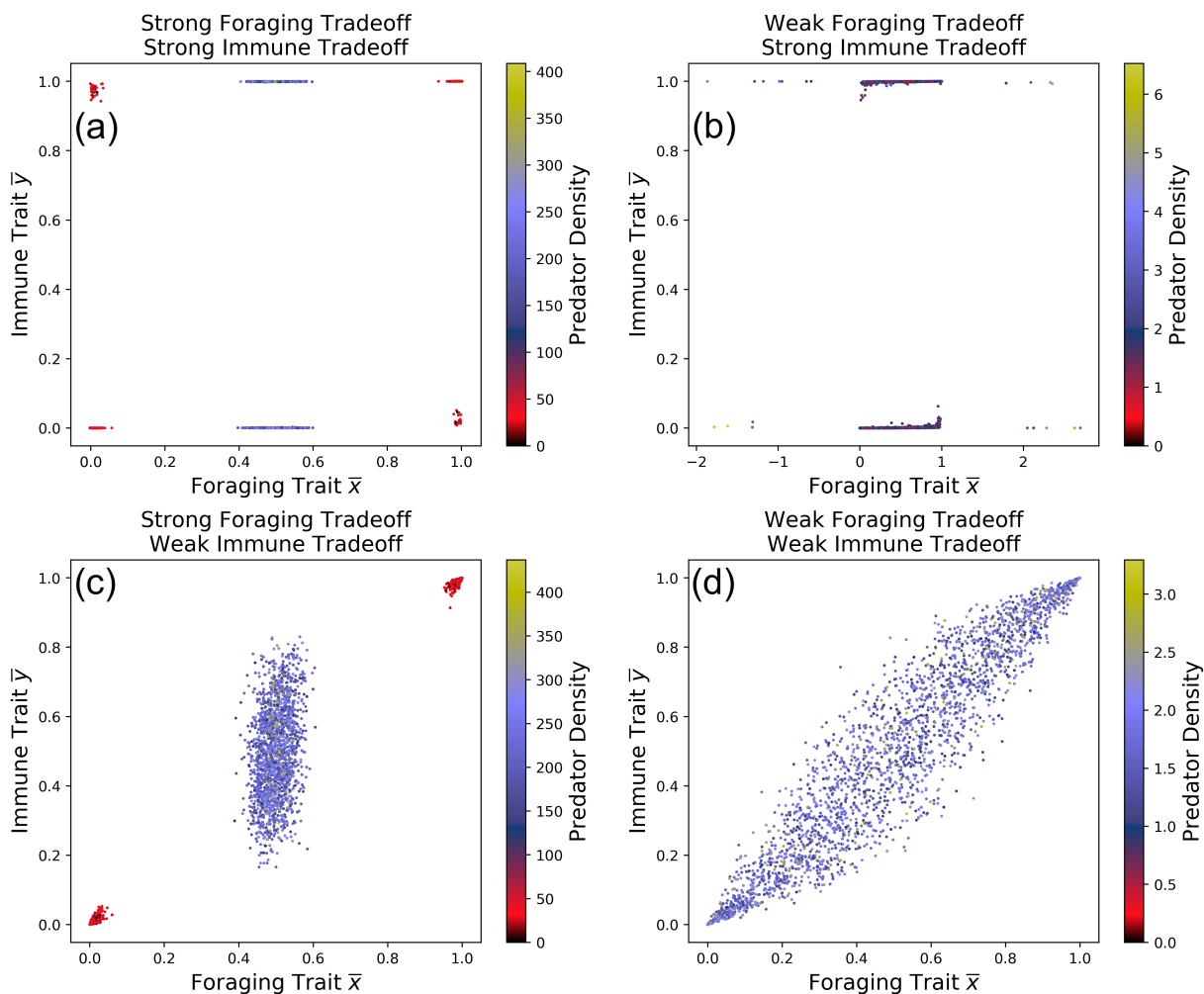


FIGURE 2.3. Locations of stable equilibria for a Latin Hypercube sample of parameter space. In (a) and (b) immune tradeoffs are strong ( $\tau_i = 0.01$ ), and in (c) and (d) immune tradeoffs are weak ( $\tau_i = 1$ ). In (a) and (c), foraging tradeoffs are strong ( $\zeta_i = 0.01$ ) and in (b) and (d) foraging tradeoffs are weak ( $\zeta_i = 1$ ). The color of each dot represents the density of the predator population at the evolutionary equilibrium.

2.3). When both tradeoffs are strong (Figure 2.3a), equilibria congregate near evolutionary specialist states, while when both tradeoffs are weak (Figure 2.3d), the predator is more likely to evolve a generalist foraging and immune strategy. If foraging tradeoffs are weak and immune tradeoffs are strong (Figure 2.3b), predators will typically evolve a generalist foraging strategy and a specialist immune strategy. In contrast, if immune tradeoffs are weak and foraging tradeoffs are strong (Figure 2.3c), then predators may evolve a generalist or specialist foraging strategy, and the immune

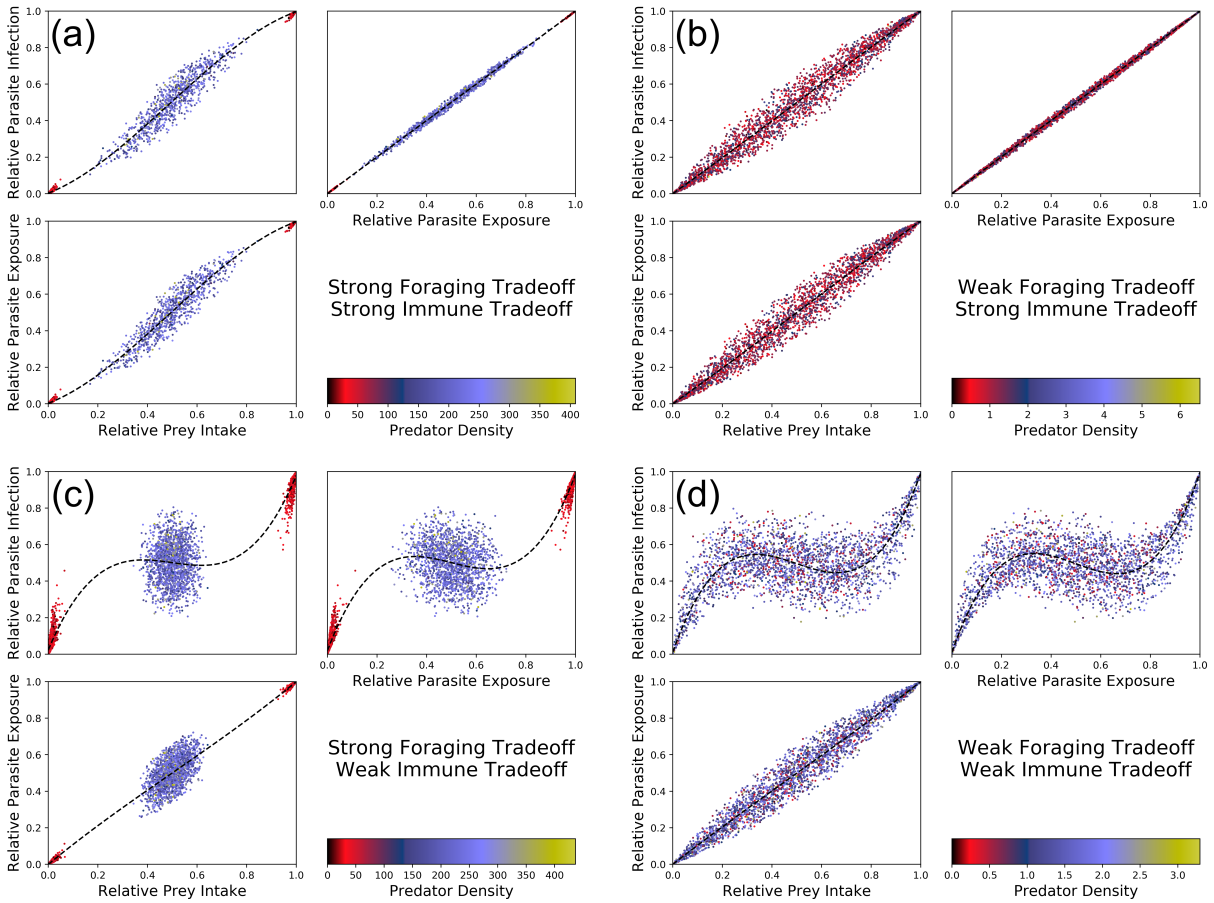


FIGURE 2.4. Prey intake, parasite exposure, and parasite infection over the same subset of parameter space given in Figure 2.3. The dots are colored as in Figure 2.3. The blue lines are splines of the data, included in order to better identify patterns between prey intake, parasite exposure, and parasite infection. In (a) and (b) immune tradeoffs are strong ( $\tau_i = 0.01$ ), and in (c) and (d) immune tradeoffs are weak ( $\tau_i = 1$ ). In (a) and (c), foraging tradeoffs are strong ( $\zeta_i = 0.01$ ) and in (b) and (d) foraging tradeoffs are weak ( $\zeta_i = 1$ ).

strategy will evolve to correspond with the foraging state. We see the same asymmetry as in Figure 2.2: generalist immune traits only evolve for generalist foragers, but generalist foraging traits may evolve regardless of immune state.

We also used the same Latin hypercube sample to understand what causes various correlations between prey intake, parasite exposure, parasite infection across predator populations (Figure 2.4). When immune tradeoffs are strong (Figure 2.4a,b), the relationship between prey intake and parasite infection does not stray far from the one-to-one line. In these scenarios, the proportion of

a predator population's diet consisting of some prey is roughly equal to the proportion of that predator's parasite load consisting of the parasites from that prey. In addition, the majority of the variation in parasite infection is caused by the relationship between prey intake and parasite exposure, and not between exposure and infection. This means that any potential nonlinear pattern between diet and infection is not caused by immune evolution if immune tradeoffs are strong.

When immune tradeoffs are weak (Figure 2.4c,d), the relationship between prey intake and parasite infection differs greatly from the one-to-one line. In these scenarios, the proportion of a predator population's diet consisting of some prey may not predict the proportion of that predator population's parasite load consisting of the parasites from that prey. In contrast to when immune tradeoffs are strong, the majority of the variation in parasite infection *is* caused by the relationship between parasite exposure and parasite infection, indicating that any potential nonlinear pattern between diet and infection is caused by immune evolution if immune tradeoffs are weak.

**Non-equilibrium eco-evolutionary dynamics.** When heritability is high, eco-evolutionary feedbacks lead to greater dynamical complexity, including cyclical and chaotic dynamics. Schreiber et al. [2011] showed niche evolution can induce cycles and chaos in the absence of immune evolution, and we found something similar for immune evolution. Regardless of immune heritability, eco-evolutionary cycles only occur for sufficiently weak immune tradeoffs (Figure 2.5a). When immune heritability is low (Figure 2.5b), chaos occurs for very weak immune tradeoffs, while for higher immune heritability (Figure 2.5c,d), chaos occurs for intermediate and possibly also very weak immune tradeoffs.

A typical chaotic eco-evolutionary trajectory is displayed in Figure 2.6. These dynamics show a positive temporal correlation between foraging and immune traits (Figure 2.6c,d). When the predator foraging trait favors one prey type over the other, its intake almost entirely consists of that prey. The immune trait has higher heritability than that the foraging trait, which is why the immune trait evolves more extreme values than the foraging trait. Once the predator over-consumes a particular prey type and the other recovers, the foraging trait faces directional selection toward the recovering, although there is a lag in the actual intake of that prey. Although it is highly heritable, the immune trait does not favor the parasite of the recovering prey until the foraging trait is near its extreme value.

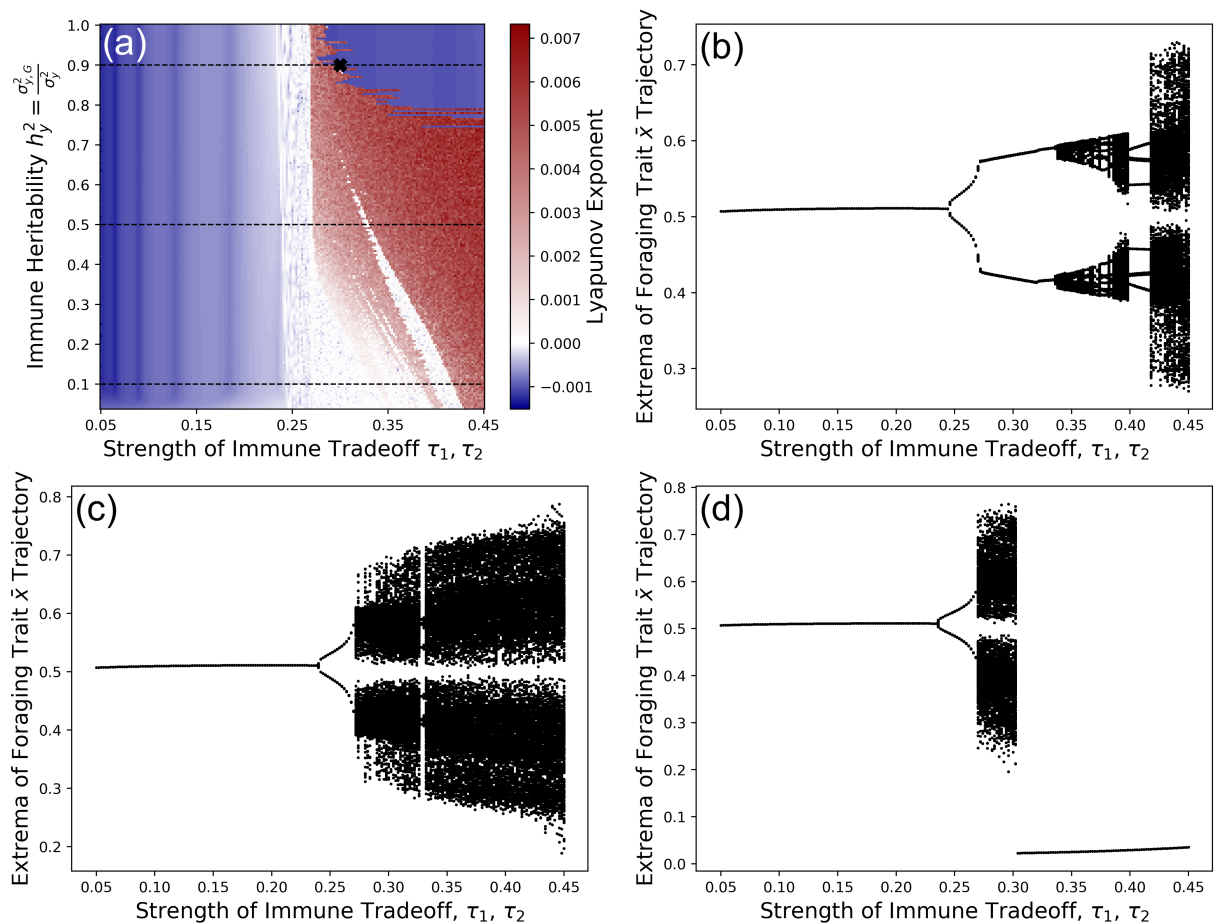


FIGURE 2.5. When immune tradeoffs are sufficiently weak, immune evolution can induce cyclic or chaotic eco-evolutionary dynamics. For weak immune tradeoffs, low heritability is destabilizing, but for intermediate immune tradeoffs, high heritability is destabilizing. (a) The blue regions denote stability (negative Lyapunov exponent) and the red regions denote chaos (positive Lyapunov exponent). (b) Local extrema of the niche trait  $\bar{x}$  along  $0.05 \leq \tau_1 = \tau_2 \leq 0.45$ ,  $h_y^2 = 0.1$ . (c) Local extrema of the niche trait  $\bar{x}$  along  $0.05 \leq \tau_1 = \tau_2 \leq 0.45$ ,  $h_y^2 = 0.5$ . (d) Local extrema of the niche trait  $\bar{x}$  along  $0.05 \leq \tau_1 = \tau_2 \leq 0.45$ ,  $h_y^2 = 0.9$ .

There is also a nonlinear correlation between diet and infection (Figure 2.6b). Because this correlation occurs within a single oscillating population, the intake-exposure relationship is one-to-one. Thus, any nonlinear correlation between diet and infection is entirely caused by the evolving immune trait  $\bar{y}$ .

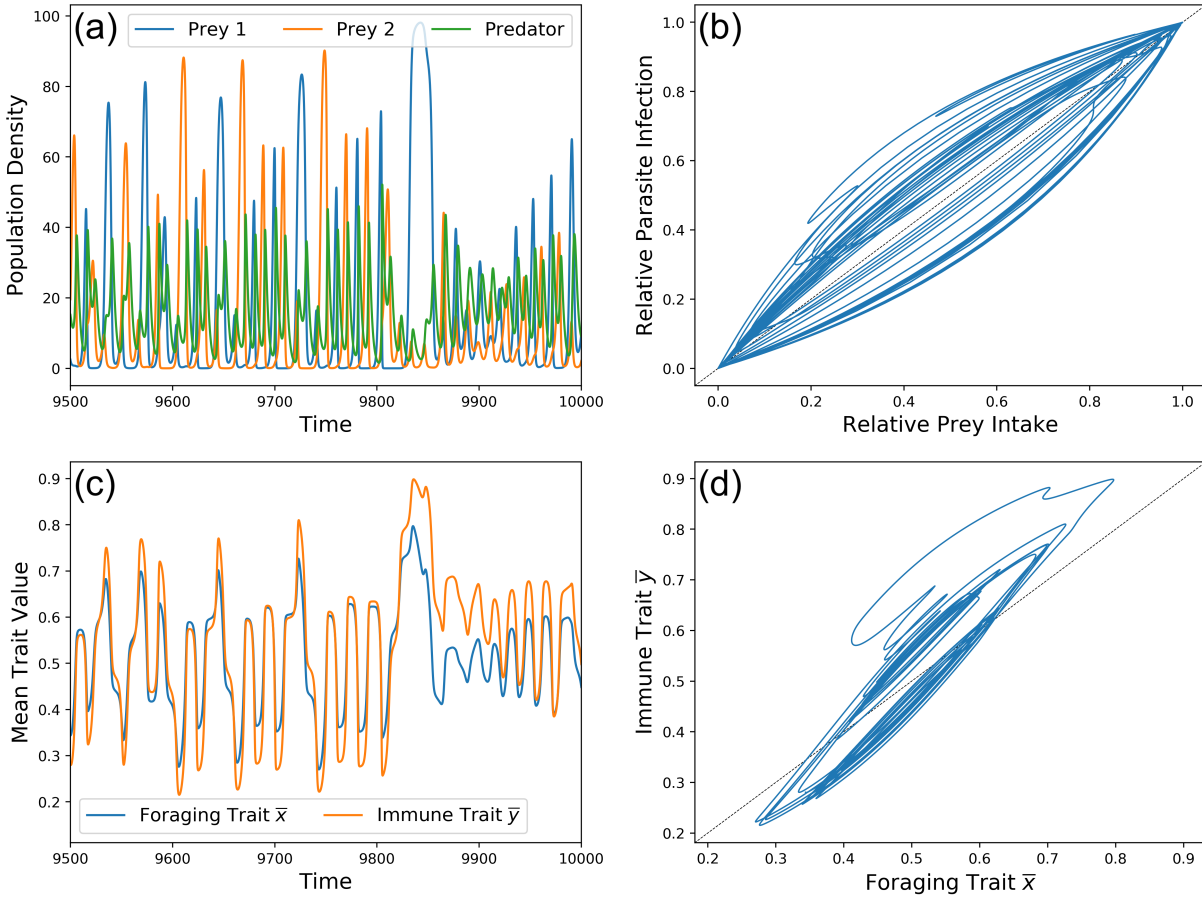


FIGURE 2.6. A chaotic eco-evolutionary trajectory. Parameters are equal to that of Figure 2.5 with  $\tau_1 = \tau_2 = 0.3$  and  $h_y^2 = 0.9$  (bold x in Figure 2.5a). (a) predator and prey densities through time. (b) Predator relative prey intake vs. relative parasite infection. (c) predator foraging and immune traits through time. (d) predator foraging trait vs. immune trait.

## 2.6. Discussion

In this study we addressed three questions: (a) how the evolution of a predator's trophic niche affects evolution of immunity to trophically transmitted parasites, and vice-versa, (b) how these traits are correlated across populations and within a single population undergoing eco-evolutionary oscillations, and (c) how the dual evolution of niche and immunity can affect the correlation between intake of and infection by parasites among populations and within a single population undergoing eco-evolutionary oscillations.

For (a), we found that even when the predator's immune state evolves faster than its niche (due to high immune heritability and low ecomorphology heritability), immune evolution does not determine niche. On the other hand, niche evolution often determines the predator's immune state, regardless of the relative speeds of evolution. Indeed, a fast-evolving immune state may reverse its evolution in response to a shifting niche, but the niche does not respond in kind to a shifting immunity.

The asymmetry between niche and immunity extends beyond the question of which trait determines the other. When niche tradeoffs are weak and immune tradeoffs are strong, the predator maintains a generalist foraging ecomorphology even though its immunity is specialized against one parasite or the other. This is true even if the parasites are abundant and detrimental to the predator's fitness. On the other hand, when niche tradeoffs are strong and immune tradeoffs are weak, the predator evolves a specialist foraging ecomorphology along with a specialist immunity against the parasites it encounters. In short, there is little fitness benefit in maintaining an immunity to a parasite rarely encountered, but there is significant benefit to maintaining a morphology suitable to consume multiple prey even when they contain parasites that confer significant fitness drawbacks.

When eco-evolutionary dynamics occur on commensurate timescales, our numerical results suggest that oscillations do not occur when immunological tradeoffs are sufficiently strong. Theory predicts evolutionary destabilization occurs more commonly when there is a tradeoffs between capturing different prey phenotypes [Abrams and Matsuda, 1997a,b, Abrams, 2000], but we find that there is a limit to this effect; if tradeoffs are too strong, all evolutionary oscillations are suppressed.

For (b) and (c), our Latin hypercube sampling results showed no correlation between trophic and immune traits when immune tradeoffs are strong. With these strong tradeoffs, predators always evolve a specialized immunity regardless of their ecomorphology. In contrast, when immune tradeoffs are weak, predators evolve an immunity to suit their niche. Here, the strength of foraging tradeoffs determine the correlation; if foraging tradeoffs are strong, then predators evolve to only a few morphological states, whereas if foraging tradeoffs are weak, then predators may evolve anywhere along the ecomorphology spectrum.

Because predators only evolve immunity to suit their niche if immune tradeoffs are weak, negative correlations between parasite intake and infection are only possible with weak immune tradeoffs. The negative correlation between intake and infection is more pronounced when there is more morphological diversity across populations, and thus is most likely to be observed if foraging tradeoffs are also weak. These results, when compared to the empirical data of Stutz et al. [2014], suggest that evolutionary trade-offs in stickleback niche (benthic or limnetic prey) and immune traits (benthic or limnetic parasite) are likely to be weak. This aligns with other studies which have shown that many stickleback populations have evolved a generalist morphology when both limnetic and benthic prey are present [Schluter and McPhail, 1992, Lavin and McPhail, 1985, Matthews et al., 2010, Snowberg et al., 2015].

We also found a nonlinear correlation between intake and infection within a single population oscillating in time. Because of the assumption that parasite abundance stays constant, this correlation is caused entirely by the evolution of immunity. Our simulations did not produce a negative correlation between intake and infection within a single oscillating population. However, the nonlinear correlation suggests that the negative correlation between diet and infection across populations observed by Stutz et al. [2014] may have resulted from oscillating populations in similar habitats rather than equilibrated populations in different habitats. However, because ecological variation among lakes is correlated with lake size (larger lakes containing more limnetic-feeding populations), this is unlikely to be the case.

It is well known that stickleback face biomechanical trade-offs that limit their ability to capture both benthic and limnetic prey [Robinson, 2000]. In contrast, it is not known whether stickleback immunity face comparable immunological trade-offs. That is, does immunity to benthic-derived parasites (e.g., nematodes) also confer protection to limnetic-derived parasites (e.g., *Schistocephalus* cestodes), or inhibit immunity to cestodes? In general, evidence suggests that different parasites are detected by different host MHC IIb alleles [Stutz and Bolnick, 2017], suggesting a possible trade-off. For certain kinds of parasites this trade-off is well documented, such as the mutual inhibition of Th1 and Th2 adaptive immune responses that, respectively, target bacterial and helminth infections. We chose to model stickleback immunity on a single bidirectional axis, with different optimal values for immunity against limnetic and benthic parasites. This choice comes with the implicit assumption

that there is a limited amount of energy allocated toward immunity, but the vertebrate immune system is complex and highly multivariate. An alternative modeling framework we considered is one unidirectional axis describing immunity for limnetic parasites, and a separate unidirectional axis for immunity to benthic parasites. Unlike our modeling framework, trade-offs would not be between immunity to either limnetic or benthic parasites, but rather between immunity to a parasite species and some other unrelated metabolic rate (i.e. death rate or conversion efficiency).

We did not choose this framework for two reasons. First, this choice would push the evolutionary dimensionality of our model from two to three, and the total dimensionality from five to six, thus increasing the complexity of analysis and decreasing mathematical tractability. Also, we expect that negative correlations between intake and infection are more likely to be seen in this more complex modeling framework. This is because there is no trade-off between immune traits, and thus slight evolutionary adjustments in immunity to one parasite can be made without affecting immunity to the other. Thus, in this framework, even when the trade-off between immunity and a metabolic rate is strong, populations can optimize immunity along both axes, allowing for a kind of immunity generalism. When populations are able to more finely tune their immunity, negative correlations between intake and infection are more likely. We were able to produce negative correlations between intake and infection in a far more conservative framework, less likely to produce this correlation, which is strong evidence in favor of the hypothesis of Stutz et al. [2014] and suggests that the cause of the negative correlation between intake and infection is indeed the evolution of immune traits in conjunction with trophic niche traits.

This study was motivated in part by the specific relationship between stickleback and their infected prey. However, trophically transmitted parasites are very common in nature [Combes, 2001]. This study helps shed light on how food web dynamics are affected by the presence of diet-derived parasites, and is a contribution to the growing body of theory regarding eco-evo dynamics in a multispecies context [Abrams, 2006, Vasseur and Fox, 2011, Cortez and Patel, 2017, Cortez and Weitz, 2014, Patel and Bürger, 2019, Fleischer et al., 2018, Patel and Schreiber, 2015, 2018, Schreiber and Patel, 2015, Schreiber et al., 2011, Saloniemi, 1993, Klauschies et al., 2016, Tien and Ellner, 2012, Abrams and Matsuda, 1997a, Cortez et al., 2020]. In particular, predator traits evolve in response to the presence and danger of parasites in prey, which results in a shift in

predator exposure and susceptibility to parasites. These eco-evo feedbacks can cause chaos or other oscillatory behavior, or cause alternative stable ecological and evolutionary states.

Conversely, we need improve our understanding of how food web dynamics play a role in the dynamics of trophically transmitted parasites, and future theoretical studies should incorporate the dynamics of parasites along with the dynamics of the community in which they reside. Prosnier et al. [2020] used an epidemiological framework to examine the effect of prey infection on predator diet. They also examined the effect of predator diet evolution on coexistence using an adaptive dynamics evolutionary framework and showed that this type of evolution generally promotes coexistence among a predator and an infected and uninfected prey. Like in this study, reductions in prey density correspond to lower consumption rates by the predator, which ultimately favors prey persistence.

Prosnier et al. [2020] modeled parasite transmission as horizontal between prey. This is not the case for stickleback prey, which become infected by parasites through consumption [Barber and Scharsack, 2009]. We therefore chose not to include explicit parasite dynamics or the epidemiological dynamics of the prey, and instead assumed that the proportion of prey which are infected stays constant. Common predators of stickleback are piscivorous birds which freely move between many lakes or ponds. Parasites lay eggs in the gut of a bird and these eggs are deposited into lakes when these birds defecate above water. This suggests that a significant proportion of the parasite load in prey results from regional recruitment rather than local population reproduction. That is, birds which consume infected stickleback from one lake or pond often defecate into another, which keeps the parasite load in each lake or pond relatively constant.

Although it may be that immunity and ecomorphology are genetically linked in some way, we chose to model the two traits as genetically independent. This choice improves mathematical tractability, as well as provides an example of a system in which the evolution of two traits drive each other, not because of genetic linkage, but rather based solely on interdependent selection pressures. Future studies should explore how correlated selection pressures can enhance, or reverse, the effects of genetic linkage of two traits.

Finally, experiments are needed to validate our model, including measurements of relevant parameters and tests of our assumptions. We know that stickleback individuals vary in their propensity to consume benthic versus limnetic resources [Snowberg et al., 2015, Matthews et al.,

2010, Robinson, 2000, Bolnick and Lau, 2008, Bolnick et al., 2014]. However, the precise nature and strength of the biomechanical (and perhaps cognitive) trade-offs remain poorly understood [Robinson, 2000, Schmid et al., 2019]. Likewise, we know that stickleback genotypes differ in their resistance to various parasites [Stutz and Bolnick, 2017, Weber et al., 2017a, Nagar and MacColl, 2016, MacColl, 2009, MacColl and Chapman, 2010, Kalbe and Kurtz, 2005, Eizaguirre et al., 2012, Weber et al., 2017b, among many others]. But, we know little about trade-offs (or synergy) between resistance to different parasites. For that matter, parasites can manipulate host immunity in ways that benefits or harms co-infecting parasites (e.g., Ezenwa et al. [2010]). We therefore need to bring together biomechanical studies of foraging trade-offs, with mechanistic immunological studies of resistance trade-offs. In addition, we lack sufficient information about the relative virulence of different parasites acquired through alternative prey, and future theoretical studies should include the effects and evolution of all three host strategies: avoidance, resistance, and tolerance.

## **2.7. Acknowledgements**

We thank Swati Patel, William Cuello, Kelsey Lyberger, Michael Culshaw-Maurer, Matthew Osmond, Nicholas Roberts, Dale Clement, Denon Start, Yoel Stuar, Jesse Weber, and Natalie Steinel for useful discussion on this topic. We gratefully acknowledge our funding sources: the U.S. National Science Foundation Grants DMS-1716803 and DMS-1714386, and the U.S. National Institute of Allergy and Infectious Diseases Grant 1R01AI123659-01A1.

## CHAPTER 3

# Predator evolution mediates permanence among competing prey

Joint work with:

**Sebastian Schreiber**

*Department of Evolution and Ecology, University of California Davis, Davis, 95616, California*

### 3.1. Abstract

Competition among prey can be qualitatively changed in the presence of predators. In some cases, the presence of one or more predators reduces diversity. In other cases, predators can mediate coexistence among prey which would not ordinarily coexist. Among the mechanisms that promote coexistence among competing prey are ontogenetic diet shifts within predators, dispersal of an inferior prey, and prey evolution in the absence of a predator. Here we study the effect of a generalist predator with an evolutionary trade-off between attack rates on two competing prey. We employ a quantitative genetics framework to analyze a Lotka-Volterra model of the three species along with an evolving predator trait. Predator evolution can promote permanence (a robust form of coexistence, in which all population densities eventually remain positive and bounded within a compact set) between prey that would not ordinarily coexist, even in the presence of a non-evolving predator. When the prey are bistable, predator-mediated permanence is more likely when evolutionary tradeoffs are weak.

### 3.2. Introduction

Nearly two decades ago, Chase et al. [2002] synthesized results from a large body of theoretical and empirical research regarding the complicated interaction between predation and competition among prey. They found that the effect of predation on interspecific competition depends on the relative competitive abilities of the prey, the relative effects of predation on each prey, and the productivity of the environment [Chase et al., 2002]. On short timescales, predators reduce

prey population densities, which reduces the total effect of competition [Sih et al., 1985]. Over longer timescales, however, the proportional reduction in population size caused by competition may increase or decrease in the presence of predation [Gurevitch et al., 2000b]. This complication is due, in part, to prey coexistence depending on the ratio of inter- to intraspecific effects, and that the effect of predation on this ratio is system specific [Chase et al., 2002].

There are a number of mechanisms in which a predator mediates coexistence among its competing prey. The presence of predators can cause prey to seek species-specific refuges where the frequency of interspecific interactions, and thus competition, is reduced, enabling coexistence [Holt and Lawton, 1994]. Predators can promote coexistence between a superior and inferior competitor if the superior competitor is more affected by predation [Abrams, 1993]. Predator switching behavior can allow predators to act as limiting factors for more than one prey, promoting coexistence [Roughgarden and Feldman, 1975]. Ontogenetic diet shifts in predators allow coexistence between a superior and inferior prey [Wollrab et al., 2013] and between a resource and an intraguild predator [Hin et al., 2011]. Dispersal of an inferior competitor causes sustained spatial heterogeneity, promoting coexistence [Amarasekare, 2008]. Other mechanisms have been hypothesized and tested, including the coexistence of *Daphnia* due to the presence of and particular feeding patterns of a predatory fish [Gliwicz and Wrzosek, 2008]. But Chase et al. [2002] noted a major gap in theory regarding the effect of evolution on the predation-competition interaction, which is surprising given this gap was originally identified a quarter-century earlier by Holt [1977] in his study of apparent competition.

The idea that ecology and evolution affect each other on commensurate timescales (also known as eco-evolutionary feedbacks) has since become mainstream [Schoener, 2011]. Many theoretical studies show how evolution of one or more species can affect the structure of its community, and conversely how community structure affects their evolution [Abrams, 2006, Geritz et al., 2007, Schreiber et al., 2011, Vasseur and Fox, 2011, Vasseur et al., 2011, Schreiber and Patel, 2015, Patel and Schreiber, 2015, Klauschies et al., 2016, Cortez and Patel, 2017, Patel and Schreiber, 2018, Fleischer et al., 2018, Patel and Bürger, 2019]. For example, Geritz et al. [2007] showed that evolution of predator handling time can cause evolutionary branching and coexistence between the two distinct predators and their shared prey. In a Lotka-Volterra competition model, Vasseur

et al. [2011] showed that a competitor with an evolving trait expressed as a tradeoff between inter- and intraspecific competition can mediate coexistence. Klauschies et al. [2016] studied a four-prey four-predator eco-evolutionary module with a prey trait tradeoff between intrinsic growth rate and a predator trait tradeoff between selectivity and half-saturation constant and found that rapid evolution promoted species coexistence, while systems with low trait heritability (and thus slower evolution) did not show increased species coexistence.

Another ecological role evolution might play is in mediating the existence of competing prey species. In a Lotka-Volterra model of two competing species, there are three qualitatively different outcomes: globally stable coexistence, globally stable dominance of a single competitor, and bistability where both single-species equilibria are stable. Hutson and Vickers [1983] fully characterized permanence of a Lotka-Volterra system with a single predator and two competing prey and found it can be permanent only if the prey coexist in the absence of the predator or one prey dominates the other, but permanence is impossible for bistable prey. Later, Schreiber [1997] showed how these conclusions extend to non-Lotka-Volterra models, such as the Schoener competition model [Schoener, 1976] and those with type II functional responses [Ayala et al., 1973].

Theoreticians have searched for ways in which one or more predators mediate permanence among bistable prey. For example, Kirlinger [1986] found two specialist predators can mediate permanence between two bistable prey. Other studies have found mechanisms for maintaining coexistence between competitors in various contexts, including stepwise predator switching between a superior dynamic prey and inferior static prey [van Baalen et al., 2001], dispersal and spatial heterogeneity in a rock-paper-scissors metacommunity [Schreiber and Killingback, 2013], and environmental temporal heterogeneity affecting interacting structured populations [Roth and Schreiber, 2013].

It may be possible, however, for a single evolving predator to mediate permanence among bistable prey. If there is a tradeoff in consumption rates between the two prey populations, then a specialist predator which suppresses population growth of a particular prey may create the conditions under which its competitor can invade. Thus, in this study we consider the evolution of the attack rates of a predator with two prey. There are numerous empirical examples of evolutionary tradeoffs between attack rates on alternative prey within generalist predators, also known as

individual specialization [Bolnick et al., 2003]. A well-studied example of heterogeneous predator populations in which diet is correlated with some physical trait is the threespine stickleback. These fish are generalists in northern temperate lakes with multiple abundant prey, but individuals' morphology is correlated with their diet [Snowberg et al., 2015]. This gives rise to potential rapid evolution of the diet-correlated trait in response to selection pressure caused by shifting prey population densities. It is possible, therefore, that predator evolution is a mechanism for maintaining prey diversity.

To test this hypothesis, we analyze a Lotka-Volterra three-species module in which a single predator population consumes two competing prey which cannot coexist in the absence of predation (either due to competitive exclusion or the priority effect). First, we find global stability conditions in the absence of evolution, extending the work of Takeuchi and Adachi [1983], whose study assumed equal assimilation efficiencies. Then, we consider an evolving quantitative trait in the predator, derive permanence conditions, and compare the regions of trait space which allow for prey coexistence. In the language of Chase et al. [2002], the measure we use to determine the effect of predator evolution on competing prey is the “ease of coexistence,” which is simply the range of parameter values producing coexistence of competitors. We conclude with an analysis of the effect of trait heritability on the type of coexistence that arises from the eco-evolutionary feedback.

### 3.3. Models and Definitions

**3.3.1. The Ecological Dynamics.** Let  $N_i(t)$  ( $i = 1, 2$ ) and  $P(t)$  be the prey and predator densities at time  $t$ , respectively. Let  $r_i$  denote the intrinsic growth rates of the prey,  $c_{12}$  and  $c_{21}$  the competition rates between the competing prey species,  $a_i$  the predator attack rates on the two prey,  $e_i$  the predator conversion efficiencies of the two prey, and  $d$  the predator death rate. Non-dimensionalizing the prey carrying capacities in the absence of other species to  $r_i$ , the Lotka-Volterra model of a predator and two competing prey is

$$(3.1) \quad \begin{aligned} \frac{dN_1}{dt} &= N_1(r_1 - N_1 - c_{12}N_2 - a_1P), \\ \frac{dN_2}{dt} &= N_2(r_2 - N_2 - c_{21}N_1 - a_2P), \\ \frac{dP}{dt} &= P(a_1e_1N_1 + a_2e_2N_2 - d). \end{aligned}$$

There are three qualitatively different outcomes of the  $N_1$ - $N_2$  subsystem of Model (3.1): (i) if  $c_{12} < \frac{r_1}{r_2}$  and  $c_{21} < \frac{r_2}{r_1}$ , then the prey converge to a globally stable equilibrium for all positive initial conditions, (ii) if  $c_{12} < \frac{r_1}{r_2}$  and  $c_{21} > \frac{r_2}{r_1}$ , then prey 1 is the superior prey and prey 2 is lost (dynamics converge to  $(r_1, 0)$  for all positive initial conditions), and (iii) if  $c_{12} > \frac{r_1}{r_2}$  and  $c_{21} > \frac{r_2}{r_1}$ , then both  $(r_1, 0)$  and  $(0, r_2)$  are locally stable, and their basins of attraction are separated by the one-dimensional stable manifold of the unstable coexistence equilibrium.

We are interested in when the prey cannot coexist in the absence of the predator, and thus we focus on cases (ii) and (iii). Extending results from Takeuchi and Adachi [1983], we determine conditions for global stability of the various equilibria of Model (3.1), as well as conditions for the existence of a Hopf Bifurcation.

**3.3.2. The Eco-Evolutionary Dynamics.** To study the role of evolution in predator-mediated coexistence, we extend Model (3.1) to include an evolving trait that determines its attack rates  $a_i$  on the two prey species. We assume the predator trait  $x$  is normally distributed with mean  $\bar{x}$  and variance  $\sigma^2$  across the predator population ( $x \sim \mathcal{N}(\bar{x}, \sigma^2)$ ), and is determined by an infinite amount of independent loci with additive effects. We also assume the trait stays normally distributed with variance  $\sigma^2$  throughout time [Lande, 1976].

Trait  $x$  affects the predator attack rate  $a_i$  on prey  $i$  such that  $a_i$  is maximized at optimal trait value  $\theta_i$  and decreases in a Gaussian manner as  $|x - \theta_i|$  increases:

$$a_i(x) = \alpha_i + \beta_i \exp\left[-\frac{(x - \theta_i)^2}{2\tau_i^2}\right],$$

where  $\alpha_i$  and  $\alpha_i + \beta_i$  are the bounding values of  $a_i$  and  $\tau_i$  is a measure of the strength of the evolutionary tradeoff between attack rates. Under these assumptions, the eco-evolutionary dynamics are

$$(3.2) \quad \begin{aligned} \frac{dN_1}{dt} &= N_1(r_1 - N_1 - c_{12}N_2 - \bar{a}_1(\bar{x})P), \\ \frac{dN_2}{dt} &= N_2(r_2 - N_2 - c_{21}N_1 - \bar{a}_2(\bar{x})P), \\ \frac{dP}{dt} &= Pf_P(N_1, N_2, P, \bar{x}), \\ \frac{d\bar{x}}{dt} &= \sigma_G^2 \frac{d}{d\bar{x}} f_P(N_1, N_2, P, \bar{x}), \end{aligned}$$

where

$$\bar{a}_i(\bar{x}) := \int_{-\infty}^{\infty} a_i(x) \cdot \frac{1}{\sqrt{2\pi\sigma^2}} \exp\left[-\frac{(x - \bar{x})^2}{2\sigma^2}\right] dx = \alpha_i + \frac{\beta_i \tau_i}{\sqrt{\sigma^2 + \tau_i^2}} \exp\left[-\frac{(\bar{x} - \theta_i)^2}{2(\sigma^2 + \tau_i^2)}\right]$$

is the average predator attack rate on prey  $i$ ,

$$f_P(N_1, N_2, P, \bar{x}) := \bar{a}_1(\bar{x})e_1N_1 + \bar{a}_2(\bar{x})e_2N_2 - d$$

is the average predator per-capita growth rate, and  $\sigma_G^2$  is the portion of the phenotypic variation due to the genotypic variation in the predator population. The population densities  $(N_1, N_2, P) \in \mathbb{R}_{\geq 0}^3 = [0, \infty)^3$ , and the trait  $\bar{x} \in K := [\theta_1, \theta_2]$ . Thus the state space for Model (3.2) is  $S := \mathbb{R}_{\geq 0}^3 \times K$ . The *extinction set*  $S_0 := \{z = (N_1, N_2, P, \bar{x}) \in S \mid N_1N_2P = 0\}$  is the set which has at least one species extinct (density equal to zero). The heritability  $h^2 \in [0, 1]$  of trait  $x$  is the ratio  $\sigma_G^2/\sigma^2$ .

**3.3.3. Coexistence: attractors, permanence, and global stability.** The word *coexistence* is used often to describe species that are able to persist for extended periods of time. This can have many meanings and has been refined in a variety of ways [see, e.g., Schreiber, 2006, for a review]. The simplest form of coexistence is a locally asymptotically stable equilibrium of positive densities. This coexistence is robust to small perturbations, but not necessarily large ones, as there may be other equilibria with one or more species extinct (zero density) that are also locally asymptotically stable. More generally, there are interior attractors, which include stable equilibria as well as stable limit cycles or chaos bounded away from zero. Again, this form of coexistence is not necessarily robust to large perturbations as there may be other asymptotically stable attractors in which one or more species is extinct. To persist after vigorous shakeups, not only gentle stirrings [Jansen and Sigmund, 1998], one requires a *global* interior attractor, which is an attractor in which all trajectories with positive initial condition eventually approach. The term *permanence* describes a case in which there is a compact global interior attractor. Hutson and Schmitt [1992] introduced *robust permanence* [see also Schreiber, 2000], which requires permanence for any sufficiently small and smooth model perturbation. Even stronger is global stability of an interior equilibrium, which guarantees asymptotic approach to one equilibrium of positive densities for all initial conditions with positive densities. To state these terms precisely, we need a few definitions.

Let  $z.t$  denote the solution to Model (3.1) or (3.2) for initial condition  $z \in S$ . For any set  $Z \in S$  and  $I \in \mathbb{R}$ , let  $Z.I := \{z.t \mid t \in I, z \in Z\}$ . Models (3.1) or (3.2) are *dissipative* if there exists a compact set  $Q \in S$  such that for all  $z \in S$ ,  $z.t \in Q$  for all  $t$  sufficiently large. The  $\omega$ -*limit set* of a set  $Z \subset S$  is  $\omega(Z) := \bigcap_{t \geq 0} \overline{Z.[t, \infty)}$ , and the  $\alpha$ -*limit set* is  $\alpha(Z) := \overline{Z.(-\infty, t]}$ . A set  $Z \subset S$  is *invariant* if  $Z.\mathbb{R} = Z$ . A set  $A \subset S$  is an *attractor* if there is a neighborhood  $U$  of  $A$  such that  $\omega(U) = A$ . The *global attractor* is  $\omega(Q)$ .

Models (3.1) or (3.2) are *permanent* if (i) they are dissipative, (ii) there exists a compact attractor  $A$  such that  $A \cap S_0 = \emptyset$ , and (iii)  $\omega(x) \subset A$  for all  $x \in S \setminus S_0$ . Equivalently, they are permanent if there is some  $\epsilon > 0$  such that for any positive initial condition,  $\liminf_{t \rightarrow \infty} N_1(t)N_2(t)P(t) > \epsilon$  and  $\limsup_{t \rightarrow \infty} N_1(t)N_2(t)P(t) < \frac{1}{\epsilon}$ . All population densities must eventually be uniformly bounded away from 0 and uniformly bounded above as long as each population has a positive initial density. If the models are permanent for sufficiently small and smooth perturbations, then they are *robustly permanent* [see Patel and Schreiber, 2018, for a precise definition]. To derive robust permanence conditions for Model (3.2), we use results from a previous study [Patel and Schreiber, 2018], which allow us to simply consider the invasion rates of missing species at the equilibria on the boundary.

Even stronger than robust permanence is global stability. An equilibrium  $z^*$  is *globally stable* if  $\omega(z) = \{z^*\}$  for all  $z \in S \setminus S_0$ . We derive conditions for global stability of Model (3.1), but do not make any claims about global stability in Model (3.2).

### 3.4. Results

We first refine the results of Hutson and Vickers [1983], who found conditions for permanence of Model (3.1), by deriving conditions for global stability of the coexistence equilibrium (extending the results of Takeuchi and Adachi [1983], who assumed  $e_1 = e_2$ ). We then discuss the dynamics when Model (3.1) is not permanent, including global stability of boundary equilibria, existence of Hopf bifurcations, and various types of bistabilities. We then present our main result: conditions for permanence of Model (3.2). We conclude with a presentation of four qualitatively different forms of permanence, including cases in which evolution stabilizes unstable communities and cases in which evolution destabilizes stable communities.

**3.4.1. Permanence and Global Stability of Model (3.1).** Generically, there are seven equilibria of Model (3.1). Each equilibrium exists if the coordinates are non-negative, but we are often interested in the cases where the variable coordinates are strictly positive, which inspires the “+” and “0” notation we use for the equilibria. The first three always exist: the origin  $E_{00}^0 = (0, 0, 0)$  and the two single-prey equilibria  $E_{+0}^0 = (r_1, 0, 0)$  and  $E_{0+}^0 = (0, r_2, 0)$ . Given  $c_{12}c_{21} \neq 1$ , we can define the predator-exclusion equilibrium  $E_{++}^0 = \left( \frac{r_1 - c_{12}r_1}{1 - c_{12}c_{21}}, \frac{r_2 - c_{21}r_1}{1 - c_{12}c_{21}}, 0 \right)$ , which exists if  $(r_1 - c_{12}r_2)(r_2 - c_{21}r_1) \geq 0$ . There are two predator-prey equilibria,  $E_{+0}^+ = \left( \frac{d}{a_1e_1}, 0, \frac{1}{a_1} \left( r_1 - \frac{d}{a_1e_1} \right) \right)$  and  $E_{0+}^+ = \left( 0, \frac{d}{a_2e_2}, \frac{1}{a_2} \left( r_2 - \frac{d}{a_2e_2} \right) \right)$ , which exist if  $d \leq a_1e_1r_1$  and  $d \leq a_2e_2r_2$ , respectively. Finally, there is one coexistence equilibrium  $E_{++}^+ = (N_1^*, N_2^*, P^*)$ , where

$$\begin{aligned} N_i^* &= \frac{\tilde{N}_i}{\Theta}, \quad i = 1, 2, & P^* &= \frac{\tilde{P}}{\Theta}, \\ \tilde{N}_1 &= d(a_1 - c_{12}a_2) - a_2e_2(a_1r_2 - a_2r_1), \\ (\diamond) \quad \tilde{N}_2 &= d(a_2 - c_{21}a_1) - a_1e_1(a_2r_1 - a_1r_2), \\ \tilde{P} &= a_1e_1(r_1 - c_{12}r_2) + a_2e_2(r_2 - c_{21}r_1) - d(1 - c_{12}c_{21}), \text{ and} \\ \Theta &= a_1^2e_1 - a_1a_2(c_{12}e_1 + c_{21}e_2) + a_2^2e_2. \end{aligned}$$

The conditions for positivity and local asymptotic stability for each equilibrium are summarized in Table 3.1, as discussed in Hutson and Vickers [1983]. Hutson and Vickers [1983] also derived necessary and sufficient conditions for permanence of Model (3.1). These conditions characterize robust permanence within the class of Lotka-Volterra models.

**THEOREM 3.1** (Hutson and Vickers, 1983, Theorems 3.4 and 3.5). *Suppose that  $E_{++}^+ = (N_1^*, N_2^*, P^*)$  of Model (3.1) satisfies  $N_1^* > 0$ ,  $N_2^* > 0$ , and  $P^* > 0$ . Model (3.1) is robustly permanent if and only if*

- (i)  $c_{12} < \frac{r_1}{r_2}$  or  $c_{21} < \frac{r_2}{r_1}$ , and
- (ii)  $\Theta > 0$ .

Condition (i) in Theorem 3.1 implies that bistable prey cannot be made permanent with the addition of a Lotka-Volterra predator. Specifically, if  $c_{12} > \frac{r_1}{r_2}$  and  $c_{21} > \frac{r_2}{r_1}$  and an interior equilibrium exists, then Hutson and Vickers [1983] show that one of  $E_{+0}^0$  and  $E_{0+}^0$  must be locally

Equilibrium	Positivity conditions	Local stability conditions (given positivity)
$E_{++}^+$	$N_1^* > 0, N_2^* > 0, P^* > 0$ (see $\blacklozenge$ )	$\begin{cases} Z_1 := (1 - c_{12}c_{21})N_1^*N_2^* \\ \quad + (a_1^2e_1N_1^* + a_2^2e_2N_2^*)P^* > 0 \\ Z_2 := (N_1^* + N_2^*)Z_1 - N_1^*N_2^*P^*\Theta > 0 \\ Z_3 := N_1^*N_2^*P^*\Theta > 0 \\ Z_1Z_2 - Z_3 > 0 \end{cases}$
$E_{+0}^+$	$d < a_1e_1r_1$	$\tilde{N}_2 < 0$
$E_{0+}^+$	$d < a_2e_2r_2$	$\tilde{N}_1 < 0$
$E_{++}^0$	$(r_1 - c_{12}r_2)(r_2 - c_{21}r_1) > 0$	$c_{12}c_{21} < 1$ and $\tilde{P} < 0$
$E_{+0}^0$	always	$\begin{cases} d > a_1e_1r_1 \\ c_{21} > \frac{r_2}{r_1} \end{cases}$
$E_{0+}^0$	always	$\begin{cases} d > a_2e_2r_2 \\ c_{12} > \frac{r_1}{r_2} \end{cases}$
$E_{00}^0$	always	never

TABLE 3.1. Existence and local stability conditions for all equilibria of Model (3.1).

asymptotically stable, preventing permanence. If condition (i) holds (and thus the prey are not bistable; one dominates the other or they coexist in the absence of predation), then condition (ii) can be interpreted as a restriction on the type of predator which ensures permanence. For example, if prey 1 dominates prey 2 ( $c_{12} < \frac{r_1}{r_2}$  and  $c_{21} > \frac{r_2}{r_1}$ ), then (3.1) is permanent if the attack rate on prey 1 is sufficiently large and the attack rate on prey 2 is sufficiently small (see, e.g., Figs. 3.4b-d).

The following theorem provides a sufficient condition for permanence to correspond to a globally stable equilibrium. Moreover, it provides sufficient conditions for boundary equilibria (i.e. where at least one species is missing) to be globally stable.

**THEOREM 3.2.** *Suppose  $c_{12}e_1 + c_{21}e_2 < 2\sqrt{e_1e_2}$ .*

(a) *If  $E_{++}^+$  exists and is positive, it is globally stable.*

(b) *If  $E_{++}^+$  is not positive, then one of  $E_{0+}^0$ ,  $E_{+0}^0$ ,  $E_{++}^0$ ,  $E_{0+}^+$ , or  $E_{+0}^+$  is globally stable.*

The condition  $c_{12}e_1 + c_{21}e_2 < 2\sqrt{e_1e_2}$  in Theorem 3.2 requires that the competition among prey is weak relative to their nutritional value for predators.

Model (3.1) may be permanent but not globally stable, in which case there is some globally stable interior non-equilibrium attractor. If Model (3.1) is not permanent, however, then either the coexistence equilibrium  $E_{++}^+$  does not exist, or condition (i) or (ii) from Theorem 3.1 does not hold.

The following theorem fully characterizes the dynamics for the cases in which Prey 1 dominates Prey 2.

**THEOREM 3.3.** *Assume Model (3.1) is not robustly permanent, and  $c_{12} < \frac{r_1}{r_2}$  and  $c_{21} > \frac{r_2}{r_1}$  (Prey 1 dominates Prey 2). Then one of the following holds:*

- (a)  $E_{++}^+$  is not positive and one of  $E_{+0}^0$ ,  $E_{+0}^+$ , or  $E_{0+}^+$  is globally stable, or
- (b)  $E_{++}^+$  is positive, and  $E_{0+}^+$  and  $E_{+0}^+$  are both asymptotically stable or  $E_{0+}^0$  and  $E_{+0}^0$  are both asymptotically stable.

When the prey are bistable ( $c_{12} > \frac{r_1}{r_2}$  and  $c_{21} > \frac{r_2}{r_1}$ ) a full characterization of the dynamics of Model (3.1) is more difficult and remains a future challenge. Both types of bistabilities described in Theorem 3.3 are also possible if the prey are bistable, as well as bistability of  $E_{+0}^0$  and  $E_{0+}^0$  if the predator is unable to sustain itself on either prey. Furthermore, while permanence is impossible in this case (Theorem 3.1), a weaker form of coexistence, existence of an internal attractor, can hold if the predator is specialized on one prey. This attractor must be bistable with some boundary equilibrium ( $E_{+0}^0$  or  $E_{0+}^0$ ). In a bistable prey community in which prey 1 is present, if a predator specialized on prey 1 invades, it suppresses the prey 1 population such that prey 2 can invade. If the predator attack rate on prey 2 is sufficiently small and the attack rate on prey 1 is intermediate, then all three species may coexist. However, the same predator cannot invade the same community while prey 2 is present. In addition, if all three species are present, sufficiently large ecological perturbations may result in all but one prey species being excluded.

Figures 3.1b-d illustrate the possible dynamics when prey 1 dominates prey 2 in the absence of the predator ( $c_{12} < \frac{r_1}{r_2}$  and  $c_{21} > \frac{r_2}{r_1}$ ). In Figure 3.1b, the global stability condition holds (Theorem 3.2), and thus exactly one equilibrium is globally stable for each combination of  $a_1$  and  $a_2$  values. In Figures 3.1c,d, the global stability condition does not hold. Permanence is possible in this case; regions with only vertical stripes indicate scenarios in which no boundary equilibrium is locally stable, and thus all attractors are in the interior, and white regions indicate scenarios in which no equilibrium is stable, including the interior equilibrium  $E_{++}^+$ , and thus all attractors are oscillatory and in the interior. If (3.1) is not permanent, multiple equilibria may be simultaneously locally stable ( $E_{0+}^+$  and either  $E_{+0}^+$  or  $E_{+0}^0$ ).

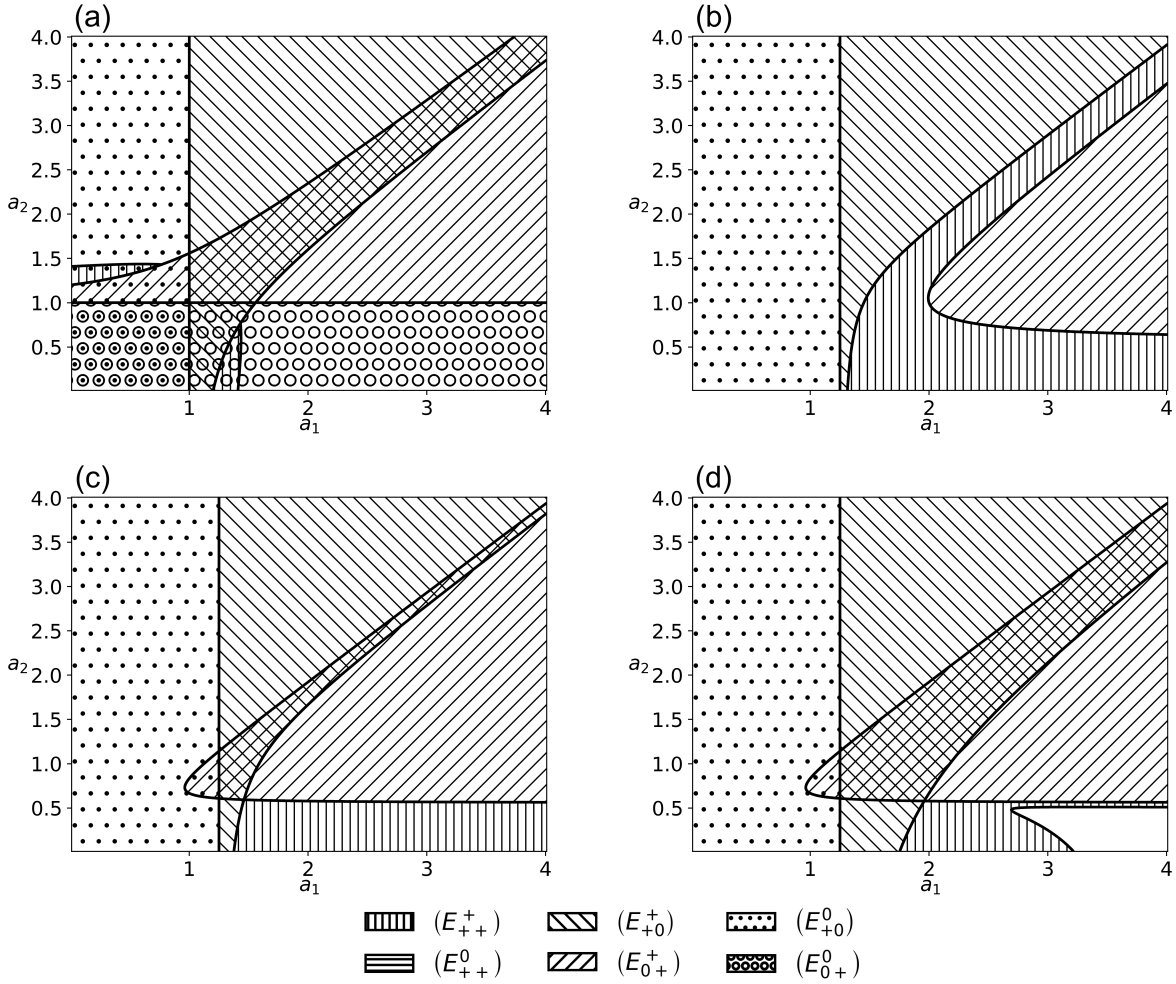


FIGURE 3.1. Existence and local stability of equilibria on the  $a_1$ - $a_2$  plane. The legend indicates which patches correspond to which equilibrium. Regions containing multiple patches indicate bistability between equilibria. White regions indicate no equilibria exist and are locally stable and thus there is some stable oscillatory solution. In (a), the prey are bistable ( $c_{12} > \frac{r_1}{r_2}$  and  $c_{21} > \frac{r_2}{r_1}$ ). In (b), (c), and (d), prey 1 dominates prey 2 ( $c_{12} < \frac{r_1}{r_2}$  and  $c_{21} > \frac{r_2}{r_1}$ ). Parameters:  $r_1 = r_2 = 1$ ,  $d = 0.5$ . In (a),  $c_{12} = c_{21} = 1.2$ ,  $e_1 = e_2 = 0.5$ . In (b),  $c_{12} = 0.2$ ,  $c_{21} = 1.05$ ,  $e_1 = 0.4$ , and  $e_2 = 0.9$ . In (c),  $c_{12} = 0.9$ ,  $c_{21} = 1.1$ ,  $e_1 = 0.4$ , and  $e_2 = 0.9$ . In (d),  $c_{12} = 0.9$ ,  $c_{21} = 1.4$ ,  $e_1 = 0.4$ , and  $e_2 = 0.9$ .

**3.4.2. Evolving Predator-Mediated Permanence.** In Model (3.2), the predator attack rates  $a_i$  are maximized at some optimal values  $\theta_i$  and monotonically decrease with distance from that value. The minimum and maximum values of  $\bar{a}_i$ ,  $i = 1, 2$ , which govern the endpoints of the trait curve in Figure 3.2a, are as follows:

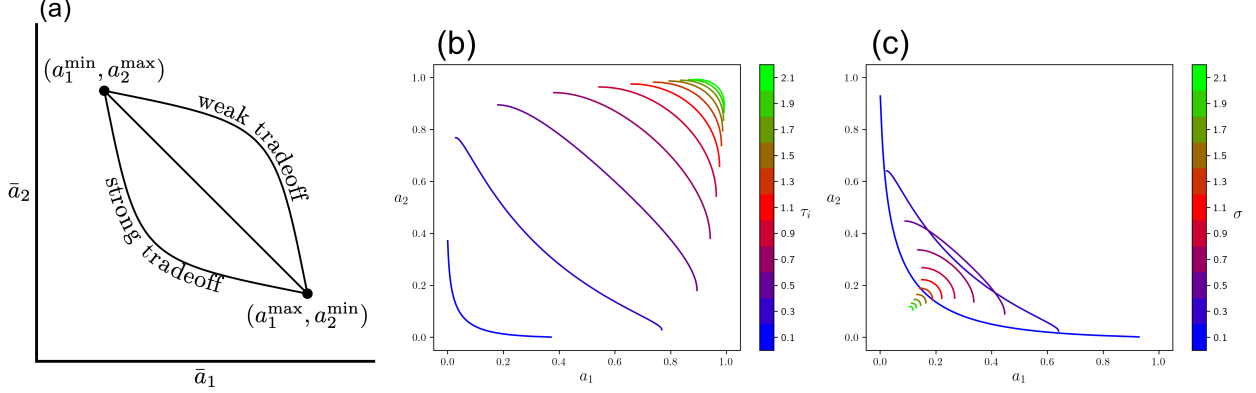


FIGURE 3.2. Evolutionary tradeoff between either attack rates  $a_i$ . (a) If  $x = \theta_i$ ,  $a_i$  is maximized and  $a_j$  is minimized. The curve connecting these two points are negatively sloped, but the concavity determines the strength of the tradeoff. Concave curves indicate a weak tradeoff, as intermediate values of  $x$  result in relatively large attack rates  $a_i$ , whereas convex curves indicate a strong tradeoff, as intermediate values of  $x$  result in relatively low attack rates  $a_i$ . The curves are convex if  $\tau_i$  and  $\sigma^2$  are sufficiently large and concave if  $\tau_i$  and  $\sigma^2$  are sufficiently small. These parameters, along with  $|\theta_2 - \theta_1|$ , determine the strength of the attack rate tradeoff. Parameters: in (b,c),  $\alpha_1 = \alpha_2 = 0$ ,  $\beta_1 = \beta_2 = 1$ ,  $\theta_1 = 0$ , and  $\theta_2 = 1$ . In (b),  $\sigma^2 = 0.25$  and  $\tau_i \in [0.1, 2.1]$ ,  $\tau_1 = \tau_2$ . In (c),  $\tau_1 = \tau_2 = 0.25$  and  $\sqrt{\sigma^2} \in [0.1, 2.1]$ .

$$\begin{aligned}
 a_1^{\max} &:= \bar{a}_1(\theta_1) = \alpha_1 + \frac{\beta_1 \tau_1}{\sqrt{\sigma^2 + \tau_1^2}}, & a_1^{\min} &:= \bar{a}_2(\theta_1) = \alpha_2 + \frac{\beta_2 \tau_2}{\sqrt{\sigma^2 + \tau_2^2}} \exp\left[-\frac{(\theta_2 - \theta_1)^2}{2(\sigma^2 + \tau_2^2)}\right], \\
 a_2^{\max} &:= \bar{a}_2(\theta_2) = \alpha_2 + \frac{\beta_2 \tau_2}{\sqrt{\sigma^2 + \tau_2^2}}, & a_2^{\min} &:= \bar{a}_1(\theta_2) = \alpha_1 + \frac{\beta_1 \tau_1}{\sqrt{\sigma^2 + \tau_1^2}} \exp\left[-\frac{(\theta_2 - \theta_1)^2}{2(\sigma^2 + \tau_1^2)}\right].
 \end{aligned}$$

We see that  $a_j^{\min}$  and  $a_i^{\max}$  increase linearly with  $\alpha_i$  and  $\beta_i$ , and increase nonlinearly with  $\tau_i$ .  $a_i^{\max}$  decreases with  $\sigma^2$ , but  $a_j^{\min}$  may be non-monotonic in  $\sigma^2$ . In particular,  $a_j^{\min}$  increases with  $\sigma^2$  if and only if  $\sigma^2 + \tau_j^2 < (\theta_2 - \theta_1)^2$ . Shifting  $\alpha_i$  or  $\beta_i$  does not change the convexity of the trait curve, but the curve is convex if  $\tau_i$  or  $\sigma^2$  are sufficiently large and concave if  $\tau_i$  or  $\sigma^2$  are sufficiently small (Figs. 3.2b,c).

Theorem 3.4 gives permanence conditions for Model (3.2) (Appendix C.4). As we are interested in when predators mediate permanence among prey who would not otherwise coexist, we limit the theorem to the cases in which the prey are bistable or one prey dominates the other (without loss of generality, prey 1 dominates prey 2). In either of these cases, permanence is only possible if (i) the predator can sustain itself of prey 1 and (ii) prey 2 has a positive per-capita growth rate at the prey 1-predator equilibrium.

THEOREM 3.4 (Permanence of Model (3.2)). *Assume*

(i) (prey 1 supports predator)  $a_1^{\max} e_1 r_1 > d$ , and

(ii) (prey 2 can invade prey 1-predator subsystem)  $d(a_2^{\min} - c_{21} a_1^{\max}) > a_1^{\max} e_1 (a_2^{\min} r_1 - a_1^{\max} r_2)$ .

**Bistable prey:** If  $c_{12} > \frac{r_1}{r_2}$  and  $c_{21} > \frac{r_2}{r_1}$ , then Model (3.2) is robustly permanent if and only if

(iii) (prey 2 supports predator)  $a_2^{\max} e_2 r_2 > d$ ,

(iv) (prey 1 can invade prey 2-predator subsystem)  $d(a_1^{\min} - c_{12} a_2^{\max}) > a_2^{\max} e_2 (a_1^{\min} r_2 - a_2^{\max} r_1)$ ,

and

(v) (predator can invade bistable prey equilibria)  $\bar{a}_1(x^*) e_1 \frac{r_1 - c_{12} r_2}{1 - c_{12} c_{21}} + \bar{a}_2(x^*) e_2 \frac{r_2 - c_{21} r_1}{1 - c_{12} c_{21}} > d$  for all  $x^* \in W$ ,

where  $W := \left\{ x \in [\theta_1, \theta_2] \mid \frac{\partial f_P}{\partial \bar{x}} \Big|_{(N_1, N_2, P, \bar{x}) = E_{++}^0(x)} = 0 \right\}$  is the set of equilibria for the trait dynamics of Model (3.2) when the prey coexist in the absence of the predator.

**Prey 1 dominates prey 2:** If  $c_{12} < \frac{r_1}{r_2}$  and  $c_{21} > \frac{r_2}{r_1}$ , then Model (3.2) is robustly permanent if and only if

$\sim$ (iii) (prey 2 does not support predator)  $a_2^{\max} e_2 r_2 < d$ , or

(iv) (prey 1 can invade prey 2-predator subsystem)  $d(a_1^{\min} - c_{12} a_2^{\max}) > a_2^{\max} e_2 (a_1^{\min} r_2 - a_2^{\max} r_1)$ .

Assumptions (i) and (ii) in Theorem 3.4 ensure the predator can invade the superior prey and the inferior prey can invade in the presence of the predator, respectively. Assumptions (iii) and (iv) ensure the predator can invade the inferior prey and the superior prey can invade in the presence of the predator, respectively. Assumption (v) ensures the predator is always able to invade if the prey are at a coexistence state. If the prey are bistable, all five assumptions must hold (Fig. 3.3a). If prey 1 dominates prey 2, either the predator must not be able to invade the inferior prey or the superior prey can invade in the presence of the predator (Fig. 3.3b,c).

Assumptions (i)-(iv) can be viewed as specifying the location of the endpoints of the trait curves  $(a_1^{\min}, a_2^{\max})$  and  $(a_1^{\max}, a_2^{\min})$  that ensure permanence of Model (3.2). When the prey are bistable, condition (v), which guarantees the predator can invade the  $E_{++}^0$  equilibria, must also be met (Fig. 3.4a). Notably, Model (3.2) can be permanent even when the prey are bistable. As proved in Theorem 3.1, this is impossible in Model (3.1), where  $a_i^{\min} = a_i^{\max}$ ,  $i = 1, 2$ . If  $a_i^{\max}$  are large and  $a_i^{\min}$  are small relative to  $a_i^{\max}$ , then permanence in Model (3.2) is guaranteed by Theorem

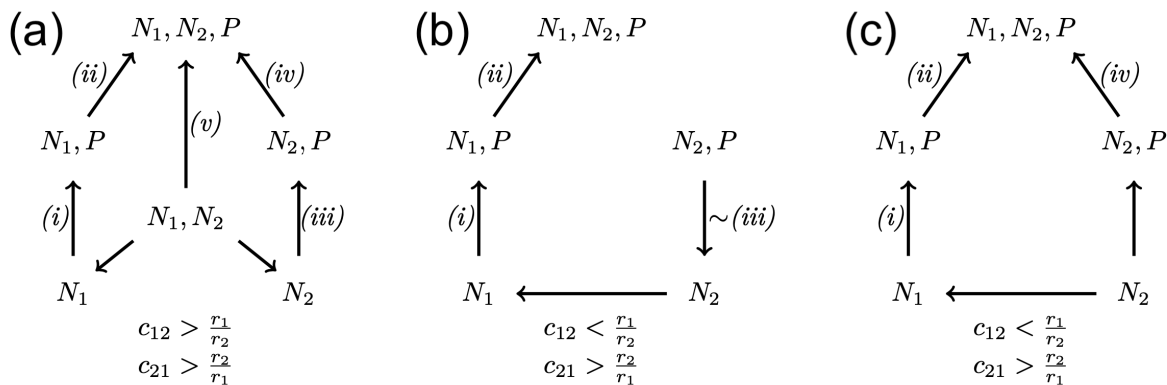


FIGURE 3.3. Diagrams depicting conditions which must be met in order to guarantee permanence. Roman numerals refer to the conditions in Theorem 3.4. In panel (a), the prey are bistable in the absence of the predator ( $c_{12} > \frac{r_1}{r_2}$  and  $c_{21} > \frac{r_2}{r_1}$ ). For the system to be permanent, the predator must always be able to invade, and each prey must be able to invade when the predator is present, even though they cannot invade when the predator is not present. In panels (b,c), prey 1 dominates prey 2 in the absence of the predator ( $c_{12} < \frac{r_1}{r_2}$  and  $c_{21} > \frac{r_2}{r_1}$ ). In panel (b), the predator is unable to invade when only prey 2 is present, and prey 2 can invade the prey 1-predator equilibrium. In panel (c), prey 1 is able to invade when the predator persists on prey 2.

3.4. This can be seen in Figure 3.4a, where there is no overlap between the hatched regions, but permanence is still possible if a trait curve straddles the bistable region. The same is true when prey 1 dominates prey 2 and global stability is not guaranteed (Figs. 3.4c,d). This case is similar to the bistable prey case when  $a_1$  and  $a_2$  are large - as long as conditions (i)-(iv) are met, permanence is guaranteed.

**3.4.3. Fast-Slow Dynamics in the Limit of Slow Evolution.** To better understand how eco-evolutionary feedbacks mediate permanence, we examine the natural case in which the evolutionary dynamics occur at a much slower time scale than the ecological dynamics. This separation of time scales occurs when the portion of phenotypic variation attributable to genotypic variation  $\sigma_G^2$  is small. In the limit as  $\sigma_G^2 \rightarrow 0$ , there is a timescale separation between the “fast” ecological

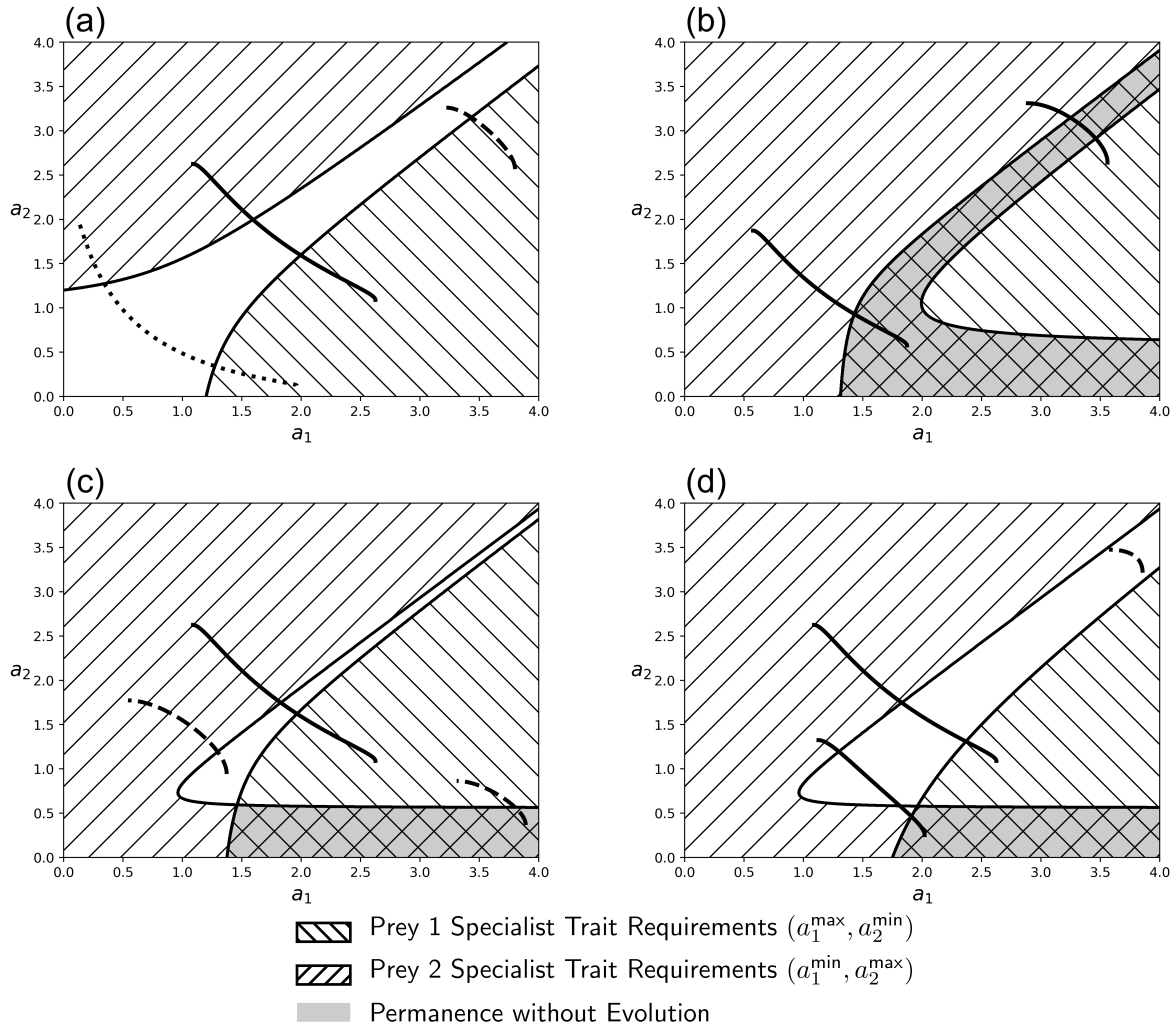


FIGURE 3.4. High specialized attack rates  $a_i^{\max}$  and strong tradeoffs ( $a_j^{\min} \ll a_i^{\max}$  for  $i \neq j$ ) ensure eco-evolutionary permanence. In order for prey 1 to invade the prey 2-predator subsystem,  $(a_1^{\min}, a_2^{\max})$  needs to lie in the right hatched regions. In order for prey 2 to invade the prey 1-predator subsystem,  $(a_1^{\max}, a_2^{\min})$  needs to lie in the left hatched regions. Gray regions indicate regions of  $a_1$ - $a_2$  parameter space in which Model (3.1) is permanent. Solid trait curves meet all requirements for permanence ((i)-(v) in Theorem 3.4). Dashed and dotted trait curves do not; dashed trait curves fail at least one of (i)-(iv), and the dotted curve fails assumption (v). Notice the endpoints of the dotted curve meet all endpoint requirements, but there is some  $\bar{x}$  equilibrium at which the predator cannot invade the  $N_1$ - $N_2$  equilibrium, and thus Model (3.2) is not permanent. Parameters: same as in Figure 3.1. In panel (a), the prey are bistable in the absence of predation. In panel (b-d), prey 1 dominates prey 2 in the absence of predation. Evolutionary parameters  $\alpha_i$ ,  $\beta_i$ ,  $\tau_i$ ,  $\sigma^2$ , and  $\theta_i$  are chosen in a variety of ways to obtain the various sample trait curves.

dynamics,

$$(3.3) \quad \begin{aligned} \frac{dN_1}{dt} &= N_1(r_1 - N_1 - c_{12}N_2 - \bar{a}_1(\bar{x})P), \\ \frac{dN_2}{dt} &= N_2(r_2 - N_2 - c_{21}N_1 - \bar{a}_2(\bar{x})P), \\ \frac{dP}{dt} &= Pf_P(N_1, N_2, P, \bar{x}), \\ \frac{d\bar{x}}{dt} &= 0, \end{aligned}$$

which is Model (3.1) with constant trait  $\bar{x}$ , and the “slow” evolutionary dynamics  $\frac{d\bar{x}}{dt}$ . To formulate the slow dynamics, we consider three cases: (i) Model (3.3) has a globally stable equilibrium  $E_{++}^+$ ,  $E_{+0}^+$ ,  $E_{0+}^+$ , or  $E_{0+}^0$ , (ii) Model (3.3) exhibits oscillatory permanence, and (iii) Model (3.3) is bistable.

For case (i), let  $G \subset [\theta_1, \theta_2]$  be such that for each  $\bar{x} \in G$ , an equilibrium  $E(\bar{x})$  of Model (3.3) is globally stable (e.g., Fig. 3.1b). Then the “slow” evolutionary dynamics for  $\bar{x} \in G$  are given by

$$(3.4) \quad \frac{d\bar{x}}{dt} = \sigma_G^2 \frac{\partial f_P}{\partial \bar{x}} \Big|_{(N_1, N_2, P, \bar{x})=E(\bar{x})}.$$

For case (ii), Hofbauer and Sigmund [1998, Theorem 5.2.3] showed that for Model (3.1), if there is a solution  $(N_1(t), N_2(t), P(t))$  whose  $\omega$ -limit set lies in  $(0, \infty)^3$ , then

$$\lim_{T \rightarrow \infty} \frac{1}{T} \int_0^T (N_1(t), N_2(t), P(t)) dt = E_{++}^+.$$

In other words, the time-averaged densities of the ecological dynamics are equal to the coexistence equilibrium  $E_{++}^+$  densities. Thus, if  $\bar{x}$  is such that (3.3) is permanent, then for any initial condition  $(N_1(0), N_2(0), P(0), \bar{x}) \in S \setminus S_0$  we have,

$$(*) \quad \lim_{T \rightarrow \infty} \frac{1}{T} \int_0^T \frac{\partial f_P}{\partial \bar{x}} \Big|_{(N_1, N_2, P, \bar{x})=(N_1(t), N_2(t), P(t), \bar{x}(t))} dt = \frac{\partial f_P}{\partial \bar{x}} \Big|_{(N_1, N_2, P, \bar{x})=E_{++}^+(\bar{x})},$$

where  $E_{++}^+(\bar{x})$  denotes the interior equilibrium of Model (3.3) given  $\bar{x}$ . Let  $H \subset [\theta_1, \theta_2]$  such that for all  $\bar{x} \in H$ , there exists a global interior oscillatory attractor for Model (3.3). The “slow” evolutionary dynamics for  $\bar{x} \in H$  are given by

$$(3.5) \quad \frac{d\bar{x}}{dt} = \sigma_G^2 \frac{\partial f_P}{\partial \bar{x}} \Big|_{(N_1, N_2, P, \bar{x})=E_{++}^+(\bar{x})}.$$

For case (iii), given an  $\bar{x}$ , there are multiple attractors for Model (3.3). Let  $I \subset [\theta_1, \theta_2]$  such that for all  $\bar{x} \in I$ , Model (3.3) contains two or more ecological attractors. If  $\bar{x} \in I$ , then either (3.4) or (3.5) applies. If the initial condition lies in the basin of attraction for one of the equilibria, then (3.4) applies. Otherwise, the attractor is in the interior, implying (\*), and therefore (3.5) applies.

The slow dynamics  $\frac{d\bar{x}}{dt}$  may be discontinuous at any  $\bar{x}$  on the boundary between the regions described in cases (i)-(iii). For example, consider a trait curve which passes over three distinct regions: at extreme trait values, global stability at  $E_{+0}^+(\bar{x})$  or  $E_{0+}^+(\bar{x})$  equilibria, and at intermediate trait values, bistability between these two equilibria (Figs. 3.5 and 3.6c,d). For  $\bar{x}$  sufficiently close to  $\theta_1$  or  $\theta_2$ ,  $E_{+0}^+$  or  $E_{0+}^+$  is globally stable, and thus case (i) applies. For intermediate  $\bar{x}$ , these equilibria are bistable and thus case (iii) applies. Asymptotic approach toward  $E_{+0}^+$  causes  $\bar{x}$  to asymptotically approach  $\theta_1$ , respectively. This pushes  $(\bar{a}_1, \bar{a}_2)$  into a parameter region in which  $E_{0+}^+$  is globally stable. Eventually, prey 2 recovers and replaces prey 1. This triggers a reversal in the direction of evolution and asymptotic evolution of  $\bar{x}$  toward  $\theta_2$ , pushing  $(\bar{a}_1, \bar{a}_2)$  back into a parameter region in which  $E_{+0}^+$  is globally stable. Prey 1 eventually recovers and replaces prey 2, and the cycle begins again. One might suspect that the trait cycle extrema occur at the discontinuities of  $\frac{d\bar{x}}{dt}$ , but this is not the case (see Discussion). Next we describe three instances of complex dynamics that arise from timescale separation and these discontinuities (Fig. 3.6).

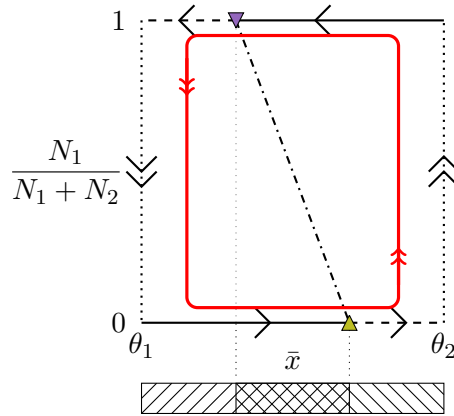


FIGURE 3.5. Eco-evolutionary fast-slow cycles in the limit as  $\sigma_G^2 \rightarrow 0$ . The trait curve in this example passes over three regions, represented by diagonal lines below the graph, matching with Figures 3.1a and 3.6c,d: at the extremes, global stability of  $E_{+0}^+$  or  $E_{0+}^+$ , and for intermediate values, bistability of  $E_{+0}^+$  and  $E_{0+}^+$ . Yellow and purple triangles also align with those from Figures 3.6c,d. The red curve represents an eco-evolutionary limit cycle.

If evolutionary parameters  $\alpha_i, \beta_i, \tau_i, \sigma^2$ , and  $\theta_i$  are such that the trait curve passes only through ecological parameter regions with a single attractor, then ecological dynamics asymptotically approach whatever attractor is globally stable given  $\bar{x}(t)$ . In Figures 3.6a,b, for example, the predator has an initial trait  $\bar{x}$  which in the absence of evolution, excludes prey 1 ( $E_{0+}^+$  is globally stable). The predator slowly evolves its trait to better suit prey 2, which pushes  $(\bar{a}_1, \bar{a}_2)$  into a parameter region in which all three species can coexist.

If the trait curve is such that Model (3.1) is bistable for some subset of  $[\theta_1, \theta_2]$ , then fast-slow oscillations can arise (Figs. 3.6c-f). The simplest example is shown in Figures 3.6c,d. Here, when the predator evolves to favor prey 1, its attack rate on prey 2 is low enough to allow prey 2 to recover and eventually replace prey 1. At this point,  $E_{0+}^+$  is globally stable. Once prey eventually replaces prey 1, the predator then evolves to favor prey 2. Its attack rate on prey 1 is then low enough to allow prey 1 to recover and eventually replace prey 2. At this point,  $E_{+0}^+$  is globally stable. So long as  $\sigma_G^2 > 0$ , Theorem 3.4 guarantees permanence even though there is no point at which the ecological subsystem is permanent in the absence of evolution.

A more complex example is shown in Figures 3.6e,f. Here, the trait curve covers five distinct regions described in the analysis of (3.1) (Section 3.4.1). In order of decreasing  $\bar{x}$ , they are (i) global stability of  $E_{+0}^+$ , (ii) bistability of  $E_{+0}^+$  and  $E_{0+}^+$ , (iii) global stability of  $E_{0+}^+$ , (iv) global stability of  $E_{++}^+$ , and (v) global stability of some interior oscillatory attractor. Unlike in Figures 3.6c,d, where the prey are bistable in the absence of predation, here prey 1 dominates prey 2 in the absence of predation and in the absence of evolution, permanence is guaranteed if the attack rate on the inferior prey is sufficiently low and the attack rate on the superior prey is sufficiently large. When the predator evolves to favor prey 1, all three species coexist in high-frequency ecological oscillations. The predator then evolves out of this region (blue triangle), leading to the exclusion of prey 1. The  $E_{0+}^+$  equilibrium remains stable until the predator completes its specialization on prey 2 (yellow triangle), allowing prey 1 to recover and nearly replace prey 2. Once this happens, the evolution of that  $\bar{x}$  reverses direction as the predator experiences directional selection to favor prey 1. Once the predator trait evolves out of the bistable region (purple triangle), prey 2 begins to recover and nearly replace prey 1, but this does not happen before the predator specializes on

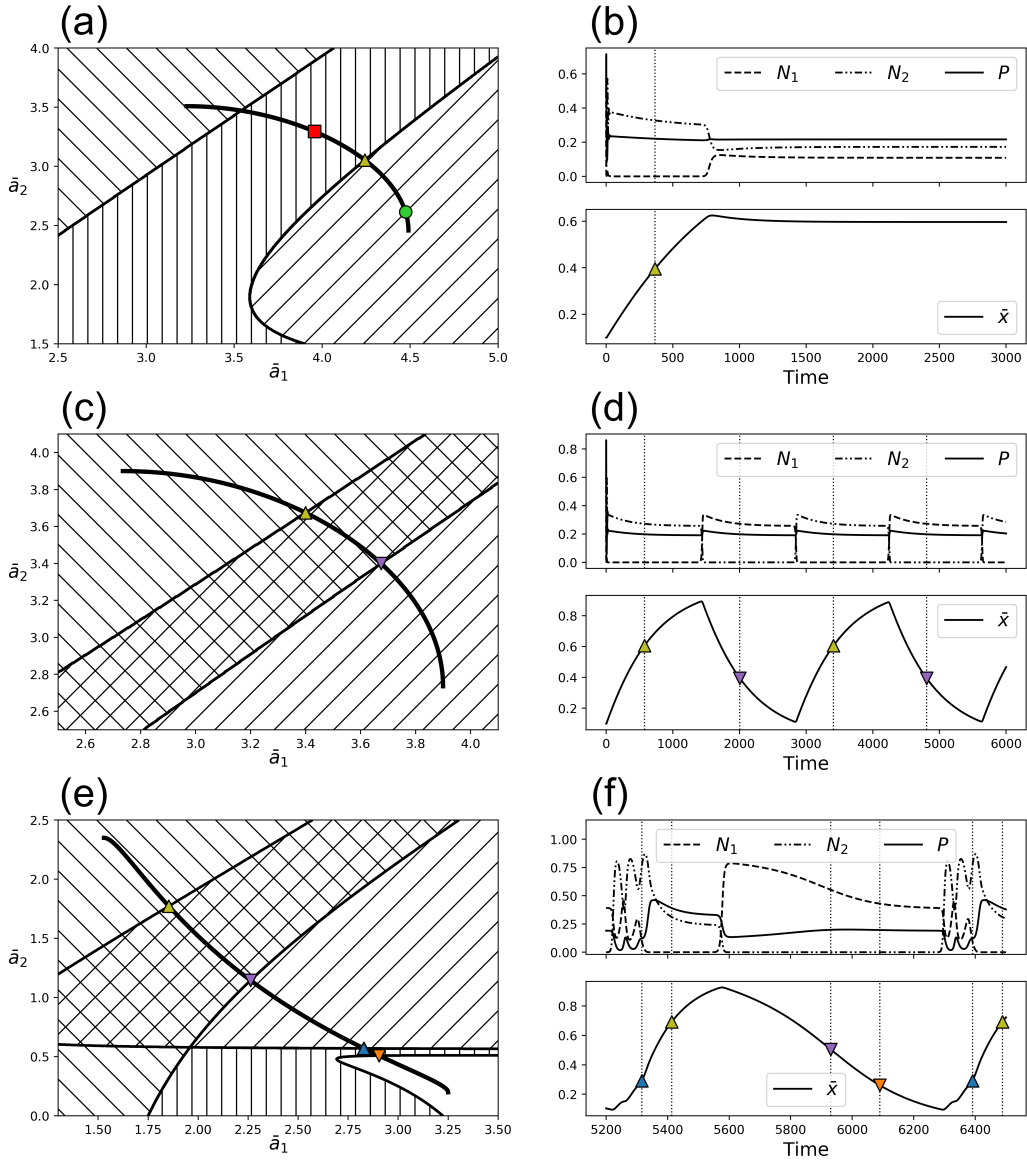


FIGURE 3.6. Eco-evolutionary fast-slow oscillations when evolution occurs at a slow time scale. In panels (a,c,e), triangles indicate the location of a discontinuity in the “slow” dynamics. The triangles and dotted vertical lines in panels (b,d,f) indicate the times at which these thresholds are passed. Upward-facing triangles indicate  $\frac{d\bar{x}}{dt} > 0$  and downward-facing triangles indicate  $\frac{d\bar{x}}{dt} < 0$ . In panel (a), a trait curve over a region of global stability for the ecological dynamics (Fig. 3.1b). The green circle and red square indicate the initial and final values for  $\bar{x}$  in the simulation shown in panel (b). In panel (c), a trait curve over a region of bistability for the ecological dynamics (Fig. 3.1a). At the times indicated by the dotted lines in panel (d), the missing prey can begin to recover. Once it eventually does it replaces the other, forcing a reversal in the direction of selection on the predator trait  $\bar{x}$ . In panel (e), a trait curve over a regions of bistability and (Continued on next page.)

FIGURE 3.6. (Previous page.) permanence for the ecological dynamics (Fig. 3.1d). Parameters:  $\theta_1 = 0$ ,  $\theta_2 = 1$ . In (a,b), same as Figure 3.1b,  $\sigma^2 = 0.0625$ ,  $\sigma_G^2 = 0.003125$ ,  $\alpha_1 = 1.6$ ,  $\alpha_2 = 1.1$ ,  $\beta_1 = 3$ ,  $\beta_2 = 2.5$ ,  $\tau_1 = \tau_2 = 0.9$ . In (c,d), same as Figure 3.1a,  $\sigma^2 = 0.12$ ,  $\sigma_G^2 = 0.004$ ,  $\alpha_1 = \alpha_2 = 1.1$ ,  $\beta_1 = \beta_2 = 3$ ,  $\tau_1 = \tau_2 = 0.9$ . In (e,f), same as in Figure 3.1d,  $\sigma^2 = 0.07$ ,  $\sigma_G^2 = 0.003$ ,  $\alpha_1 = 1.45$ ,  $\alpha_2 = 0.1$ ,  $\beta_1 = 2.4$ ,  $\beta_2 = 3$ ,  $\tau_1 = \tau_2 = 0.3$ .

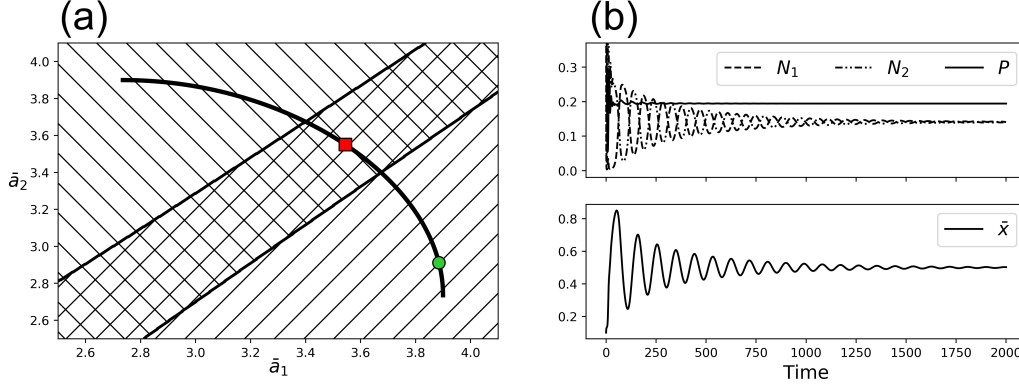


FIGURE 3.7. Faster evolution can stabilize ecologically unstable equilibria. In panel (a), a trait curve over a region of bistability for the ecological dynamics (Fig. 3.1a). The green circle and red square indicate the initial and final values for  $\bar{x}$  in the simulation shown in panel (b). Parameters as in Figures 3.6c,d but with  $\sigma_G^2 = 0.12$ .

prey 1 (orange triangle), allowing for the oscillatory coexistence of all three species, and the cycle begins again.

#### 3.4.4. Rapid Evolution Stabilizes an Otherwise Unstable Coexistence Equilibrium.

If evolution and ecology change on commensurate timescales, then cyclic permanence may be stabilized. Figure 3.7 shows dynamics of Model (3.2) in an environment equivalent to that of Figures 3.6c,d, but with genetic variation significantly greater. For these parameters, whether  $\sigma_G^2$  is small or large, Theorem 3.4 implies the system is permanent due to the eco-evolutionary feedbacks. However, when evolution occurs at a faster time scale, stabilizing selection forces the ecological dynamics to asymptotically approach the otherwise unstable coexistence equilibrium. This type of permanence is fundamentally different than what is seen in Figure 3.6; when evolution occurs quickly, ecological dynamics do not necessarily match with what one might expect from Model (3.1). In particular, if  $\sigma_G^2$  is sufficiently large there may be some asymptotically stable equilibrium  $E_{++}^+(\bar{x})$  of Model (3.2) which is asymptotically unstable in Model (3.1).

### 3.5. Discussion

We found conditions for global stability (Appendix A), as well as conditions for a Hopf bifurcation (Appendix B), in a general Lotka-Volterra model with a predator and two competing prey (Model 3.1). These results extend those of Takeuchi and Adachi [1983], who assumed equal predator conversion efficiencies ( $e_1 = e_2$ ). We also fully characterized the dynamics if (3.1) is not permanent and Prey 1 dominates Prey 2 in the absence of the predator (Theorem 3.3, Appendix C). When the prey are bistable in the absence of the predator, any form of coexistence co-occurs with a stable boundary equilibrium [Hutson and Vickers, 1983]. This eliminates the possibility for predator-mediated permanence between bistable prey. However, if the predator has an evolving trait which determines attack rates on the two prey, and if there is a tradeoff between these two attack rates, then permanence is possible (Theorem 3.4, Appendix D).

Eco-evolutionary mediated permanence in Model (3.2) can take on many qualitatively different forms. If the predator trait curve overlaps with a region of the  $\bar{a}_1$ - $\bar{a}_2$  space in which the coexistence equilibrium is globally stable, then the predator may evolve into this region and the ecological dynamics may asymptotically approach the coexistence equilibrium (Figs. 3.6a,b). However, trait curve overlap with a globally stable coexistence equilibrium region does not guarantee asymptotic evolution into that space. For example, whereas both trait curves in Figures 3.6a and 3.6e overlap with the region with globally stable coexistence (region with vertical lines), only in Figure 3.6a does evolution lead to an eco-evolutionary stable equilibrium in that region. Figure 3.6e, on the other hand, shows a scenario in which there is directional selection at any ecologically-stable coexistence equilibrium. Thus, even if there is a predator trait which allows for globally stable coexistence in the absence of evolution, evolution may select for oscillatory coexistence. Conversely, provided evolution occurs sufficiently quickly, a globally asymptotically stable eco-evolutionary equilibrium can arise even when the prey are bistable and the ecological subsystem (3.1) never admits permanence (Fig. 3.7). This effect is similar to one found by Patel et al. [2018], who generalized the eco-evolutionary competition model first analyzed by Vasseur et al. [2011]. These studies found that rapid or slow evolution can destabilize the eco-evolutionary dynamics, depending on the details of the evolutionary tradeoffs.

In our model, if the predator trait has very low heritability and evolves much slower than ecological processes (i.e. a timescale separation between the  $N_1$ - $N_2$ - $P$  and  $\bar{x}$  subsystems), then permanence may take on the form of an eco-evolutionary limit cycle. When this occurs, the amplitude of the oscillation increases as  $\sigma_G^2 \rightarrow 0$ . This type of parameter-dependent amplitude shift has been seen in many other settings, including food chain systems, predation on an age-structured prey, and competitive coexistence [Rinaldi and Muratori, 1992], although to our knowledge this study is the first to show this effect in scenarios with type 1 (linear) functional responses. Consider the case described for Figures 3.5 and 3.6c,d. In this limit, the system spends more time approaching  $E_{+0}^+$  or  $(E_{0+}^+)$ , which means prey 2 (or prey 1) spends more time with a negative invasion rate, reducing its density by orders of magnitude. This means it takes more time for prey 2 (or prey 1) to recover once its invasion rate becomes positive as  $\bar{x}$  passes the critical value. While a mathematically rigorous analysis required to derive the location of the “take-off” point [see, e.g., Hek, 2009] is beyond the scope of this study, there is a natural conjecture. Let  $T_0$  be the earliest time at which  $N_1 \leq \epsilon$  for some  $0 < \epsilon \ll 1$ . Denote  $T^*$  as the earliest time with  $T^* > T_0$  such that  $\frac{1}{N_1} \frac{dN_1}{dt} = 0$ . For all  $t \in (T_0, T^*)$ ,  $\frac{1}{N_1} \frac{dN_1}{dt} < 0$ . Denote  $T_f$  as the earliest time with  $T_f > T^* > T_0$  such that  $\int_{T^*}^{T_f} \frac{1}{N_1} \frac{dN_1}{dt} dt = - \int_{T_0}^{T^*} \frac{1}{N_1} \frac{dN_1}{dt} dt$ . We conjecture that the length of time in which  $(N_1, N_2, P, \bar{x})$  spends within an  $\epsilon$  distance from the  $N_1 = 0$  hyperplane is approximately  $T_f - T_0$ , which increases as  $\sigma_G \rightarrow 0$ . We leave verifying this conjecture as a challenge for a future study.

Evolution need not be slow in order to produce cyclic dynamics. Although what follows is a departure from true evolution, consider the case in which  $\sigma^2$  is held constant while  $\sigma_G^2 \rightarrow \infty$  [Cortez and Ellner, 2010]. Then there is a timescale separation between the “evolution” and ecology of Model (3.2), but the ecology is the slow system. For a given ecological state, the predator optimizes its trait such that its fitness is locally maximized. This type of dynamic resembles optimal foraging and prey switching that involves a behavioral trait rather than a genetic one. For such behavioral traits, van Baalen et al. [2001] showed optimal foraging mediates permanence between two competing prey. Future theoretical studies could follow the groundwork laid out by Patel et al. [2018] and consider the limit as  $\sigma_G^2 \rightarrow \infty$  in Model (3.2) to confirm their results in a Lotka-Volterra context.

Chase et al. [2002] challenged theoreticians and experimentalists to uncover how evolution can mediate permanence between bistable prey. Our study provides one such mechanism with an evolving predator. Vasseur et al. [2011] considered evolution of a competitor without predators. There, the evolving trait exhibited a tradeoff between inter- and intraspecific competition. Interestingly, increased heritability has different effects between their model and ours. In both studies, there is an eco-evolutionary Hopf bifurcation, but the direction is reversed. In our study, increased heritability can lead to asymptotic equilibrium stability, and cycles occur if heritability is sufficiently low. In their study, if eco-evolutionary cycles are possible at all, it is only if heritability is sufficiently large. The question remains: are there other ways for evolution to mediate permanence between bistable competitors? Recent theoretical studies have shown that evolution of different traits affects ecological dynamics in asymmetrical ways [Fleischer et al., 2018, 2020]. For example, if a predator has an evolving trait expressed as a tradeoff between the conversion efficiencies of the two prey, rather than the attack rates, is predator-mediated permanence possible in the case of bistable prey?

Theoreticians should also expand the community contexts in which eco-evo feedbacks mediate coexistence. For example, Lafferty et al. [2006] found that parasites are ubiquitous in food-webs. Thus future studies might consider the effect of multitrophic parasites on permanence between bistable prey [Fleischer et al., 2020]. Parasites which require predation to complete their lifecycle may benefit from increased predation on their intermediate host. This can increase parasite prevalence, which can depress the predator population and allow for the other prey population to recover. Predation on the newly recovered prey can then increase, boosting the predator population. But this increase also comes with an increase in the transmission of the parasites in this recovered prey, and the cycle begins again. Evolution of predator or prey resistance or immunity to parasitism, evolution of parasite transmissibility, and evolution of parasite-induced behavior changes in a host may also complicate dynamics and mediate permanence.

Finally, there is a need to understand the role of environmental stochasticity on eco-evolutionary dynamics. One consequence of the deterministic model is the need for condition (v) in Theorem 3.4. If that condition does not hold, then there is a stable manifold of the  $N_1$ - $N_2$  equilibrium that passes through the interior. This prevents permanence because not all positive initial conditions lead to dynamics in the interior. We suspect that some form of stochasticity essentially solves this

problem, as any dynamics on this stable manifold are almost surely guaranteed to be pushed off, allowing for almost-sure permanence for any positive initial condition. Indeed, this has been shown for a stochastic ordinary differential equation model of two prey with a switching predator [Hening et al., 2020]. Future studies may show that in a stochastic version of Model (3.2), Theorem 3.4 may still hold even without the condition that predators must be able to invade at the otherwise unstable  $N_1$ - $N_2$  equilibrium.

## APPENDIX A

### Chaper 1 (Pick Your Tradeoffs Wisely) Appendices

#### A.1. Model Derivation

**A.1.1. Identities.** Recall the following:

$$\int_{\mathbb{R}} \frac{1}{\sqrt{2\pi\sigma^2}} \exp\left[-\frac{(x-\bar{x})^2}{2\sigma^2}\right] dx = 1,$$

and for  $X > 0$ ,

$$\int_{\mathbb{R}} \exp[-(Xx^2 + Yx + Z)] dx = \sqrt{\frac{\pi}{X}} \exp\left[\frac{Y^2}{4X} - Z\right].$$

**A.1.2. Average Attack Rate.** For predators with trait value  $p$  and prey with trait value  $n$ , the attack rate  $a(p, n)$  is given by

$$a(p, n) = \alpha \exp\left[-\frac{((p-n)-\theta)^2}{2\tau_a^2}\right].$$

Since the distributions of predator and prey traits,  $q_p$  and  $q_n$ , respectively, are given by

$$q_p(p, \bar{p}) = \frac{1}{\sqrt{2\pi\sigma^2}} \exp\left[-\frac{(p-\bar{p})^2}{2\sigma^2}\right] \quad \text{and} \quad q_n(n, \bar{n}) = \frac{1}{\sqrt{2\pi\beta^2}} \exp\left[-\frac{(n-\bar{n})^2}{2\beta^2}\right],$$

then the average attack rate  $\bar{a}(\bar{p}, \bar{n})$  is given by

$$\begin{aligned} \bar{a}(\bar{p}, \bar{n}) &= \int_{\mathbb{R}^2} a(p, n) q_p(p, \bar{p}) q_n(n, \bar{n}) dp dn \\ &= \frac{\alpha}{2\pi\sigma\beta} \int_{\mathbb{R}^2} \exp\left[-\frac{((p-n)-\theta)^2}{2\tau_a^2} - \frac{(p-\bar{p})^2}{2\sigma^2} - \frac{(n-\bar{n})^2}{2\beta^2}\right] dp dn \\ &= \frac{\alpha}{2\pi\sigma\beta} \int_{\mathbb{R}} \exp\left[-\frac{(n-\bar{n})^2}{2\beta^2}\right] \int_{\mathbb{R}} \exp[-(Xp^2 + Yp + Z)] dp dn, \end{aligned}$$

where  $X = \frac{\sigma^2 + \tau_a^2}{2\sigma^2\tau_a^2}$ ,  $Y = -\frac{\sigma^2(n + \theta) + \tau_a^2\bar{p}}{\tau_a^2\sigma^2}$ , and  $Z = \frac{\sigma^2(n + \theta)^2 + \tau_a^2\bar{p}^2}{2\sigma^2\tau_a^2}$ . Then

$$\sqrt{\pi}X \exp\left[\frac{Y^2}{4X} - Z\right] = \frac{\sigma\tau_a\sqrt{2\pi}}{\sqrt{\sigma^2 + \tau_a^2}} \exp\left[-\frac{((\bar{p} - n) - \theta)^2}{2(\sigma^2 + \tau_a^2)}\right].$$

Thus,

$$\begin{aligned} \bar{a}(\bar{p}, \bar{n}) &= \frac{\alpha\tau_a}{\beta\sqrt{2\pi(\sigma^2 + \tau_a^2)}} \int_{\mathbb{R}} \exp\left[-\frac{((\bar{p} - n) - \theta)^2}{2(\sigma^2 + \tau_a^2)} - \frac{(n - \bar{n})^2}{2\beta^2}\right] dn \\ &= \frac{\alpha\tau_a}{\beta\sqrt{2\pi(\sigma^2 + \tau_a^2)}} \int_{\mathbb{R}} \exp[-(Xn^2 + Yn + Z)] dn, \end{aligned}$$

where  $X = \frac{\tau_a^2 + \sigma^2 + \beta^2}{2\beta^2(\sigma^2 + \tau_a^2)}$ ,  $Y = -\frac{(\bar{p} - \theta)\beta^2 + (\sigma^2 + \tau_a^2)\bar{n}}{\beta^2(\sigma^2 + \tau_a^2)}$ , and  $Z = \frac{(\bar{p} - \theta)^2\beta^2 + \bar{n}^2(\sigma^2 + \tau_a^2)}{2\beta^2(\sigma^2 + \tau_a^2)}$ .

Then

$$\sqrt{\pi}X \exp\left[\frac{Y^2}{4X} - Z\right] = \frac{\beta\sqrt{2\pi(\sigma^2 + \tau_a^2)}}{\sqrt{\beta^2 + \sigma^2 + \tau_a^2}} \exp\left[-\frac{((\bar{p} - \bar{n}) - \theta)^2}{2(\beta^2 + \sigma^2 + \tau_a^2)}\right].$$

Thus,

$$\bar{a}(\bar{p}, \bar{n}) = \frac{\alpha\tau_a}{\sqrt{\tau_a^2 + \sigma^2 + \beta^2}} \exp\left[-\frac{((\bar{p} - \bar{n}) - \theta)^2}{2(\tau_a^2 + \sigma^2 + \beta^2)}\right].$$

**A.1.3. Average Growth Rate.** The growth rate of prey individuals with trait value  $n$  is given by

$$r(n) = \rho \exp\left[-\frac{(n - \theta_r)^2}{2\tau_r^2}\right].$$

Given the same normal distribution of prey traits as above, then the average growth rate  $\bar{r}(\bar{n})$  is given by

$$\begin{aligned} \bar{r}(\bar{n}) &= \int_{\mathbb{R}} r(n)q_n(n, \bar{n})dn \\ &= \frac{\rho}{\beta\sqrt{2\pi}} \int_{\mathbb{R}} \exp[-(Xn^2 + Yn + Z)] dn, \end{aligned}$$

where  $X = \frac{\beta^2 + \theta_r^2}{2\beta^2\theta_r^2}$ ,  $Y = -\frac{\theta_r\beta^2 + \bar{n}\theta_r^2}{\beta^2\theta_r^2}$ , and  $Z = \frac{\theta_r^2\beta^2 + \bar{n}^2\theta_r^2}{2\beta^2\theta_r^2}$ . Then

$$\sqrt{\frac{\pi}{X}} \exp\left[\frac{Y^2}{4X} - Z\right] = \frac{\beta\theta_r\sqrt{2\pi}}{\sqrt{\beta^2 + \theta_r^2}} \exp\left[-\frac{(\bar{n} - \theta_r)^2}{2(\beta^2 + \theta_r^2)}\right].$$

Thus,

$$\bar{r}(\bar{n}) = \frac{\rho\theta_r}{\sqrt{\beta^2 + \theta_r^2}} \exp\left[-\frac{(\bar{n} - \theta_r)^2}{2(\beta^2 + \theta_r^2)}\right].$$

**A.1.4. Average Predator Fitness.** Let  $W(N, n, p) = ea(p, n)N - d$ , where  $e$  and  $d$  are constant and  $a(p, n)$  is as above. Then the average predator fitness  $\bar{W}(N, \bar{n}, \bar{p})$  is given by

$$\bar{W}(N, \bar{n}, \bar{p}) = \int_{\mathbb{R}^2} W(N, n, p)q_p(p, \bar{p})q_n(n, \bar{n})dpdn,$$

where  $q_p$  and  $q_n$  are given above. Then

$$\begin{aligned} \bar{W}(N, \bar{n}, \bar{p}) &= eN \int_{\mathbb{R}^2} a(p, n)q_p(p, \bar{p})q_n(n, \bar{n})dpdn - d \int_{\mathbb{R}^2} q_p(p, \bar{p})q_n(n, \bar{n})dpdn \\ &= e\bar{a}(\bar{p}, \bar{n})N - d \end{aligned}$$

**A.1.5. Average Prey Fitness – Model 1.** Let  $Y(N, P, n, p) = r(n)\left(1 - \frac{N}{K}\right) - a(p, n)P$ , where  $r(n)$  and  $a(p, n)$  are given above. Then the average prey fitness  $\bar{Y}(N, P, \bar{n}, \bar{p})$  is given by

$$\bar{Y}(N, P, \bar{n}, \bar{p}) = \int_{\mathbb{R}^2} Y(N, P, n, p)q_p(p, \bar{p})q_n(n, \bar{n})dpdn,$$

where  $q_p$  and  $q_n$  are given above. Then

$$\begin{aligned} \bar{Y}(N, P, \bar{n}, \bar{p}) &= \left(1 - \frac{N}{K}\right) \int_{\mathbb{R}^2} r(n)q_p(p, \bar{p})q_n(n, \bar{n})dpdn - P \int_{\mathbb{R}^2} a(p, n)q_p(p, \bar{p})q_n(n, \bar{n})dpdn \\ &= \bar{r}(\bar{n})\left(1 - \frac{N}{K}\right) - \bar{a}(\bar{p}, \bar{n})P. \end{aligned}$$

**A.1.6. Average Prey Fitness – Model 2.** The resource use parameter for prey individuals with trait value  $n$  is given by

$$K(n) = \kappa \exp \left[ -\frac{(n - \theta_K)^2}{2\tau_K^2} \right].$$

Let the fitness of prey with trait value  $n$  interacting with predators with trait value  $p$  be

$$Y(N, P, n, p) = r \left( 1 - \frac{N}{K(n)} \right) - a(p, n)P.$$

Then the average prey fitness  $\bar{Y}(N, P, \bar{n}, \bar{p})$  is given by

$$\bar{Y}(N, P, \bar{n}, \bar{p}) = \int_{\mathbb{R}^2} Y(N, P, n, p) q_p(p, \bar{p}) q_n(n, \bar{n}) dp dn,$$

where the predator and prey trait distributions  $q_p$  and  $q_n$  are given above. Then

$$\begin{aligned} \bar{Y}(N, P, \bar{n}, \bar{p}) &= r \int_{\mathbb{R}^2} q_p(p, \bar{p}) q_n(n, \bar{n}) dp dn \\ &\quad - rN \int_{\mathbb{R}^2} \frac{1}{K(n)} q_p(p, \bar{p}) q_n(n, \bar{n}) dp dn \\ &\quad - P \int_{\mathbb{R}^2} a(p, n) q_p(p, \bar{p}) q_n(n, \bar{n}) dp dn \\ &= r - rN \int_{\mathbb{R}^2} \frac{1}{K(n)} q_n(n, \bar{n}) dn - \bar{a}(\bar{p}, \bar{n})P. \end{aligned}$$

However,

$$\begin{aligned} \int_{\mathbb{R}^2} \frac{1}{K(n)} q_n(n, \bar{n}) dn &= \frac{1}{\kappa \sqrt{2\pi\beta^2}} \int_{\mathbb{R}} \exp \left[ \frac{(n - \theta_K)^2}{2\tau_K^2} - \frac{(n - \bar{n})^2}{2\beta^2} \right] dn \\ &= \frac{1}{\kappa \sqrt{2\pi\beta^2}} \int_{\mathbb{R}} \exp[-(Xn^2 + Yn + Z)] dn, \end{aligned}$$

where  $X = \frac{\tau_K^2 - \beta^2}{2\tau_K^2\beta^2}$ ,  $Y = \frac{\beta^2\theta_K - \tau_K^2\bar{n}}{\tau_K^2\beta^2}$ , and  $Z = \frac{\tau_K^2\bar{n}^2 - \beta^2\theta_K^2}{2\tau_K^2\beta^2}$ . Then

$$\sqrt{\frac{\pi}{X}} \exp \left[ \frac{Y^2}{4X} - Z \right] = \frac{\tau_K\beta\sqrt{2\pi}}{\sqrt{\tau_K^2 - \beta^2}} \exp \left[ \frac{(\bar{n} - \theta_K)^2}{2(\tau_K^2 - \beta^2)} \right].$$

Thus,

$$\int_{\mathbb{R}^2} \frac{1}{K(n)} q_n(n, \bar{n}) dn = \frac{\tau_K}{\kappa \sqrt{\tau_K^2 - \beta^2}} \exp \left[ \frac{(\bar{n} - \theta_K)^2}{2(\tau_K^2 - \beta^2)} \right].$$

Thus,

$$\bar{Y}(N, P, \bar{n}, \bar{p}) = r \left( 1 - \frac{N}{\bar{K}(\bar{n})} \right) - \bar{a}(\bar{p}, \bar{n})P,$$

where

$$\bar{K}(\bar{n}) = \frac{\kappa \sqrt{\tau_K^2 - \beta^2}}{\tau_K} \exp \left[ -\frac{(\bar{n} - \theta_K)^2}{2(\tau_K^2 - \beta^2)} \right].$$

Note that  $\bar{K}(\bar{n})$  is the harmonic mean of prey carrying capacity over the population:

$$\bar{K}(\bar{n}) = \left( \int_{\mathbb{R}} \frac{1}{K(n)} q_K(n, \bar{n}) dn \right)^{-1}.$$

## A.2. Model 1 Analysis

**A.2.1. Equilibria.** Model 1 is

$$\begin{aligned} f_1 &= \frac{dP}{dt} = P[e\bar{a}(\bar{p}, \bar{n})N - d] \\ f_2 &= \frac{dN}{dt} = N \left[ \bar{r}(\bar{n}) \left( 1 - \frac{N}{\bar{K}} \right) - \bar{a}(\bar{p}, \bar{n})P \right] \\ f_3 &= \frac{d\bar{p}}{dt} = \sigma_G^2 \frac{eN(\theta_a - (\bar{p} - \bar{n}))}{A} \bar{a}(\bar{p}, \bar{n}) \\ f_4 &= \frac{d\bar{n}}{dt} = \beta_G^2 \left[ \bar{r}(\bar{n}) \left( 1 - \frac{N}{\bar{K}} \right) \frac{\theta_r - \bar{n}}{B} + \frac{P(\theta_a - (\bar{p} - \bar{n}))}{A} \bar{a}(\bar{p}, \bar{n}) \right] \end{aligned}$$

where

$$\begin{aligned} A &= \tau_a^2 + \sigma^2 + \beta^2, & B &= \beta^2 + \tau_r^2, \\ \bar{a}(\bar{p}, \bar{n}) &= \frac{\alpha \tau_a}{\sqrt{A}} \exp \left[ -\frac{((\bar{p} - \bar{n}) - \theta_a)^2}{2A} \right], & \text{and} & \quad \bar{r}(\bar{n}) = \frac{\rho \tau_r}{\sqrt{B}} \exp \left[ -\frac{(\bar{n} - \theta_r)^2}{2B} \right]. \end{aligned}$$

Set  $f_1 = f_2 = f_3 = f_4 = 0$  to find equilibria:

$$\begin{aligned}
f_1 = 0 &\implies P = 0 \quad \text{or} & N &= \frac{d}{e\bar{a}(\bar{p}, \bar{n})} \\
f_2 = 0 &\implies N = 0 \quad \text{or} & P &= \frac{\bar{r}(\bar{n})}{\bar{a}(\bar{p}, \bar{n})} \left(1 - \frac{N}{K}\right) \\
f_3 = 0 &\implies N = 0 \quad \text{or} & \bar{p} - \bar{n} &= 0 \\
f_4 = 0 &\implies P = 0 \quad \text{or} & \bar{r}(\bar{n}) \left(1 - \frac{N}{K}\right) \frac{\theta_r - \bar{n}}{B} &= \frac{P((\bar{p} - \bar{n}) - \theta_a)}{A} \bar{a}(\bar{p}, \bar{n})
\end{aligned}$$

If  $P = N = 0$ , then equilibrium is satisfied and  $\bar{p}$  and  $\bar{n}$  are arbitrary. This gives the extinction equilibria. Suppose  $P = 0$  but  $N \neq 0$ . Then  $f_2 = 0 \implies N = K$  and  $f_3 = 0 \implies \bar{p} - \bar{n} = \theta_a$ . This gives the exclusion equilibria. Suppose  $P \neq 0$  and  $N \neq 0$ . Then  $f_3 = 0 \implies \bar{p} - \bar{n} = \theta_a \implies \bar{a}(\bar{p}, \bar{n}) = \frac{\alpha\tau_a}{\sqrt{A}}$ . Since  $\bar{p} - \bar{n} = \theta_a$ , then  $f_4 = 0 \implies \bar{n} = \theta_r$  or  $N = K$ . But if  $N = K$ , then  $f_2 = 0 \implies P = 0$ , which is a contradiction. Thus  $\bar{n} = \theta_r$ , which implies  $\bar{p} = \theta_r + \theta_a$  and  $P = \frac{\rho\tau_r\sqrt{A}}{\alpha\tau_a\sqrt{B}} \left(1 - \frac{\sqrt{A}}{Ke\alpha\tau_a}\right)$ . By exhaustion, this gives the only other equilibrium: the coexistence equilibrium point.

**A.2.2. Stability Conditions.** To solve for local stability conditions, we find the eigenvalues of the community matrix  $J$  evaluated at each equilibrium point. Let the extinction, exclusion, and coexistence equilibria be denoted as

$$\begin{aligned}
E_{\text{ext}} &= (0, 0, \mu^*, \nu^*), \\
E_{\text{excl}} &= (0, K, \nu^* + \theta_a, \nu^*), \\
E_{\text{coex}} &= \left( \frac{\rho\tau_r\sqrt{A}}{\alpha\tau_a\sqrt{B}} \left(1 - \frac{N^*}{K}\right), \frac{d\sqrt{A}}{e\alpha\tau_a}, \theta_r + \theta_a, \theta_r \right).
\end{aligned}$$

The Jacobia evaluated at the extinction equilibria are

$$J|_{E_{\text{ext}}} = \begin{pmatrix} -d & 0 & 0 & 0 \\ 0 & \frac{\rho\tau_r}{\sqrt{B}} \exp\left[-\frac{(\nu^* - \theta_r)^2}{2B}\right] & 0 & 0 \\ 0 & \frac{\sigma_G^2 e(\theta_a - (\mu^* - \nu^*)) \bar{a}(\mu^*, \nu^*)}{A} & 0 & 0 \\ \frac{\beta_G^2 (\theta_a - (\mu^* - \nu^*)) \bar{a}(\mu^*, \nu^*)}{A} & -\frac{\beta_G^2 \bar{r}(\nu^*)}{K} \cdot \frac{\theta_r - \nu^*}{B} & 0 & \frac{\beta_G^2 \bar{r}(\nu^*)}{B} \left(\frac{(\theta_r - \nu^*)^2}{B} - 1\right) \end{pmatrix}$$

This is an upper-triangular matrix, and thus the eigenvalues are the entries on the main diagonal:  $-d$ ,  $\frac{\rho\tau_r}{\sqrt{B}} \exp\left[-\frac{(\nu^*-\theta_r)^2}{2B}\right]$ , 0, and  $\frac{\beta_G^2 \bar{r}(\nu^*)}{B} \left(\frac{\theta_r-\nu^*}{B} - 1\right)$ . Since one of the eigenvalues is positive, namely  $\frac{\rho\tau_r}{\sqrt{B}} \exp\left[-\frac{(\nu^*-\theta_r)^2}{2B}\right]$ , then  $E_{\text{ext}}$  is locally unstable. The Jacobian evaluated at the exclusion equilibria are

$$J|_{E_{\text{excl}}} = \begin{pmatrix} \frac{Ke\alpha\tau_a}{\sqrt{A}} - d & 0 & 0 & 0 \\ -\frac{K\alpha\tau_a}{\sqrt{A}} & -\frac{\rho\tau_r}{\sqrt{B}} \exp\left[-\frac{(\mu^*-\theta_r)^2}{2B}\right] & 0 & 0 \\ 0 & 0 & -\frac{\sigma_G^2 Ke\alpha\tau_a}{A^{3/2}} & \frac{\sigma_G^2 Ke\alpha\tau_a}{A^{3/2}} \\ 0 & -\frac{\beta_G^2 \rho\tau_r}{K\sqrt{B}} \exp\left[-\frac{(\nu^*-\theta_r)^2}{2B}\right] \cdot \frac{\theta_r-\mu^*}{B} & 0 & 0 \end{pmatrix}$$

The eigenvalues are  $\frac{Ke\alpha\tau_a}{\sqrt{A}} - d$ ,  $-\frac{\rho\tau_r}{\sqrt{B}} \exp\left[-\frac{(\mu^*-\theta_r)^2}{2B}\right]$ ,  $-\frac{\sigma_G^2 Ke\alpha\tau_a}{A^{3/2}}$ , and 0 (by swapping the third and fourth rows and columns, we obtain an upper-triangular matrix). Since all of these are non-positive if  $d > \frac{Ke\alpha\tau_a}{\sqrt{A}}$ , the exclusion equilibria are not unstable, but since one of the eigenvalues is 0 and the manifold of equilibria is unbounded, we cannot say the equilibria are stable. However, all of our simulations suggest stability if  $d > \frac{Ke\alpha\tau_a}{\sqrt{A}}$ . The Jacobian evaluated at the coexistence equilibrium point is

$$J|_{E_{\text{coex}}} = \begin{pmatrix} 0 & \frac{e\rho\tau_r}{\sqrt{B}} \left(1 - \frac{N^*}{K}\right) & 0 & 0 \\ -\frac{d}{e} & -\frac{\rho\tau_r N^*}{K\sqrt{B}} & 0 & 0 \\ 0 & 0 & -\frac{\sigma_G^2 d}{A} & \frac{\sigma_G^2 d}{A} \\ 0 & 0 & -\frac{\beta_G^2 \rho\tau_r}{A\sqrt{B}} \left(1 - \frac{N^*}{K}\right) & \frac{\beta_G^2 \rho\tau_r}{A\sqrt{B}} \left(1 - \frac{N^*}{K}\right) \left(\frac{1}{A} - \frac{1}{B}\right) \end{pmatrix}$$

This is a block-diagonal matrix, and so the eigenvalues of  $J|_{E_{\text{coex}}}$  are simply the eigenvalues of each block,

$$J_1 = \begin{pmatrix} 0 & \frac{e\rho\tau_r}{\sqrt{B}} \left(1 - \frac{N^*}{K}\right) \\ -\frac{d}{e} & -\frac{\rho\tau_r N^*}{K\sqrt{B}} \end{pmatrix} \text{ and } J_2 = \begin{pmatrix} -\frac{\sigma_G^2 d}{A} & \frac{\sigma_G^2 d}{A} \\ -\frac{\beta_G^2 \rho\tau_r}{A\sqrt{B}} \left(1 - \frac{N^*}{K}\right) & \frac{\beta_G^2 \rho\tau_r}{A\sqrt{B}} \left(1 - \frac{N^*}{K}\right) \left(\frac{1}{A} - \frac{1}{B}\right) \end{pmatrix}$$

The eigenvalues of  $J_1$  are

$$\lambda_{1,2} = \frac{1}{2} \left[ -\frac{\rho\tau_r N^*}{K\sqrt{B}} \pm \sqrt{\left(\frac{\rho\tau_r N^*}{K\sqrt{B}}\right)^2 - \frac{4\rho\tau_r d}{\sqrt{B}} \left(1 - \frac{N^*}{K}\right)} \right].$$

Biological feasibility requires  $N^* < K$ , and so  $\sqrt{\left(\frac{\rho\tau_r N^*}{K\sqrt{B}}\right)^2 - \frac{4\rho\tau_r d}{\sqrt{B}}\left(1 - \frac{N^*}{K}\right)} < \left|\frac{\rho\tau_r N^*}{K\sqrt{B}}\right|$ . Thus,  $\text{Re}(\lambda_{1,2}) < 0$ . For ease, define

$$F := \frac{d\sigma_G^2}{A} \quad \text{and} \quad G := \frac{\beta_G^2 \rho\tau_r}{\sqrt{B}} \left(1 - \frac{N^*}{K}\right).$$

Then the eigenvalues of  $J_2$  are

$$\lambda_{3,4} = \frac{1}{2} \left[ - \left( F + G \left( \frac{1}{B} - \frac{1}{A} \right) \right) \pm \sqrt{\Delta} \right],$$

where

$$\Delta = \left( F + G \left( \frac{1}{B} - \frac{1}{A} \right) \right)^2 - \frac{4FG}{A}.$$

Again, since  $N^* < K$ , then  $G > 0$ . If  $\Delta > 0$ , then  $\sqrt{\Delta} < \left| F + G \left( \frac{1}{B} - \frac{1}{A} \right) \right|$ . Then

$$\begin{aligned} \text{Re}(\lambda_{3,4}) < 0 &\iff F + G \left( \frac{1}{B} - \frac{1}{A} \right) > 0 \\ &\iff \frac{\sigma_G^2}{\beta_G^2} > \frac{\rho\tau_r}{d\sqrt{B}} \left( 1 - \frac{d\sqrt{A}}{Ke\alpha\tau_a} \right) \left( 1 - \frac{A}{B} \right) \end{aligned}$$

If  $\Delta \leq 0$ , then  $2\text{Re}(\lambda_{3,4}) = -\left( F + G \left( \frac{1}{B} - \frac{1}{A} \right) \right)$ , and thus  $\text{Re}(\lambda_{3,4}) < 0$  if and only if the same exact condition holds.

Note the existence of a Hopf bifurcation when  $F + G \left( \frac{1}{B} - \frac{1}{A} \right) = 0$ , which is equivalent to

$$\frac{\sigma_G^2}{\beta_G^2} = \frac{\rho\tau_r}{d\sqrt{B}} \left( 1 - \frac{d\sqrt{A}}{Ke\alpha\tau_a} \right) \left( 1 - \frac{A}{B} \right).$$

Hopf Bifurcations occur when eigenvalues are complex (which is always true since  $\Delta < 0 \iff \frac{4d\sigma_G^2\beta_G^2\rho\tau_r}{A^2\sqrt{B}} \left( 1 - \frac{N^*}{K} \right) > 0$  and biological feasibility requires  $N^* < K$ ) and when the real part of the eigenvalues cross the imaginary axis as a parameter is shifted. As the real part of the eigenvalues becomes positive, the equilibrium becomes unstable, resulting in cyclic behavior around the equilibrium.

### A.3. Model 2 Analysis

**A.3.1. Equilibria.** Model 2 is given by

$$\begin{aligned}
 f_1 &= \frac{dP}{dt} = P[e\bar{a}(\bar{p}, \bar{n})N - d] \\
 f_2 &= \frac{dN}{dt} = N \left[ r \left( 1 - \frac{N}{\bar{K}(\bar{n})} \right) - \bar{a}(\bar{p}, \bar{n})P \right] \\
 f_3 &= \frac{d\bar{p}}{dt} = \sigma_G^2 \frac{eN(\theta - (\bar{p} - \bar{n}))}{A} \bar{a}(\bar{p}, \bar{n}) \\
 f_4 &= \frac{d\bar{n}}{dt} = \beta_G^2 \left[ -\frac{rN(\bar{n} - \theta_K)}{\bar{K}(\bar{n})C} + \frac{P(\theta - (\bar{p} - \bar{n}))}{A} \bar{a}(\bar{p}, \bar{n}) \right]
 \end{aligned}$$

where

$$A = \tau_a^2 + \sigma^2 + \beta^2, \quad C = \tau_K^2 - \beta^2,$$

$$\bar{a}(\bar{p}, \bar{n}) = \frac{\alpha\tau_a}{\sqrt{A}} \exp \left[ -\frac{((\bar{p} - \bar{n}) - \theta)^2}{2A} \right], \quad \text{and} \quad \bar{K}(\bar{n}) = \frac{\kappa\sqrt{C}}{\tau_K} \exp \left[ -\frac{(\bar{n} - \theta_K)^2}{2C} \right].$$

Set  $f_1 = f_2 = f_3 = f_4 = 0$  to find equilibria:

$$\begin{aligned}
 f_1 = 0 &\implies P = 0 \quad \text{or} \quad N = \frac{d}{e\bar{a}(\bar{p}, \bar{n})} \\
 f_2 = 0 &\implies N = 0 \quad \text{or} \quad P = \frac{r}{\bar{a}(\bar{p}, \bar{n})} \left( 1 - \frac{N}{\bar{K}(\bar{n})} \right) \\
 f_3 = 0 &\implies N = 0 \quad \text{or} \quad \bar{p} - \bar{n} = \theta \\
 f_4 = 0 &\implies P = 0 \quad \text{or} \quad \frac{rN(\bar{n} - \theta_K)}{\bar{K}(\bar{n})C} = \frac{P(\theta - (\bar{p} - \bar{n}))}{A} \bar{a}(\bar{p}, \bar{n})
 \end{aligned}$$

If  $P = N = 0$ , then equilibrium is satisfied and  $\bar{p}$  and  $\bar{n}$  are arbitrary. This gives the extinction equilibria. Suppose  $P = 0$  but  $N \neq 0$ . Then  $f_2 = 0 \implies N = \bar{K}(\bar{n})$  and  $f_3 = 0 \implies \bar{p} - \bar{n} = \theta$ .  $f_4 = 0 \implies \bar{n} = \theta_K \implies \bar{p} = \theta_K + \theta \implies N = \bar{K}(\theta_K) = \frac{\kappa\sqrt{C}}{\tau_K}$ . This gives the exclusion equilibria. Suppose  $P \neq 0$  and  $N \neq 0$ . Then  $f_3 = 0 \implies \bar{p} - \bar{n} = \theta \implies \bar{a}(\bar{p}, \bar{n}) = \frac{\alpha\tau_a}{\sqrt{A}}$ . Then  $f_1 = 0 \implies N = \frac{d\sqrt{A}}{e\alpha\tau_a}$ . Since  $\bar{p} - \bar{n} = \theta$ , then  $f_4 = 0 \implies \bar{n} = \theta_K \implies \bar{p} = \theta_K + \theta$ . Then  $f_2 = 0 \implies P = \frac{r\sqrt{A}}{\alpha\tau_a} \left( 1 - \frac{N}{\bar{K}(\theta_K)} \right)$ . By exhaustion, this gives the only other equilibrium: the coexistence equilibrium point.

**A.3.2. Stability Conditions.** To solve for local stability conditions, we find the eigenvalues of the community matrix  $J$  evaluated at each equilibrium point. Let the extinction, exclusion, and coexistence equilibria be denoted as

$$\begin{aligned} E_{\text{ext}} &= (0, 0, \mu^*, \nu^*), \\ E_{\text{excl}} &= (0, K, \theta_K + \theta, \theta_K), \\ E_{\text{coex}} &= \left( \frac{r\sqrt{A}}{\alpha\tau_a} \left( 1 - \frac{N^*\tau_K}{\kappa\sqrt{C}} \right), \frac{d\sqrt{A}}{e\alpha\tau_a}, \theta_K + \theta, \theta_K \right). \end{aligned}$$

Then

$$J|_{E_{\text{ext}}} = \begin{pmatrix} -d & 0 & 0 & 0 \\ 0 & r & 0 & 0 \\ 0 & \frac{\sigma_G^2 e(\theta - (\mu^* - \nu^*))\bar{a}(\mu^*, \nu^*)}{A} & 0 & 0 \\ \frac{\beta_G^2 (\theta - (\mu^* - \nu^*))\bar{a}(\mu^*, \nu^*)}{A} & \frac{\beta_G^2 r(\theta_K - \nu^*)}{K(\nu^*)C} & 0 & 0 \end{pmatrix}$$

This is an upper-triangular matrix, and thus the eigenvalues are the entries on the main diagonal:  $-d$ ,  $r$ , and  $0$ . Since one of the eigenvalues is positive, namely  $r$ , then  $E_{\text{ext}}$  is locally unstable.

$$J|_{E_{\text{excl}}} = \begin{pmatrix} \frac{e\alpha\tau_a\kappa\sqrt{C}}{\tau_K\sqrt{A}} - d & 0 & 0 & 0 \\ -\frac{\alpha\tau_a\kappa\sqrt{C}}{\tau_K\sqrt{A}} & -r & 0 & 0 \\ 0 & 0 & -\frac{\sigma_G^2 e\alpha\tau_a\kappa\sqrt{C}}{\tau_K A^{3/2}} & \frac{\sigma_G^2 e\alpha\tau_a\kappa\sqrt{C}}{\tau_K A^{3/2}} \\ 0 & 0 & 0 & -\frac{\beta_G^2 r}{C} \end{pmatrix}$$

This is a block-diagonal matrix, and so the eigenvalues of  $J|_{E_{\text{excl}}}$  are simply the eigenvalues of each block. Each block is triangular, so the eigenvalues are the entries on the diagonals:  $\frac{e\alpha\tau_a\kappa\sqrt{C}}{\tau_K\sqrt{A}} - d$ ,  $-r$ ,  $-\frac{\sigma_G^2 e\alpha\tau_a\kappa\sqrt{C}}{\tau_K A^{3/2}}$ , and  $-\frac{\beta_G^2 r}{C}$ . All of these are non-positive, indicating local asymptotic stability, if  $d > \frac{e\alpha\tau_a\kappa\sqrt{C}}{\tau_K\sqrt{A}}$ .

$$J|_{E_{\text{coex}}} = \begin{pmatrix} 0 & er\left(1 - \frac{N^*}{\bar{K}(\theta_K)}\right) & 0 & 0 \\ -\frac{d}{e} & -\frac{rN^*}{\bar{K}(\theta_K)} & 0 & 0 \\ 0 & 0 & -\frac{\sigma_G^2 d}{A} & \frac{\sigma_G^2 d}{A} \\ 0 & 0 & -\frac{\beta_G^2 r}{A}\left(1 - \frac{N^*}{\bar{K}(\theta_K)}\right) & \frac{\beta_G^2 r}{A}\left(1 - \frac{N^*}{\bar{K}(\theta_K)}\left(1 + \frac{A}{C}\right)\right) \end{pmatrix}$$

This is a block-diagonal matrix, and so the eigenvalues of  $J|_{E_{\text{coex}}}$  are simply the eigenvalues of each block,

$$J_1 = \begin{pmatrix} 0 & er\left(1 - \frac{N^*}{\bar{K}(\theta_K)}\right) \\ -\frac{d}{e} & -\frac{rN^*}{\bar{K}(\theta_K)} \end{pmatrix} \quad \text{and} \quad J_2 = \begin{pmatrix} -\frac{\sigma_G^2 d}{A} & \frac{\sigma_G^2 d}{A} \\ -\frac{\beta_G^2 r}{A}\left(1 - \frac{N^*}{\bar{K}(\theta_K)}\right) & \frac{\beta_G^2 r}{A}\left(1 - \frac{N^*}{\bar{K}(\theta_K)}\left(1 + \frac{A}{C}\right)\right) \end{pmatrix}$$

The eigenvalues of  $J_1$  are

$$\lambda_{1,2} = \frac{1}{2} \left( -\frac{rN^*}{\bar{K}(\theta_K)} \pm \sqrt{\left(\frac{rN^*}{\bar{K}(\theta_K)}\right)^2 - 4rd\left(1 - \frac{N^*}{\bar{K}(\theta_K)}\right)} \right)$$

Biological feasibility requires  $N^* < \bar{K}(\theta_K)$ , and so  $\sqrt{\left(\frac{rN^*}{\bar{K}(\theta_K)}\right)^2 - 4rd\left(1 - \frac{N^*}{\bar{K}(\theta_K)}\right)} < \left|\frac{rN^*}{\bar{K}(\theta_K)}\right|$ . Thus,  $\text{Re}(\lambda_{1,2}) < 0$ . Note the trace and determinant of  $J_2$  are

$$\begin{aligned} \text{tr}(J_2) &= -\frac{\sigma_G^2 d}{A} + \frac{\beta_G^2 r}{A} \left(1 - \frac{N^*}{\bar{K}(\theta_K)} \left(1 + \frac{A}{C}\right)\right) \\ \det(J_2) &= -\frac{\sigma_G^2 \beta_G^2 dr}{A^2} \left(1 - \frac{N^*}{\bar{K}(\theta_K)} \left(1 + \frac{A}{C}\right)\right) + \frac{\sigma_G^2 \beta_G^2 dr}{A^2} \left(1 - \frac{N^*}{\bar{K}(\theta_K)}\right) \\ &= \frac{\sigma_G^2 \beta_G^2 dr}{A^2} \left(1 - \frac{N^*}{\bar{K}(\theta_K)} - 1 + \frac{N^*}{\bar{K}(\theta_K)} \left(1 + \frac{A}{C}\right)\right) \\ &= \frac{\sigma_G^2 \beta_G^2 dr N^*}{AC \bar{K}(\theta_K)} \end{aligned}$$

Note  $\det(J_2) > 0$  since  $N^* < \bar{K}(\theta_K)$ ,  $A > 0$ , and  $C > 0$ . Then the eigenvalues of  $J_2$  are

$$\lambda_{3,4} = \frac{1}{2} \left[ -\text{tr}(J_2) \pm \sqrt{\Delta} \right], \quad \text{where} \quad \Delta = (\text{tr}(J_2))^2 - 4\det(J_2).$$

$\lambda_{3,4}$  have negative real part if and only if  $\text{tr}(J_2) > 0$ . This gives us our coexistence local stability condition

$$\frac{\sigma_G^2}{\beta_G^2} > \frac{r}{d} \left( 1 - \frac{N^*}{K(\theta_K)} \left( 1 - \frac{A}{C} \right) \right).$$

Note the existence of a Hopf bifurcation when  $(\text{tr}(J_2))^2 - 4\det(J_2) < 0$  and when  $\text{tr}(J_2) = 0$ . Hopf bifurcations occur when the eigenvalues are complex and when the real part of the eigenvalues cross the imaginary axis as a parameter is shifted. As the real part of the eigenvalues becomes positive, the equilibrium becomes unstable, resulting in cyclic behavior around the equilibrium.

#### A.4. Model without Stabilizing Selection and Ecological Pleiotropy

Suppose prey growth rate  $r$  and prey carrying capacity  $K$  are constant, i.e., there is no ecological pleiotropy in the prey. The prey mean trait  $\bar{p}$  and predator mean trait  $\bar{n}$  only affect the average attack rate  $\bar{a}$ , which is given by

$$\bar{a}(\bar{p}, \bar{n}) = \frac{\alpha\tau_a}{\sqrt{A}} \exp \left[ -\frac{((\bar{p} - \bar{n}) - \theta_a)^2}{2A} \right],$$

where  $A := \tau_a^2 + \sigma^2 + \beta^2$ . The four-dimensional eco-evolutionary system is given by

$$\begin{aligned} \frac{dP}{dt} &= P[e\bar{a}(\bar{p}, \bar{n})N - d], \\ \frac{dN}{dt} &= N \left[ r \left( 1 - \frac{N}{K} \right) - \bar{a}(\bar{p}, \bar{n})P \right], \\ \frac{d\bar{p}}{dt} &= \sigma_G^2 \frac{\partial \left( \frac{1}{P} \frac{dP}{dt} \right)}{\partial \bar{p}} = \sigma_G^2 \frac{eN(\theta_a - (\bar{p} - \bar{n}))}{A} \bar{a}(\bar{p}, \bar{n}), \\ \frac{d\bar{n}}{dt} &= \sigma_G^2 \frac{\partial \left( \frac{1}{N} \frac{dN}{dt} \right)}{\partial \bar{n}} = \beta_G^2 \frac{P(\theta_a - (\bar{p} - \bar{n}))}{A} \bar{a}(\bar{p}, \bar{n}). \end{aligned}$$

We can define  $x := \bar{p} - \bar{n}$  since all functions of  $\bar{p}$  and  $\bar{n}$  are only functions of their difference. We can redefine average attack rate  $\bar{a}$  in terms of  $x$ :

$$\bar{a}(x) = \frac{\alpha\tau_a}{\sqrt{A}} \exp \left[ -\frac{(x - \theta_a)^2}{2A} \right],$$

and, since differentiation is linear, we recover a three-dimensional eco-evolutionary system:

$$\begin{aligned}
f_1 &:= \frac{dP}{dt} = P[e\bar{a}(x)N - d], \\
f_2 &:= \frac{dN}{dt} = N \left[ r \left( 1 - \frac{N}{K} \right) - \bar{a}(x)P \right], \\
f_3 &:= \frac{dx}{dt} = \frac{d\bar{p}}{dt} - \frac{d\bar{n}}{dt} = (\sigma_G^2 eN - \beta_G^2 P) \left[ \frac{\theta_a - x}{A} \right] \bar{a}(x)
\end{aligned}$$

**A.4.1. Equilibria.** There are four types of equilibria of the model: predator and prey extinction, predator exclusion, coexistence, and arms-race coexistence. Set  $f_1 = f_2 = f_3 = 0$  to find equilibria:

$$\begin{aligned}
f_1 = 0 &\implies P = 0 && \text{or } N = \frac{d}{e\bar{a}(x)} \\
f_2 = 0 &\implies N = 0 && \text{or } P = \frac{r}{\bar{a}(x)} \left( 1 - \frac{N}{K} \right) \\
f_3 = 0 &\implies P = \frac{\sigma_G^2}{\beta_G^2} eN && \text{or } x = \theta_a
\end{aligned}$$

Clearly  $P = N = 0$  satisfies equilibrium, so  $(P^*, N^*, x^*) = (0, 0, x)$  are the “extinction” equilibria for arbitrary  $x$  values. Denote  $E_{\text{ext}}$  as the set of extinction equilibria. If  $N \neq 0$  and  $P = 0$ , then  $f_2 = 0$  implies  $N = K$ . Then  $f_3 = 0 \implies x = \theta_a$ . This means  $\bar{p}^* = \bar{n}^* + \theta_a$  at these “predator exclusion” equilibria. Denote the set of predator exclusion equilibria as  $E_{\text{excl}}$ . If  $P \neq 0$  and  $N \neq 0$ , then  $f_1 = 0$  implies  $N = \frac{d}{e\bar{a}(x)}$ , and so  $f_2 = 0$  implies  $P = \frac{r}{\bar{a}(x)} \left( 1 - \frac{d}{Ke\bar{a}(x)} \right)$ . If  $P = \frac{\sigma_G^2}{\beta_G^2} eN$ , then we can solve this for  $x$ :

$$\frac{r}{\bar{a}(x)} \left( 1 - \frac{d}{Ke\bar{a}(x)} \right) = \frac{\sigma_G^2}{\beta_G^2} \cdot e \cdot \frac{d}{e\bar{a}(x)} \implies x = \theta_a \pm \sqrt{2A \ln \left( \frac{Ke\alpha\tau_a \left( 1 - \frac{\sigma_G^2 d}{\beta_G^2 r} \right)}{d\sqrt{A}} \right)}$$

For ease, define  $\xi := \frac{\sigma_G^2 d}{\beta_G^2 r}$  and define  $Z$  as the interior of the square root:

$$Z := 2A \ln \left( \frac{Ke\alpha\tau_a(1 - \xi)}{d\sqrt{A}} \right)$$

and define  $x^+$  and  $x^-$  as the two respective solutions:

$$x^+ = \theta_a + \sqrt{Z} \quad \text{and} \quad x^- = \theta_a - \sqrt{Z}$$

Note that these solutions only exist if  $Z > 0$ , which requires

$$\frac{Ke\alpha\tau_a(1-\xi)}{d\sqrt{A}} > 1,$$

which is equivalent to

$$\frac{\sigma_G^2}{\beta_G^2} < \frac{r}{d} \left( 1 - \frac{d\sqrt{A}}{Ke\alpha\tau_a} \right)$$

This gives a unique coexistence equilibrium if the above condition does not hold:

$$(P^*, N^*, x^*) = \left( \frac{r}{\bar{a}(\theta_a)} \left( 1 - \frac{d}{Ke\bar{a}(\theta_a)} \right), \frac{d}{e\bar{a}(\theta_a)}, \theta_a \right)$$

and two additional coexistence equilibria, called the arms race equilibria, if the above condition does hold:

$$(P^*, N^*, x^*) = \left( \frac{r}{\bar{a}(x^*)} \left( 1 - \frac{d}{Ke\bar{a}(x^*)} \right), \frac{d}{e\bar{a}(x^*)}, x^* \right)$$

where  $x^* = x^+$  or  $x^-$ . Denote the three coexistence equilibria as  $E_{\text{coex}}$ ,  $E^+$ , and  $E^-$ , respectively.

Note that

$$\bar{a}(x^+) = \bar{a}(x^-) = \frac{d}{Ke(1-\xi)}$$

and so the two additional coexistence equilibria are given by

$$(P^*, N^*, x^*) = \left( \frac{rKe}{d} \xi(1-\xi), K(1-\xi), x^* \right)$$

where  $x^* = x^+$  or  $x^-$ .

**A.4.2. Local Stability Analysis.** To solve for local stability conditions, we find the eigenvalues of the Jacobian matrix evaluated at the equilibria. The Jacobian is given by

$$J = \begin{pmatrix} e\bar{a}(x)N - d & Pe\bar{a}(x) & Pe\bar{a}'(x)N \\ -\bar{a}(x)N & r - 2r\frac{N}{K} - \bar{a}(x)P & -N\bar{a}'(x)P \\ -\beta_G^2\left(\frac{\theta_a - x}{A}\right)\bar{a}(x) & \sigma_G^2 e\left(\frac{\theta_a - x}{A}\right)\bar{a}(x) & \frac{\sigma_G^2 eN - \beta_G^2 P}{A}[(\theta_a - x)\bar{a}'(x) - \bar{a}(x)] \end{pmatrix}$$

where

$$\bar{a}'(x) = \frac{d}{dx}\bar{a}(x) = \frac{\theta_a - x}{A} \cdot \bar{a}(x).$$

At the extinction equilibria,

$$J_{\text{ext}} = \begin{pmatrix} -d & 0 & 0 \\ 0 & r & 0 \\ \beta_G^2\left(\frac{\theta_a - x}{A}\right)\bar{a}(x) & \sigma_G^2 e\left(\frac{\theta_a - x}{A}\right)\bar{a}(x) & 0 \end{pmatrix}$$

which has eigenvalues  $-d$ ,  $r$ , and  $0$ . Since  $r > 0$ , these equilibria are unstable. At the predator exclusion equilibria,

$$J_{\text{excl}} = \begin{pmatrix} e\bar{a}(\theta_a)K - d & 0 & 0 \\ -\bar{a}(\theta_a)K & -r & 0 \\ 0 & 0 & -\frac{\sigma_G^2 eK}{A}\bar{a}(\theta_a) \end{pmatrix}$$

which has eigenvalues  $\frac{Ke\alpha\tau_a}{\sqrt{A}} - d$ ,  $-r$ , and  $-\frac{\sigma_G^2 eK}{A}\bar{a}(\theta_a)$ . These are all negative if  $d > \frac{Ke\alpha\tau_a}{\sqrt{A}}$ . At the coexistence equilibrium (where  $x^* = \theta_a$ ),

$$J_{\text{coex}} = \begin{pmatrix} 0 & re\left(1 - \frac{d\sqrt{A}}{Ke\alpha\tau_a}\right) & 0 \\ -\frac{d}{e} & -\frac{rd\sqrt{A}}{Ke\alpha\tau_a} & 0 \\ 0 & 0 & -\frac{1}{A}\left(\sigma_G^2 d - \beta_G^2 r\left(1 - \frac{d\sqrt{A}}{Ke\alpha\tau_a}\right)\right) \end{pmatrix}$$

which has eigenvalues

$$\lambda_{1,2} = \frac{1}{2}\left(\text{tr} \pm \sqrt{\text{tr}^2 - 4\text{det}}\right), \quad \lambda_3 = -\frac{1}{A}\left(\sigma_G^2 d - \beta_G^2 r\left(1 - \frac{d\sqrt{A}}{Ke\alpha\tau_a}\right)\right)$$

where

$$\begin{aligned}\text{tr} &= -\frac{rd\sqrt{A}}{Ke\alpha\tau_a} \\ \det &= rd\left(1 - \frac{d\sqrt{A}}{Ke\alpha\tau_a}\right)\end{aligned}$$

Since  $\text{tr} < 0$  and  $\det > 0$  (due to biological feasibility), then  $\text{Re}[\lambda_{1,2}] < 0$ , and so all three eigenvalues have negative real part if

$$\frac{\sigma_G^2}{\beta_G^2} > \frac{r}{d}\left(1 - \frac{d\sqrt{A}}{Ke\alpha\tau_a}\right).$$

Finally, at the arms race equilibria (where  $x^* = x^+$  or  $x^-$ ),

$$J_{\text{arms}}^{\pm} = \begin{pmatrix} 0 & re\xi & \mp \frac{rKe}{A}\xi(1-\xi)\sqrt{Z} \\ -\frac{d}{e} & -r(1-\xi) & \pm \frac{rK}{A}\xi(1-\xi)\sqrt{Z} \\ \pm \frac{\beta_G^2 d}{KAe(1-\xi)}\sqrt{Z} & \mp \frac{\sigma_G^2 d}{KA(1-\xi)}\sqrt{Z} & 0 \end{pmatrix}.$$

The characteristic polynomial for 3x3 matrices  $M = (m_{ij})$  is given by

$$P(\lambda) = \lambda^3 - \text{tr}(M)\lambda^2 + Q(M)\lambda - \det(M)$$

where  $\text{tr}(M)$  is the trace of  $M$ ,  $\det(M)$  is the determinant of  $M$ , and  $Q(M) := (m_{11}m_{22} - m_{21}m_{12}) + (m_{11}m_{33} - m_{31}m_{13}) + (m_{22}m_{33} - m_{32}m_{23})$ . For the matrix  $J_{\text{arms}}$ , these coefficients are given by

$$\begin{aligned}-\text{tr}(J_{\text{arms}}) &= r(1-\xi) \\ Q(J_{\text{arms}}) &= rd\xi\left(1 + \frac{Z}{A^2}(\beta_G^2 + \sigma_G^2)\right) \\ -\det(J_{\text{arms}}) &= \frac{\beta_G^2 dr^2 \xi(1-\xi)Z}{A^2}\end{aligned}$$

The Routh-Hurwitz criteria for 3rd degree polynomials  $P(\lambda) = \lambda^3 + a_2\lambda^2 + a_1\lambda + a_0$ , which guarantees all three roots lie on the left side of the complex plane, are  $a_0 > 0$ ,  $a_2 > 0$ , and  $a_1a_2 > a_0$ . Since  $1 - \xi > 0$  is guaranteed by biological feasibility of the existence of  $E^+$  and  $E^-$ , then  $-\text{tr}(J_{\text{arms}}) > 0$  and  $-\det(J_{\text{arms}}) > 0$ . The third condition is

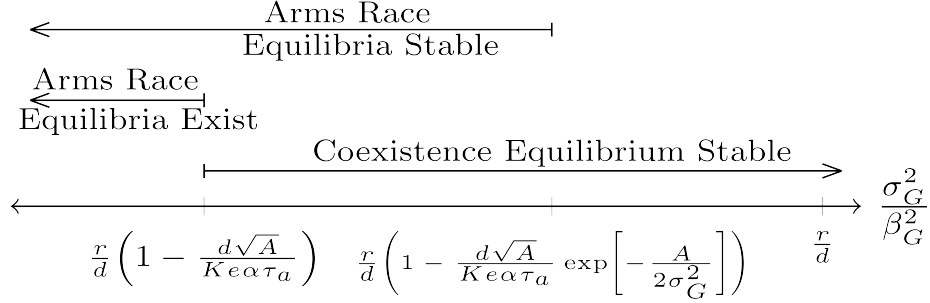


FIGURE A.1. **Bifurcation Diagram in terms of the ratio of speeds of predator to prey speeds of evolution,  $\frac{\sigma_G^2}{\beta_G^2}$ .** This diagram shows which equilibria exist and are stable, under the assumption that the coexistence equilibrium exists:  $d < \frac{Ke\alpha\tau_a}{\sqrt{A}}$ . In this region, the predator exclusion equilibrium is unstable. If  $d > \frac{Ke\alpha\tau_a}{\sqrt{A}}$ , the coexistence and arms race equilibria do not exist, and the predator exclusion equilibrium is stable.

$$rd\xi\left(1 + \frac{Z}{A^2}(\beta_G^2 + \sigma_G^2)\right) \cdot r(1 - \xi) > \frac{\beta_G^2 dr^2 \xi(1 - \xi)Z}{A^2}$$

which is equivalent to

$$\frac{\sigma_G^2}{\beta_G^2} < \frac{r}{d} \left(1 - \frac{d\sqrt{A}}{Ke\alpha\tau_a} \exp\left[-\frac{A}{2\sigma_G^2}\right]\right)$$

Since the arms race equilibria only exist if

$$\frac{\sigma_G^2}{\beta_G^2} < \frac{r}{d} \left(1 - \frac{d\sqrt{A}}{Ke\alpha\tau_a}\right),$$

and it is always true that

$$\frac{r}{d} \left(1 - \frac{d\sqrt{A}}{Ke\alpha\tau_a}\right) < \frac{r}{d} \left(1 - \frac{d\sqrt{A}}{Ke\alpha\tau_a} \exp\left[-\frac{A}{2\sigma_G^2}\right]\right),$$

provided  $d < \frac{Ke\alpha\tau_a}{\sqrt{A}}$ , then the two arms race equilibria are always asymptotically stable if they exist. Figure A.1 is a diagram describing regions of existence and stability for each equilibrium. Figure A.2 shows all possible dynamics of this system for positive density initial conditions.

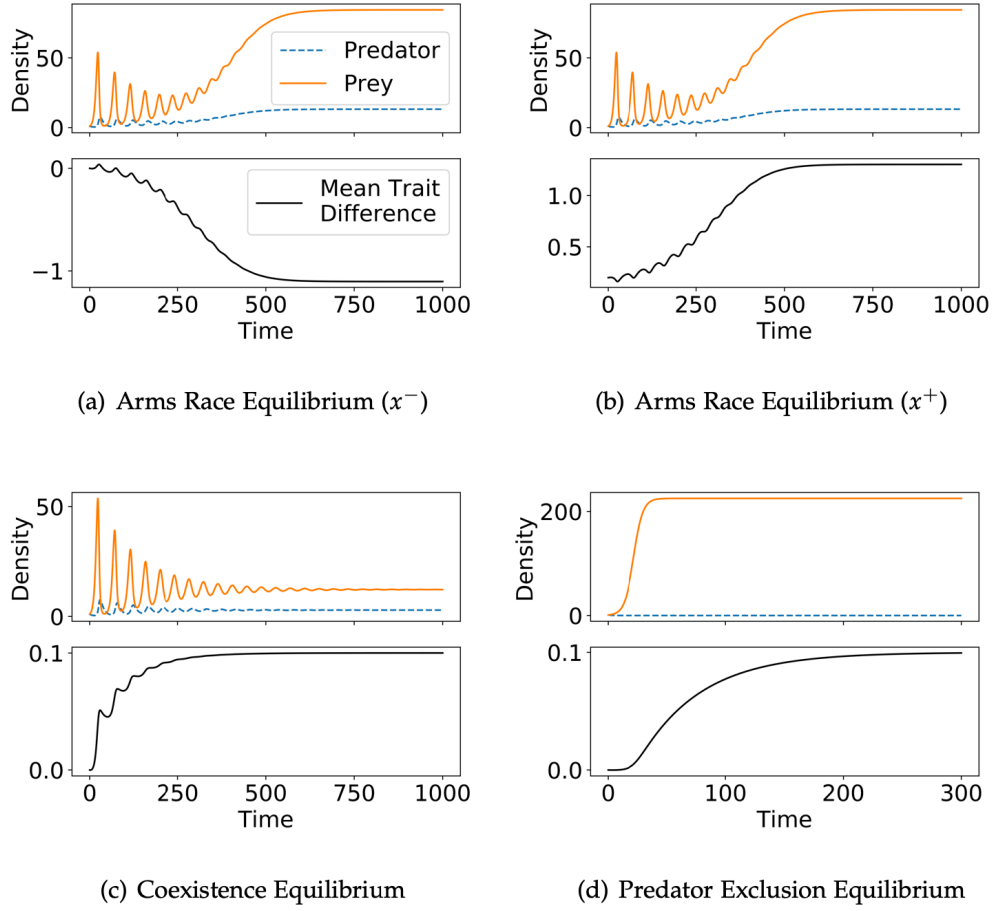


FIGURE A.2. **All Four Possible Dynamics.** Panels (a,b) parameter values:  $\sigma = \beta = 0.25$ ,  $\sigma_G = 0.25$ ,  $\beta_G = 0.2$ ,  $d = e = \alpha = \theta_a = 0.1$ ,  $\tau_a = 0.5$ ,  $r = 0.25$ ,  $K = 225$ . Panels (a,b) differ only in initial condition. Panel (c) parameter values: same as panels (a,b) except  $\beta_G = 0.1$ . Panel (d) parameter values: same as panel (c) except  $d = 0.3$  and  $e = \alpha = 0.025$ . All initial density conditions are  $P_0 = N_0 = 1$ . Panels (a,c,d) initial mean trait difference  $x_0 = 0$ . Panel (b) initial mean trait difference  $x_0 = 0.2$ .

## APPENDIX B

### Chaper 2 (Sick of Eating) Appendices

#### B.1. Derivation of average prey and predator fitness

Recall the probability distributions  $p_x(x, \bar{x})$  and  $p_y(y, \bar{y})$ :

$$(B.1) \quad p_x(x, \bar{x}) = \frac{1}{\sqrt{2\pi\sigma_x^2}} \exp\left[-\frac{(x - \bar{x})^2}{2\sigma_x^2}\right] \quad \text{and} \quad p_y(y, \bar{y}) = \frac{1}{\sqrt{2\pi\sigma_y^2}} \exp\left[-\frac{(y - \bar{y})^2}{2\sigma_y^2}\right]$$

Given  $W(x, y) = \sum_{i=1}^2 \left[ (b_i - c_i m_i S_i(y)) a_i(x) N_i \right] - d$ , then through the linearity of sums and integrals, we have

$$(B.2) \quad \bar{W}(\bar{x}, \bar{y}) = \int_{\mathbb{R} \times \mathbb{R}} W(x, y) p_x(x, \bar{x}) p_y(y, \bar{y}) dx dy = \sum_{i=1}^2 \left[ (b_i - c_i m_i \bar{S}_i(\bar{y})) \bar{a}_i(\bar{x}) N_i \right] - d$$

where

$$(B.3) \quad \bar{a}_i(\bar{x}) = \int_{\mathbb{R}} a_i(x) p_x(x, \bar{x}) dx \quad \text{and} \quad \bar{S}_i(\bar{y}) = \int_{\mathbb{R}} S_i(y) p_y(y, \bar{y}) dy$$

are the average attack rate of the predator on prey  $i$  and the susceptibility rate of the predator to infection by the parasite in prey  $i$ , respectively. Similary, given  $Y_i(x) = r_i \left( 1 - \frac{N_i}{K_i} \right) - a_i(x) P$  for  $i = 1, 2$ , we have

$$(B.4) \quad \bar{Y}_i(\bar{x}) = \int_{\mathbb{R}} Y_i(x) p_x(x, \bar{x}) dx = r_i \left( 1 - \frac{N_i}{K_i} \right) - \bar{a}_i(\bar{x}) P.$$

Finally, since

$$(B.5) \quad a_i(x) = \alpha_i \exp\left[-\frac{(x - \theta_i)^2}{2\zeta_i^2}\right] \quad \text{and} \quad S_i(y) = \beta_i - (\beta_i - \gamma_i) \exp\left[-\frac{(y - \phi_i)^2}{2\tau_i^2}\right],$$

we have

$$(B.6) \quad \bar{a}_i(\bar{x}) = \int_{\mathbb{R}} \alpha_i \exp \left[ -\frac{(x - \theta_i)^2}{2\zeta_i^2} \right] \frac{1}{\sqrt{2\pi\sigma_x^2}} \exp \left[ -\frac{(x - \bar{x})^2}{2\sigma_x^2} \right] dx$$

$$(B.7) \quad = \frac{\alpha_i}{\sqrt{2\pi\sigma_x^2}} \int_{\mathbb{R}} \exp \left[ -\frac{(x - \theta_i)^2}{2\zeta_i^2} - \frac{(x - \bar{x})^2}{2\sigma_x^2} \right] dx$$

$$(B.8) \quad = \frac{\alpha_i}{\sqrt{2\pi\sigma_x^2}} \int_{\mathbb{R}} \exp \left[ -\frac{1}{2\zeta_i^2\sigma_x^2} ((\sigma_x^2 + \zeta_i^2)x^2 - (2\theta_i\sigma_x^2 + 2\bar{x}\zeta_i^2)x + (\theta_i^2\sigma_x^2 + \bar{x}^2\zeta_i^2)) \right] dx$$

$$(B.9) \quad = \frac{\alpha_i}{\sqrt{2\pi\sigma_x^2}} \frac{\sqrt{\pi}}{\sqrt{A}} \exp \left[ \frac{B^2}{4A} - C \right]$$

where  $A = \frac{\sigma_x^2 + \zeta_i^2}{2\zeta_i^2\sigma_x^2}$ ,  $B = \frac{2\theta_i\sigma_x^2 + 2\bar{x}\zeta_i^2}{2\zeta_i^2\sigma_x^2}$ , and  $C = \frac{\theta_i^2\sigma_x^2 + \bar{x}^2\zeta_i^2}{2\zeta_i^2\sigma_x^2}$ . So,

$$(B.10) \quad \frac{B^2}{4A} - C = -\frac{(\bar{x} - \theta_i)^2}{2(\sigma_x^2 + \zeta_i^2)}$$

and thus

$$(B.11) \quad \bar{a}_i(\bar{x}) = \frac{\alpha_i\zeta_i}{\sqrt{\sigma_x^2 + \zeta_i^2}} \exp \left[ -\frac{(\bar{x} - \theta_i)^2}{2(\sigma_x^2 + \zeta_i^2)} \right].$$

Also,

$$(B.12) \quad \bar{S}_i(\bar{y}) = \int_{\mathbb{R}} \left( \beta_i - (\beta_i - \gamma_i) \exp \left[ -\frac{y - \phi_i}{2\tau_i^2} \right] \right) \frac{1}{\sqrt{2\pi\sigma_y^2}} \exp \left[ -\frac{(y - \bar{y})^2}{2\sigma_y^2} \right] dy$$

$$(B.13) \quad = \beta_i \int_{\mathbb{R}} \frac{1}{\sqrt{2\pi\sigma_y^2}} \exp \left[ -\frac{(y - \bar{y})^2}{2\sigma_y^2} \right] dy - \frac{\beta_i - \gamma_i}{\sqrt{2\pi\sigma_y^2}} \int_{\mathbb{R}} \exp \left[ -\frac{(y - \phi_i)^2}{2\tau_i^2} - \frac{(y - \bar{y})^2}{2\sigma_y^2} \right] dy$$

Through an identical calculation as for  $\bar{a}_i(\bar{x})$ , we have

$$(B.14) \quad \bar{S}_i(\bar{y}) = \beta_i - \frac{(\beta_i - \gamma_i)\tau_i}{\sqrt{\sigma_y^2 + \tau_i^2}} \exp \left[ -\frac{(\bar{y} - \phi_i)^2}{2(\sigma_y^2 + \tau_i^2)} \right].$$

Parameter	Baseline Value
$K_1, K_2$	100
$\alpha_1, \alpha_2$	0.7
$\beta_1, \beta_2$	0.95
$\gamma_1, \gamma_2$	0.05
$\sigma_x, \sigma_y$	0.25
$\sigma_{x,G}, \sigma_{y,G}$	0.1
$\tau_1, \tau_2$	0.1
$\zeta_1, \zeta_2$	0.1
$\theta_1, \phi_1$	0
$\theta_2, \phi_2$	1
$b_1, b_2$	1
$c_1, c_2$	0.9
$m_1, m_2$	0.9
$r_1, r_2$	1
$d$	0.4

TABLE B.1. Baseline parameter values.

Figure(s)	Parameter	Value
Figure 2.2a-c,g-i	$\zeta_1, \zeta_2$	0.01
Figure 2.2d-f,j-l	$\zeta_1, \zeta_2$	1
Figure 2.2a-f	$\tau_1, \tau_2$	0.01
Figure 2.2g-l	$\tau_1, \tau_2$	1
Figure 2.2a,d,g,j	$\sigma_{x,G}$	0.005
Figure 2.2a,d,g,j	$\sigma_{y,G}$	0.25
Figure 2.2b,e,h,k	$\sigma_{x,G}$	0.25
Figure 2.2b,e,h,k	$\sigma_{y,G}$	0.005
Figure 2.2c,f,i,l	$c_1, c_2, m_1, m_2$	0.1

TABLE B.2. Figure 2.2 parameters. All parameters not given here are given in Table B.1.

## B.2. Model parameters

### B.3. Numerical approximation of Lyapunov exponents

Consider a system of ordinary differential equations

$$(B.15) \quad \dot{\mathbf{x}} = f(\mathbf{x})$$

and an initial condition  $\mathbf{x}_0$  on or near an attractor of (B.15). Let  $\mathbf{x}_s(t)$  be the solution of (B.15) with  $\mathbf{x}_s(0) = \mathbf{x}_0$ . Let  $g(f, \mathbf{x}_0, t)$  denote a stable numerical algorithm that approximates the solution

Figure(s)	Parameter	Value
Figures 2.3a-d and 2.4a-d	$K_1, K_2$	[10, 1000]
Figures 2.3a-d and 2.4a-d	$\alpha_1, \alpha_2$	[0.5, 0.9]
Figures 2.3a-d and 2.4a-d	$\beta_1, \beta_2$	[0.9, 1]
Figures 2.3a-d and 2.4a-d	$\gamma_1, \gamma_2$	[0, 0.1]
Figures 2.3a-d and 2.4a-d	$\sigma_{x,G}, \sigma_{y,G}$	0.25
Figures 2.3a-d and 2.4a-d	$b_1, b_2$	[0.8, 1.2]
Figures 2.3a-d and 2.4a-d	$c_1, c_2, m_1, m_2$	[0.5, 1]
Figures 2.3a-d and 2.4a-d	$r_1, r_2$	[0.5, 1.5]
Figures 2.3a-d and 2.4a-d	$d$	[0.25, 0.55]
Figures 2.3a,b and 2.4a,b	$\tau_1, \tau_2$	0.01
Figures 2.3c,d and 2.4c,d	$\tau_1, \tau_2$	1
Figures 2.3a,c and 2.4a,c	$\zeta_1, \zeta_2$	0.01
Figures 2.3b,d and 2.4b,d	$\zeta_1, \zeta_2$	1

TABLE B.3. Figures 2.3 and 2.4 parameters. All parameters not given here are given in Table B.1.

to (B.15) (i.e. Python's `scipy.integrate.odeint()`). That is,

$$(B.16) \quad g(f, \mathbf{x}_0, t) \approx \mathbf{x}_s(t).$$

Let  $\epsilon$  be a small positive number and choose a vector  $\mathbf{y}_0 \neq \mathbf{x}_0$ . For  $i = 0, 1, \dots, n$ , define

$$d_i := \|\mathbf{y}_i - \mathbf{x}_i\| \quad \text{and} \quad \mathbf{y}_i^* := \mathbf{x}_i + \frac{\epsilon}{d_i} (\mathbf{y}_i - \mathbf{x}_i),$$

where  $\mathbf{y}_i$  is defined for  $i = 1, \dots, n$  as

$$(B.17) \quad \mathbf{y}_i := g(f, \Delta t, \mathbf{y}_{i-1}^*).$$

See Figure B.1 for a graphical depiction of this process.

Finally, define

$$(B.18) \quad L_i := \ln \left( \frac{d_i}{\epsilon} \right).$$

If  $L_i > 0$  ( $< 0$ ), then nearby solutions at that point move away from (towards) the reference solution  $\mathbf{x}_s$ , indicating chaotic (stable) dynamics. Then the Lyapunov exponent  $L$  for the reference

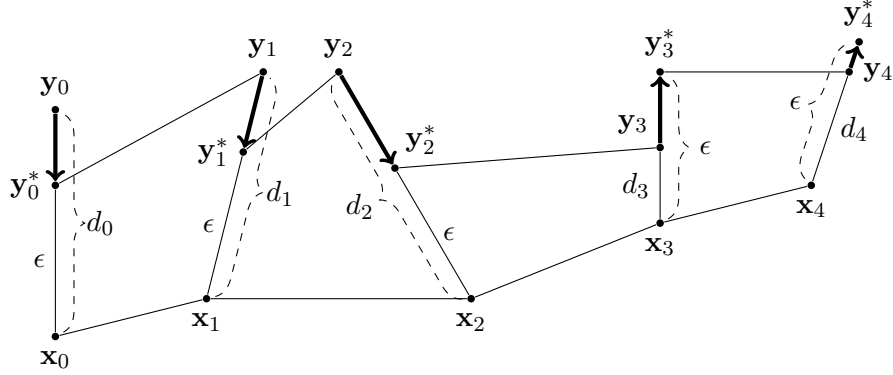


FIGURE B.1. Cartoon of the numerical approximation of the Lyapunov exponent for the solution  $\mathbf{x}_s$  of some system  $\dot{\mathbf{x}} = f(\mathbf{x})$  with initial condition  $\mathbf{x}(0) = \mathbf{x}_0$ . The initial  $\epsilon$ -perturbation of  $\mathbf{x}_0$  is  $\mathbf{y}_0^*$ . Each  $\mathbf{y}_i$  is rescaled to a distance of  $\epsilon$  from  $\mathbf{x}_i$ .

trajectory  $\mathbf{x}_s$  is defined as

$$(B.19) \quad L := \frac{1}{n} \sum_{i=1}^n L_i.$$

If  $L < 0$ , we say  $\dot{\mathbf{x}} = f(\mathbf{x})$  is stable around  $\mathbf{x}_s$  (and that  $\mathbf{x}_s$  is a stable trajectory). If  $L > 0$ , we say  $\dot{\mathbf{x}} = f(\mathbf{x})$  is chaotic around  $\mathbf{x}_s$  [Sprott, 2003].

Parameters for Figure 2.4 are in Table B.3.

#### B.4. Determining global stability of the ecological subsystem for constant traits $\bar{x}$ and $\bar{y}$

This appendix addresses the global stability of ecological equilibria of Equation (3.1). In particular, for constant predator mean traits  $\bar{x}$  and  $\bar{y}$ , we have

$$(B.20) \quad \begin{aligned} \dot{N}_1 &= N_1 \left( r_1 \left( 1 - \frac{N_1}{K_1} \right) - a_1 P \right) \\ \dot{N}_2 &= N_2 \left( r_2 \left( 1 - \frac{N_2}{K_2} \right) - a_2 P \right) \\ \dot{P} &= P (a_1 e_1 N_1 + a_2 e_2 N_2 - d) \end{aligned}$$

where  $a_i$  is shorthand for  $\bar{a}_i(\bar{x})$  and  $e_i$  is shorthand for  $b_i - m_i c_i \bar{S}_i(\bar{y})$ .

Note that  $e_i$  may be negative. We will first discuss global stability of (B.20) in the case that  $e_i > 0$  for  $i = 1, 2$ . We will then discuss the case that  $e_1 < 0$  and  $e_2 > 0$  (which is symmetrical to the case that  $e_1 > 0$  and  $e_2 < 0$ ). We will conclude with the case that both  $e_i < 0$  for  $i = 1, 2$ .

**Case 1: Two positive conversion efficiencies.** First, we nondimensionalize (B.20):

$$(B.21) \quad \begin{aligned} \dot{x}_1 &= x_1(r_1 - x_1 - a_1 y) \\ \dot{x}_2 &= x_2(r_2 - x_2 - a_2 y) \\ \dot{y} &= y(a_1 e_1 x_1 + a_2 e_2 x_2 - d) \end{aligned}$$

In this case, there are seven ecologically relevant equilibria of (B.21):

$$\begin{aligned} (E_{+++}) &= \frac{1}{|\Theta|} (\tilde{x}_1, \tilde{x}_2, \tilde{y}), \text{ where} \\ \tilde{x}_1 &= a_1 d + a_2 e_2 (a_2 r_1 - a_1 r_2) \\ \tilde{x}_2 &= a_2 d + a_1 e_1 (a_1 r_2 - a_2 r_1) \\ \tilde{y} &= a_1 e_1 r_1 + a_2 e_2 r_2 - d \\ |\Theta| &= a_1^2 e_1 + a_2^2 e_2 \\ (E_{+0+}) &= \left( \frac{d}{a_1 e_1}, 0, \frac{1}{a_1} \left( r_1 - \frac{d}{a_1 e_1} \right) \right) \\ (E_{0++}) &= \left( 0, \frac{d}{a_2 e_2}, \frac{1}{a_2} \left( r_2 - \frac{d}{a_2 e_2} \right) \right) \\ (E_{++0}) &= (r_1, r_2, 0) \\ (E_{+00}) &= (r_1, 0, 0) \\ (E_{0+0}) &= (0, r_2, 0) \\ (E_{000}) &= (0, 0, 0) \end{aligned}$$

The zero-species equilibrium ( $E_{000}$ ) and the one-species equilibria ( $E_{+00}$ ) and ( $E_{0+0}$ ) are unstable. The two-species equilibria ( $E_{+0+}$ ), ( $E_{0++}$ ), and ( $E_{++0}$ ) are globally stable if  $\tilde{x}_2 < 0$ ,  $\tilde{x}_1 < 0$ , and  $\tilde{y} < 0$ , respectively. It is impossible for any two of  $\tilde{x}_1$ ,  $\tilde{x}_2$ , and  $\tilde{y}$  to be negative simultaneously. If

$(E_{+++})$  is positive, then  $(E_{+++})$  is globally stable. Thus in order to determine which equilibrium is globally stable, it suffices to check the signs of  $\tilde{x}_1$ ,  $\tilde{x}_2$ , and  $\tilde{y}$ .

**Case 2: One negative and one positive conversion efficiency.** In order to keep all parameters positive, we write a new system:

$$(B.22) \quad \begin{aligned} \dot{x}_1 &= x_1 (r_1 - x_1 - a_1 y) \\ \dot{x}_2 &= x_2 (r_2 - x_2 - a_2 y) \\ \dot{y} &= y (-a_1 e_1 x_1 + a_2 e_2 x_2 - d) \end{aligned}$$

In this case, there are six ecologically relevant equilibria of (B.22):

$$\begin{aligned} (E_{+++}) &= \frac{1}{|\Theta|} (\tilde{x}_1, \tilde{x}_2, \tilde{y}), \text{ where} \\ \tilde{x}_1 &= a_1 d - a_2 e_2 (a_1 r_2 - a_2 r_1) \\ \tilde{x}_2 &= a_2 d + a_1 e_1 (a_2 r_1 - a_1 r_2) \\ \tilde{y} &= -a_1 e_1 r_1 + a_2 e_2 r_2 - d \\ |\Theta| &= -a_1^2 e_1 + a_2^2 e_2 \\ (E_{0++}) &= \left( 0, \frac{d}{a_2 e_2}, \frac{1}{a_2} \left( r_2 - \frac{d}{a_2 e_2} \right) \right) \\ (E_{++0}) &= (r_1, r_2, 0) \\ (E_{+00}) &= (r_1, 0, 0) \\ (E_{0+0}) &= (0, r_2, 0) \\ (E_{000}) &= (0, 0, 0) \end{aligned}$$

As in the previous case, the zero-species and one-species equilibria are unstable. The two-species equilibria  $(E_{0++})$  and  $(E_{++0})$  are globally stable if  $\tilde{x}_1 < 0$  and  $\tilde{y} < 0$ , respectively. At this time we cannot make a statement about the global stability of  $(E_{+++})$ . However, if  $(E_{0++})$  and  $(E_{++0})$  are unstable, then the trajectory (i) approaches  $(E_{+++})$  asymptotically, (ii) approaches a stable limit cycle, or (iii) is chaotic. In any case, because all solutions of (B.22) are bounded, the time-average of

the solution approaches  $(E_{+++})$ . This is the only requirement for Equation (2.2) to be an accurate approximation of Equation (3.1b) in the limit of slow evolution.

**Case 3: Two negative conversion efficiencies.** In order to keep all parameters positive, we write a new system:

$$(B.23) \quad \begin{aligned} \dot{x}_1 &= x_1 (r_1 - x_1 - a_1 y) \\ \dot{x}_2 &= x_2 (r_2 - x_2 - a_2 y) \\ \dot{y} &= y (-a_1 e_1 x_1 - a_2 e_2 x_2 - d) \end{aligned}$$

In this case, predator fitness is always negative, and so there are only four ecologically relevant equilibria of (B.23):

$$\begin{aligned} (E_{+++}) &= (r_1, r_2, 0) \\ (E_{+00}) &= (r_1, 0, 0) \\ (E_{0+0}) &= (0, r_2, 0) \\ (E_{000}) &= (0, 0, 0) \end{aligned}$$

As in the previous cases, the zero-species and one-species equilibria are unstable. The two species equilibrium  $(E_{+++})$  is globally stable.

### B.5. Unimodality condition for $\bar{W}$ with respect to $\bar{y}$

In this appendix, we assume the widths of the two susceptibility curves are equal:  $\tau := \tau_1 = \tau_2$ . The predator fitness is thus

$$(B.24) \quad \bar{W} = (b_1 - m_1 c_1 \bar{S}_1(\bar{y})) \bar{a}_1(\bar{x}) N_1 + (b_2 - m_2 c_2 \bar{S}_2(\bar{y})) \bar{a}_2(\bar{x}) N_2 - d.$$

where

$$\bar{S}_i(\bar{y}) = \beta_i - \frac{(\beta_i - \gamma_i)\tau}{\sqrt{\sigma_y^2 + \tau^2}} \exp\left[-\frac{(\bar{y} - \phi_i)^2}{2(\sigma_y^2 + \tau^2)}\right], \quad i = 1, 2.$$

Thus,  $\bar{y}$  fitness gradient is

$$(B.25) \quad \frac{\partial \bar{W}}{\partial \bar{y}} = -m_1 c_1 \bar{S}'_1(\bar{y}) \bar{a}_1(\bar{x}) N_1 - m_2 c_2 \bar{S}'_2(\bar{y}) \bar{a}_2(\bar{x}) N_2$$

$$= m_1 c_1 \left( \frac{(\beta_1 - \gamma_1) \tau (\phi_1 - \bar{y})}{(\sigma_y^2 + \tau^2)^{\frac{3}{2}}} \exp \left[ -\frac{(\bar{y} - \phi_1)^2}{2(\sigma_y^2 + \tau^2)} \right] \right) \bar{a}_1(\bar{x}) N_1$$

$$(B.26) \quad + m_2 c_2 \left( \frac{(\beta_2 - \gamma_2) \tau (\phi_2 - \bar{y})}{(\sigma_y^2 + \tau^2)^{\frac{3}{2}}} \exp \left[ -\frac{(\bar{y} - \phi_2)^2}{2(\sigma_y^2 + \tau^2)} \right] \right) \bar{a}_2(\bar{x}) N_2$$

For simplicity, we introduce a composite parameter  $A := \sigma_y^2 + \tau^2$  and  $Z_i := \frac{m_i c_i (\beta_i - \gamma_i) \tau \bar{a}_i(\bar{x}) N_i}{A^{\frac{3}{2}}}$  and so

$$(B.27) \quad \frac{\partial \bar{W}}{\partial \bar{y}} = Z_1 (\phi_1 - \bar{y}) \exp \left[ -\frac{(\bar{y} - \phi_1)^2}{2A} \right] + Z_2 (\phi_2 - \bar{y}) \exp \left[ -\frac{(\bar{y} - \phi_2)^2}{2A} \right]$$

We also rescale so that  $\phi_1 = 0$ ,  $\phi_2 = \phi$ , and  $\bar{y} = \tilde{y}\phi$ . Thus,

$$(B.28) \quad \frac{\partial \bar{W}}{\partial \bar{y}} = -Z_1 \phi \tilde{y} \exp \left[ -\frac{\tilde{y}^2 \phi^2}{2A} \right] + Z_2 \phi (1 - \tilde{y}) \exp \left[ -\frac{\phi^2 (\tilde{y} - 1)^2}{2A} \right]$$

To find critical points, we set  $\frac{d\bar{W}}{d\bar{y}} = 0$ :

$$(B.29) \quad Z_1 \tilde{y} \exp \left[ -\frac{\tilde{y}^2 \phi^2}{2A} \right] = Z_2 (1 - \tilde{y}) \exp \left[ -\frac{\phi^2 (\tilde{y} - 1)^2}{2A} \right]$$

Let  $\Psi := \frac{Z_2}{Z_1} = \frac{m_2 c_2 (\beta_2 - \gamma_2) \bar{a}_2(\bar{x}) N_2}{m_1 c_1 (\beta_1 - \gamma_1) \bar{a}_1(\bar{x}) N_1}$ , the ratio of the differences between maximally and minimally effective individual parasites. With this notation, we have

$$(B.30) \quad \exp \left[ -\frac{\phi^2 (\tilde{y} - \frac{1}{2})}{A} \right] = \Psi \left( \frac{1}{\tilde{y}} - 1 \right)$$

This is the same form as Equation (A2) from Appendix A in Patel and Schreiber [2015]. The remainder of this appendix is a restatement of their analytical results applied to this model.

Thus, if  $\Psi = 1$ , then  $\tilde{y} = \frac{1}{2}$  is always a critical point. If  $\phi^2 < 4A$ , this point is stable and if  $\phi^2 > 4A$ , this point is unstable. Graphical analysis shows that two additional stable equilibria exist if  $\phi^2 > 4A$  (one less than  $\frac{1}{2}$  and one more than  $\frac{1}{2}$ ), and so the fitness function is bimodal when  $\phi^2 > 4A$ , and this corresponds to a pitchfork bifurcation.

If  $\Psi \neq 1$ , then the symmetry of the bifurcation breaks. If  $\Psi < 1$ , then parasite 1 has a greater effect on predator fitness than the parasite 2, and so we predict the critical points to be closer to  $\tilde{y} = 0$  so the predator is less susceptible to limnetic parasitism. If  $\Psi > 1$ , we likewise expect the critical points to be closer to  $\tilde{y} = 1$ . We can check this by solving for  $\frac{d\tilde{y}}{d\Psi}$ :

$$(B.31) \quad \frac{d\tilde{y}}{d\Psi} = \frac{\frac{1}{\tilde{y}} - 1}{\frac{\Psi}{\tilde{y}^2} - \frac{\phi^2}{A} \exp\left[-\frac{\phi^2(\tilde{y} - \frac{1}{2})}{A}\right]}.$$

For all relevant values of  $\tilde{y}$  ( $\tilde{y} \in (0, 1)$ ), the numerator is positive. The denominator is positive for stable critical points and thus  $\frac{d\tilde{y}}{d\Psi} > 0$  for stable critical points in  $(0, 1)$ . Thus, the stable phenotype values of  $\tilde{y}$  increase as  $\Psi$  increases.

## Chaper 3 (Predator Evolution-Mediated Permanence) Appendices

### C.1. Global Stability of Model (3.1)

There are seven equilibria of Model (3.1):

**The coexistence equilibrium:**  $E_{++}^+ = (N_1^*, N_2^*, P^*)$ , where

$$\begin{aligned} N_i^* &= \frac{\tilde{N}_i}{\Theta}, \quad i = 1, 2, & P^* &= \frac{\tilde{P}}{\Theta}, \\ \tilde{N}_1 &= d(a_1 - c_{12}a_2) - a_2e_2(a_1r_2 - a_2r_1), \\ \tilde{N}_2 &= d(a_2 - c_{21}a_1) - a_1e_1(a_2r_1 - a_1r_2), \\ \tilde{P} &= a_1e_1(r_1 - c_{12}r_2) + a_2e_2(r_2 - c_{21}r_1) - d(1 - c_{12}c_{21}), \\ \Theta &= a_1^2e_1 - a_1a_2(c_{12}e_1 + c_{21}e_2) + a_2^2e_2, \end{aligned}$$

**The two prey-exclusion equilibria:**  $E_{+0}^+ = \left( \frac{d}{a_1e_1}, 0, \frac{1}{a_1} \left( r_1 - \frac{d}{a_1e_1} \right) \right)$  and

$$E_{0+}^+ = \left( 0, \frac{d}{a_2e_2}, \frac{1}{a_2} \left( r_2 - \frac{d}{a_2e_2} \right) \right),$$

**The predator-exclusion equilibrium:**  $E_{++}^0 = \left( \frac{r_1 - c_{12}r_2}{1 - c_{12}c_{21}}, \frac{r_2 - c_{21}r_1}{1 - c_{12}c_{21}}, 0 \right)$ ,

**The two single-prey equilibria:**  $E_{+0}^0 = (r_1, 0, 0)$  and  $E_{0+}^0 = (0, r_2, 0)$ , and

**The extinction equilibrium:**  $E_{00}^0 = (0, 0, 0)$ .

$E_{+0}^+$  exists if  $d < a_1e_1r_1$ ,  $E_{0+}^+$  exists if  $d < a_2e_2r_2$ , and  $E_{++}^+$  exists if  $(r_1 - c_{12}r_2)(r_2 - c_{21}r_1) > 0$ .  $E_{+0}^+$  is asymptotically stable if  $\tilde{N}_2 < 0$ ,  $E_{0+}^+$  is asymptotically stable if  $\tilde{N}_1 < 0$ ,  $E_{++}^+$  is asymptotically stable if  $c_{12}c_{21} < 1$  and  $\tilde{P} < 0$ ,  $E_{+0}^0$  is asymptotically stable if  $E_{+0}^+$  does not exist and  $c_{21} > \frac{r_2}{r_1}$ , and  $E_{0+}^0$  is asymptotically stable if  $E_{0+}^+$  does not exist and  $c_{12} > \frac{r_1}{r_2}$ . Hutson and Vickers [1983, Theorem 3.2] provide conditions for asymptotic stability of  $E_{++}^+$ .

Let  $\tilde{\mathcal{X}}^n$  denote the space of positive-semidefinite  $n \times n$  matrices. Let  $\mathcal{X}_d^n$  denote the space of diagonal positive-definite  $n \times n$  matrices. Define  $\tilde{S}_W$  as follows:

$$(C.1) \quad \tilde{S}_W := \left\{ A \in \mathbb{R}^{n \times n} \mid \exists W \in \mathcal{X}_d^n \text{ such that } WA + A^T W \in \tilde{\mathcal{X}}^n \right\}.$$

Consider the generalized Volterra system:

$$(C.2) \quad \frac{d}{dt} x_i(t) = x_i(t) \left[ b_i - \sum_{j=1}^n a_{ij} x_j(t) \right], \quad i = 1, 2, \dots, n.$$

Let  $x^* = (x_1^*, \dots, x_n^*)$  be a non-negative equilibrium of (C.2). Define  $N := \{1, \dots, n\}$  and  $I, J \subset N$  defined as

$$I := \{i \in N \mid x_i^* = 0\}, \quad \text{and} \quad J := N \setminus I.$$

Then define  $\mathbb{R}_I^n$  as

$$\mathbb{R}_I^n := \{x \in \mathbb{R}^n \mid x_i \geq 0 \forall i \in I \text{ and } x_j > 0 \forall j \in J\}.$$

LEMMA C.1. *Let  $A$  be the following matrix:*

$$A := \begin{pmatrix} 1 & c_{12} & a_1 \\ c_{21} & 1 & a_2 \\ -a_1 e_1 & -a_2 e_2 & 0 \end{pmatrix}.$$

*Then  $A \in \tilde{S}_W$  if and only if  $c_{12}e_1 + c_{21}e_2 \leq 2\sqrt{e_1 e_2}$ .*

PROOF OF LEMMA C.1. Suppose  $c_{12}e_1 + c_{21}e_2 \leq 2\sqrt{e_1 e_2}$ . Let  $w = (e_1, e_2, 1)$  and define  $W := \text{diag}(w_i)$ . Then

$$WA + A^T W = \begin{pmatrix} 2e_1 & c_{12}e_1 + c_{21}e_2 & 0 \\ c_{12}e_1 + c_{21}e_2 & 2e_2 & 0 \\ 0 & 0 & 0 \end{pmatrix}.$$

The principal minors are  $2e_1$ ,  $4e_1e_2 - (c_{12}e_1 + c_{21}e_2)^2$ , and 0, each of which is non-negative, and thus  $WA + A^T$  is positive-semidefinite, or  $A \in \tilde{S}_W$ .

Conversely, suppose  $A \in \tilde{S}_W$ . Thus there exists  $W = \text{diag}(w_i)$  with  $w_i > 0$  such that  $WA + A^T W$

is positive semidefinite. Then all the principal minors of  $WA + A^T W$  are non-negative.

$$(C.3) \quad WA + A^T W = \begin{pmatrix} 2w_1 & c_{12}w_1 + c_{21}w_2 & a_1w_1 - a_1e_1w_3 \\ c_{12}w_1 + c_{21}w_2 & 2w_2 & a_2w_2 - a_2e_2w_3 \\ a_1w_1 - a_1e_1w_3 & a_2w_2 - a_2e_2w_3 & 0 \end{pmatrix}$$

All diagonal terms must be non-negative (which is true because  $w_i > 0$  for all  $i$ ), and the principal minors must be non-negative, which means

$$(C.4) \quad \begin{vmatrix} 2w_2 & a_2w_2 - a_2e_2w_3 \\ a_2w_2 - a_2e_2w_3 & 0 \end{vmatrix} = -(a_2w_2 - a_2e_2w_3)^2 \geq 0 \implies w_2 = e_2w_3,$$

$$(C.5) \quad \begin{vmatrix} 2w_1 & a_1w_1 - a_1e_1w_3 \\ a_1w_1 - a_1e_1w_3 & 0 \end{vmatrix} = -(a_1w_1 - a_1e_1w_3)^2 \geq 0 \implies w_1 = e_1w_3,$$

$$(C.6)$$

and

$$(C.7) \quad \begin{vmatrix} 2w_1 & c_{12}w_1 + c_{21}w_2 \\ c_{12}w_1 + c_{21}w_2 & 2w_2 \end{vmatrix} = 4w_1w_2 - (c_{12}w_1 + c_{21}w_2)^2 \geq 0$$

Since  $w_2 = e_2w_3$  and  $w_1 = e_1w_3$ , the third condition is  $c_{12}w_1 + c_{21}w_2 \leq 2\sqrt{e_1e_2}$ , which completes the proof.  $\square$

**THEOREM C.2** (Theorem 3, Takeuchi and Adachi [1983]). *Suppose that there exists a non-negative equilibrium  $x^*$  of (C.2). Then  $x^*$  is globally stable if*

(i)  $A := (a_{ij}) \in \tilde{S}_W$ ,

(ii)  $b_i - \sum_{j=1}^n a_{ij}x_j^* \leq 0$  for all  $i \in I$ , and

(iii) the function

$$-(x - x^*)^T (WA + A^T W)(x - x^* + 2) + 2 \sum_{i \in I} w_i x_i \left( b_i - \sum_{j=1}^n a_{ij} x_j^* \right)$$

does not vanish identically along any solution of (C.2) except for  $x = x^*$  in  $\mathbb{R}^n$ .

PROOF OF THEOREM 3.2. (i) We will use Theorem C.2. Lemma C.1 satisfies (i) in Theorem C.2. (ii) in Theorem C.2 holds because  $I = \emptyset$  for  $E_{+++}^+$ . Finally, the expression in (iii) in Theorem C.2 reduces to

$$(C.8) \quad -(x - E_{+++}^+)^T \begin{pmatrix} 2e_1 & c_{12}e_1 + c_{21}e_2 & 0 \\ c_{12}e_1 + c_{21}e_2 & 2e_2 & 0 \\ 0 & 0 & 0 \end{pmatrix} (x - E_{+++}^+).$$

This clearly vanishes identically along  $x = E_{+++}^+$  and does not vanish identically along any other solution in  $\mathbb{R}_{>0}^3$  since  $c_{12}e_1 + c_{21}e_2 < 2\sqrt{e_1e_2}$  ensures the matrix is positive-semidefinite. Thus by Theorem C.2,  $E_{+++}^+$  is globally stable.

(ii) The condition  $c_{12}e_1 + c_{21}e_2 < 2\sqrt{e_1e_2}$  ensures that

$$\begin{aligned} a_1^2e_2 - a_1a_2(c_{12}e_1 + c_{21}e_2) + a_2^2e_2 &> a_1^2e_1 - 2\sqrt{e_1e_2}a_1a_2 + a_2^2e_2 \\ &= (a_1\sqrt{e_1} - a_2\sqrt{e_2})^2 \\ &\geq 0 \end{aligned}$$

Thus if  $E_{+++}^+$  is not non-negative, the either  $\tilde{N}_1 \leq 0$  or  $\tilde{N}_2 \leq 0$  or  $\tilde{P} \leq 0$ . Also, at least one of  $c_{12} < \frac{r_1}{r_2}$  and  $c_{21} < \frac{r_2}{r_1}$  must be true, because if  $c_{12} \geq \frac{r_1}{r_2}$  and  $c_{21} \geq \frac{r_2}{r_1}$ , then we have  $c_{12}c_{21} \geq 1$  and

$$\begin{aligned} 0 &\leq (c_{12}e_1 - c_{21}e_2)^2 \\ &= c_{12}^2e_1^2 - 2c_{12}c_{21}e_1e_2 + c_{21}^2e_2^2 \\ &\leq c_{12}^2e_1^2 - 2e_1e_2 + c_{21}^2e_2^2 \\ \implies 4e_1e_2 &\leq c_{12}^2e_1^2 + 2e_1e_2 + c_{21}^2e_2^2 \\ &\leq c_{12}^2e_1^2 + 2c_{12}c_{21}e_1e_2 + c_{21}^2e_2^2 \\ &= (c_{12}e_1 + c_{21}e_2)^2 \\ \implies 2\sqrt{e_1e_2} &\leq c_{12}e_1 + c_{21}e_2, \end{aligned}$$

which is a contradiction. Next, if  $c_{12} \neq \frac{r_1}{r_2}$  and  $c_{21} \neq \frac{r_2}{r_1}$ , then none of  $\tilde{N}_1 = 0$ ,  $\tilde{N}_2 = 0$ , and  $\tilde{P} = 0$  intersect. This is because the non-zero  $a_1$  coordinates of the points of intersection of  $\tilde{N}_1 = 0$  and  $\tilde{N}_2 = 0$  are

$$a_1 = \frac{d(c_{12}e_1(c_{21}r_1 + r_2) + c_{21}e_2(c_{21}r_1 - r_2) - 2e_1r_1) \pm d(c_{21}r_1 - r_2)\sqrt{(c_{12}e_1 + c_{21}e_2)^2 - 4e_1e_2}}{2e_1(r_1r_2(c_{12}e_1 + c_{21}e_2 - 2\sqrt{e_1e_2}) - (r_1\sqrt{e_1} - r_2\sqrt{e_2})^2)}$$

which are only real-valued if  $c_{12}e_1 + c_{21}e_2 \geq 2\sqrt{e_1e_2}$ . These are the same non-zero  $a_1$  coordinates of the points of intersection of  $\tilde{P} = 0$  and  $\tilde{N}_2 = 0$ . The analysis is symmetrical to finding the points of intersection of  $\tilde{P} = 0$  and  $\tilde{N}_1 = 0$ . Finally, if  $c_{12} = \frac{r_1}{r_2}$  then  $\tilde{P} = 0$  is a subset of  $\tilde{N}_1 = 0$  and is equivalent to  $a_2 = \frac{d(1-c_{12}c_{21})}{e_2(r_2-c_{21}r_1)} = \frac{d}{e_2r_2}$ .  $\tilde{N}_1 = 0$  is equivalent to  $a_2 = \frac{d}{e_2r_2}$  and  $a_1 = c_{12}a_2$ . Likewise, if  $c_{21} = \frac{r_2}{r_1}$  then  $\tilde{P} = 0$  is a subset of  $\tilde{N}_2 = 0$ . Because  $\tilde{N}_1 = 0$  and  $\tilde{N}_2 = 0$  do not intersect, then at least one of  $\tilde{N}_1 > 0$  and  $\tilde{N}_2 > 0$  is true. If  $\tilde{N}_1 < 0$ , then  $E_{0+}^+$  or  $E_{0+}^0$  is globally stable if  $\tilde{P} > 0$  or  $\tilde{P} < 0$ , respectively (Theorem C.2, Fig. C.1). Similarly, if  $\tilde{N}_2 < 0$ , then  $E_{+0}^+$  or  $E_{+0}^0$  is globally stable if  $\tilde{P} > 0$  or  $\tilde{P} < 0$ , respectively. Finally, it is possible for  $\tilde{P} < 0$  when  $\tilde{N}_1 > 0$  and  $\tilde{N}_2 > 0$ , in which case  $E_{++}^0$  is globally stable.

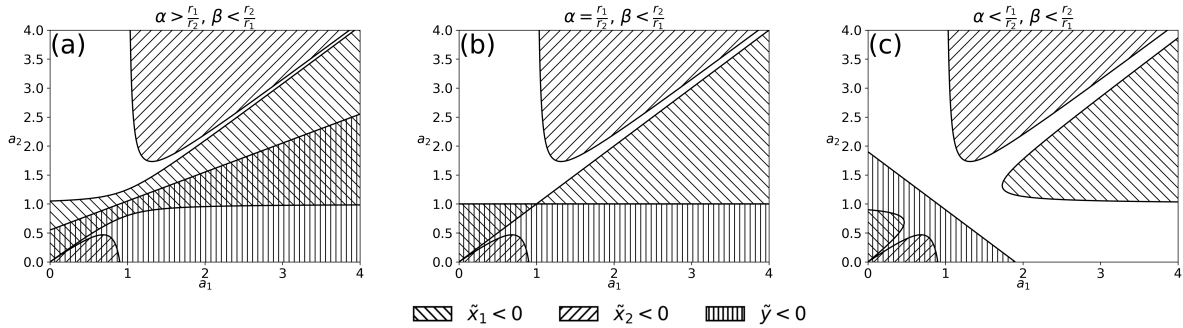


FIGURE C.1.  $a_1$ - $a_2$  bifurcation diagrams under the condition  $c_{12}e_1 + c_{21}e_2 < 2\sqrt{e_1e_2}$ . In (a), (b), and (c), we have  $c_{12} > \frac{r_1}{r_2}$ ,  $c_{12} = \frac{r_1}{r_2}$ , and  $c_{12} < \frac{r_1}{r_2}$ , respectively. Parameters:  $r_1 = r_2 = 1$ ,  $c_{21} = 0.9$ ,  $e_1 = e_2 = d = 0.5$ .  $c_{12} = 1.05, 1$ , and  $0.9$ , in (a), (b), and (c), respectively. If  $c_{21} > \frac{r_2}{r_1}$  or  $c_{21} = \frac{r_2}{r_1}$ , then  $c_{12} < \frac{r_1}{r_2}$  and plots are symmetric to (a) and (b), respectively. White regions indicate the coexistence equilibrium exists in the positive orthant and is globally stable.

□

## C.2. Hopf Bifurcation

**THEOREM C.3 (Hopf Bifurcation).** *Suppose  $c_{12}e_1 + c_{21}e_2 > 2\sqrt{e_1e_2}$  and  $c_{12}c_{21} > 1$ .*

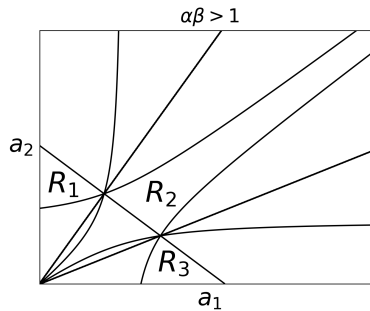
(a) In regions where  $(E_{++}^+)$  exists in the positive orthant and  $\Theta > 0$ , there exists at least one Hopf Bifurcation parametric value  $a_2^*$  (or  $a_1^*$ ) for any  $a_1$  (or  $a_2$ ) fixed if

$$(C.9) \quad \frac{d}{da_2} Z_3 \Big|_{a_2=a_2^*} \neq 0 \quad (\text{or } \frac{d}{da_1} Z_3 \Big|_{a_1=a_1^*} \neq 0).$$

(b) In regions where  $(E_{++}^+)$  exists in the positive orthant and  $\Theta < 0$ , there exist no periodic solution of the Hopf type.

PROOF. Let  $c_{12}e_1 + c_{21}e_2 > 2\sqrt{e_1e_2}$  and  $c_{12}c_{21} > 1$ .

(a) The curves  $N_i^* = 0$  ( $i = 1, 2$ ) and  $P^* = 0$  are simultaneously satisfied at exactly two points  $(a_1^1, a_2^1)$  and  $(a_1^2, a_2^2)$  in the positive  $a_1$ - $a_2$  plane. The intersections of these curves produce 14 distinct regions in the positive  $a_1$ - $a_2$  plane, three of which are regions in which  $(E_{++}^+)$  exists. The regions are  $R_1$ ,  $R_2$ , and  $R_3$ , as shown in the figure below.



For all  $(a_1, a_2) \in \overset{\circ}{R}_1$ , we have  $Z_0 > 0$  and  $Z_2 > 0$ .  $\partial R_1$  consists of the curves  $P^* = 0$  (the line),  $N_2^* = 0$  (the hyperbola), and the  $a_2$ -axis. On  $P^* = 0 |_{\partial R_1}$ , we have  $Z_2 = 0$  and  $Z_1 < 0$  (and thus  $Z_3 < 0$ ). On  $N_2^* = 0 |_{\partial R_1}$ , we have  $Z_2 = 0$  and  $Z_1 > 0$  (and thus  $Z_3 > 0$ ). Since  $Z_3$  as a function of  $a_1$  and  $a_2$  is continuous over  $R_1$ , then by the Intermediate Value Theorem,  $\forall a_1 \in \{a_1 \mid (a_1, a_2) \in \overset{\circ}{R}_1\}$ ,  $\exists a_2^* > 0$  such that  $(a_1, a_2^*) \in \overset{\circ}{R}_1$  and such that  $Z_3 |_{(a_1, a_2)=0}$ . Denote the minimum  $a_2^*$  as  $a_2^*$ . At this point, we have  $Z_i |_{(a_1, a_2^*)} > 0$  for  $i = 0, 1, 2$ .

For  $a_2$  less than  $a_2^*$ ,  $Z_i |_{(a_1, a_2)} > 0$  for  $i = 0, 1, 2, 3$ . By the Routh-Hurwitz criteria, this implies all eigenvalues of the linearized system are negative. At  $a_2 = a_2^*$ ,  $Z_3 = 0$ , which implies  $Z_2 = Z_0 Z_1$ . Thus the eigenvalues of the linearized system are  $-Z_0$  and  $\pm\sqrt{-Z_1}$ . Finally, by assumption, we have  $\frac{d}{da_2} Z_3 \Big|_{a_2=a_2^*} \neq 0$ . Thus there is a Hopf Bifurcation at  $(a_1, a_2^*)$ . A similar proof can be given for  $R_3$ .

(b) In  $R_2$ , we have  $\Theta < 0$  and  $(N_1^*, N_2^*, P^*) > 0$ . Thus  $Z_0 > 0$  and  $Z_2 < 0$ . If the linearized matrix has a conjugate pair of purely imaginary eigenvalues  $\pm \xi i$ , then the other eigenvalue is real and has the opposite sign of the constant term of the characteristic polynomial, which is  $Z_2 < 0$ , and thus the other eigenvalue is positive, which proves there is no Hopf Bifurcation in  $R_2$ .

□

### C.3. Dynamics when Model 3.1 is not permanent

PROOF OF THEOREM 3.3. Assume Model (3.1) is not robustly permanent,  $c_{12} < \frac{r_1}{r_2}$ , and  $c_{21} > \frac{r_2}{r_1}$  (Prey 1 dominates Prey 2).

Since Model (3.1) is not robustly permanent, either  $E_{++}^+$  is not positive or condition (ii) from Theorem 3.1 does not hold ( $\Theta \leq 0$ ). Condition (i) from Theorem 3.1 holds by assumption.

If  $E_{++}^+$  is not positive, then all  $\omega$ -limit points lie on the boundary of  $[0, \infty)^3$  [Hofbauer and Sigmund, 1998, Theorem 5.2.1]. Since  $c_{12} < \frac{r_1}{r_2}$  and  $c_{21} > \frac{r_2}{r_1}$ , then  $E_{++}^0$  is not feasible and  $E_{0+}^0$  is unstable. Since  $E_{00}^0$  is always unstable, only  $E_{+0}^0$ ,  $E_{+0}^+$ , and  $E_{0+}^+$  may be asymptotically stable. This results in the following possible cases:

**Case 1** ( $d > a_1 e_1 r_1$ ):  $E_{+0}^0$  is asymptotically stable and  $E_{+0}^+$  is not feasible.

**Case 1.1** ( $d > a_2 e_2 r_2$ ):  $E_{0+}^+$  is not feasible.

**Case 1.2** ( $d < a_2 e_2 r_2$ ):  $E_{0+}^+$  is feasible.

**Case 1.2.1** ( $\tilde{N}_1 < 0$ ):  $E_{0+}^+$  is asymptotically stable.

**Case 1.2.2** ( $\tilde{N}_1 < 0$ ):  $E_{0+}^+$  is unstable.

**Case 2** ( $d < a_1 e_1 r_1$ ):  $E_{+0}^0$  is unstable and  $E_{+0}^+$  is feasible.

**Case 2.1** ( $d > a_2 e_2 r_2$ ):  $E_{0+}^+$  is not feasible.

**Case 2.1.1** ( $\tilde{N}_2 < 0$ ):  $E_{+0}^+$  is asymptotically stable.

**Case 2.1.2** ( $\tilde{N}_2 > 0$ ):  $E_{+0}^+$  is unstable, and thus there are no  $\omega$ -limit points on the boundary, which is a contradiction.

**Case 2.2** ( $d < a_2 e_2 r_2$ ):  $E_{0+}^+$  is feasible.

**2.2.1** ( $\tilde{N}_1 < 0$ ,  $\tilde{N}_2 < 0$ ):  $E_{+0}^+$  and  $E_{0+}^+$  are asymptotically stable.

**2.2.2** ( $\tilde{N}_1 < 0$ ,  $\tilde{N}_2 > 0$ ):  $E_{+0}^+$  is unstable and  $E_{0+}^+$  is asymptotically stable.

**2.2.3** ( $\tilde{N}_1 > 0$ ,  $\tilde{N}_2 < 0$ ):  $E_{+0}^+$  is asymptotically stable and  $E_{0+}^+$  is unstable.

**2.2.4** ( $\tilde{N}_1 > 0, \tilde{N}_2 > 0$ ):  $E_{+0}^+$  and  $E_{0+}^+$  are unstable, and thus there are no  $\omega$ -limit points on the boundary, which is a contradiction.

In cases 1.1 and 1.2.2,  $E_{+0}^0$  is the only locally stable equilibrium on the boundary and any stable manifold of the other equilibria on the boundary lie in the boundary. Thus in these cases  $E_{+0}^0$  is globally stable. In case 1.2.1,  $E_{+0}^0$  and  $E_{0+}^+$  are stable. In cases 2.1.1 and 2.2.3,  $E_{+0}^+$  is the only locally stable equilibrium on the boundary and any stable manifold of the other equilibria on the boundary lie in the boundary. Thus in these cases  $E_{+0}^+$  is globally stable. In case 2.2.2,  $E_{0+}^+$  is the only locally stable equilibrium on the boundary and any stable manifold of the other equilibria on the boundary are on the boundary. Thus in this case  $E_{0+}^+$  is globally stable. In case 2.2.1,  $E_{+0}^+$  and  $E_{0+}^+$  are stable. In Cases 2.1.2 and 2.2.4, Model (3.1) is permanent, which is a contradiction.

Next, assume  $E_{++}^+$  is positive but condition (ii) from Theorem 3.1 does not hold ( $\Theta \leq 0$ ). Since  $E_{++}^+$  is positive, then  $\Theta \neq 0$ , and so  $\Theta < 0$ . Thus  $\tilde{N}_1 < 0, \tilde{N}_2 < 0$ , and  $\tilde{P} < 0$ . On the  $a_1$ - $a_2$  plane, the hyperbolas defined by  $\tilde{N}_1 = 0$  and  $\tilde{N}_2 = 0$  intersect at the origin. If  $c_{12}e_1 + c_{21}e_2 < 2\sqrt{e_1e_2}$ , there are no other intersections, and existence of  $E_{++}^+$  implies its global stability (Theorem 3.2). But this implies  $\Theta > 0$ , which is a contradiction. Thus  $c_{12}e_1 + c_{21}e_2 \geq 2\sqrt{e_1e_2}$ , and there are at most two additional points of intersection of the hyperbolas  $\tilde{N}_1 = 0$  and  $\tilde{N}_2 = 0$ . The line defined by  $\tilde{P} = 0$  in the  $a_1$ - $a_2$  plane also passes through these points. If  $c_{12}e_1 + c_{21}e_2 > 2\sqrt{e_1e_2}$ , then these points also fall on  $\Theta = 0$ , which consists of two lines through the origin, each with a positive slope. Denote the intersection points  $\vec{x}_1 = (a_{11}, a_{21})$  and  $\vec{x}_2 = (a_{12}, a_{22})$ , with  $a_{11} < a_{12}$ .  $\vec{x}_1$  and  $\vec{x}_2$  are each either in the first quadrant **QI** or the third quadrant **QIII** of the  $a_1$ - $a_2$  plane.

**Case 3** ( $\vec{x}_1, \vec{x}_2 \in \mathbf{QIII}$ ): In this case, the curves  $\tilde{N}_1 = 0, \tilde{N}_2 = 0, \tilde{P} = 0$ , and  $\Theta = 0$  split the first quadrant into eight distinct regions. In none of the eight regions is  $E_{++}^+$  positive and  $\Theta < 0$  (Fig. C.2a).

**Case 4** ( $\vec{x}_1 \in \mathbf{QIII}, \vec{x}_2 \in \mathbf{QI}$ ): In this case,  $\vec{x}_2$  is such that  $d < a_{i2}e_i r_i, i = 1, 2$  or  $d > a_{i2}e_i r_i, i = 1, 2$ . The curves  $\tilde{N}_1 = 0, \tilde{N}_2 = 0, \tilde{P} = 0$ , and  $\Theta = 0$  split the first quadrant into eleven distinct regions (Fig. C.2b,c).

**Case 4.1** ( $\frac{e_1(r_1 - c_{12}r_2)}{r_2(c_{21}r_1 - r_2)} > \frac{r_2}{r_1}$ ): In this case,  $d < a_{i2}e_i r_i, i = 1, 2$  and in none of the eleven regions is  $E_{++}^+$  positive and  $\Theta < 0$  (Fig. C.2b).

- Case 4.2** ( $\frac{e_1(r_1 - c_{12}r_2)}{r_2(c_{21}r_1 - r_2)} < \frac{r_2}{r_1}$ ): In this case,  $d > a_{i2}e_i r_i$ ,  $i = 1, 2$ . There is one region in which  $E_{++}^+$  is positive and  $\Theta < 0$ . This region is such that  $d < a_2 e_2 r_2$  (Fig. C.2c).
- Case 5** ( $\vec{x}_1, \vec{x}_2 \in \mathbf{QI}$ ): In this case, the curves  $\tilde{N}_1 = 0$ ,  $\tilde{N}_2 = 0$ ,  $\tilde{P} = 0$ , and  $\Theta = 0$  split the first quadrant into fourteen distinct regions (Fig. C.2d-f).
- Case 5.1** ( $a_{21} < a_{22} < \frac{d}{e_2 r_2}$ ): In none of the fourteen regions is  $E_{++}^+$  positive and  $\Theta < 0$  (Fig. C.2d).
- Case 5.2** ( $a_{21} < \frac{d}{e_2 r_2} < a_{22}$ ): There is one region in which  $E_{++}^+$  is positive and  $\Theta < 0$ . This region is such that  $d < a_2 e_2 r_2$  (Fig. C.2e).
- Case 5.3** ( $\frac{d}{e_2 r_2} < a_{21} < a_{22}$ ): There is one region in which  $E_{++}^+$  is positive and  $\Theta < 0$ . This region is such that  $d < a_2 e_2 r_2$  (Fig. C.2f).

Every region in which  $E_{++}^+$  exists and  $\Theta < 0$  is such that  $d < a_2 e_2 r_2$ . Thus  $E_{0+}^+$  is asymptotically stable. If  $d < a_1 e_1 r_1$ , then  $E_{+0}^+$  is asymptotically stable. If  $d > a_1 e_1 r_1$ , then  $E_{+0}^0$  is asymptotically stable. In either case,  $E_{++}^+$  positive and  $\Theta < 0$  implies Model (3.1) has two stable boundary equilibria.  $\square$

#### C.4. Permanence

Consider a general system

$$(C.10) \quad \begin{aligned} \frac{dx_i}{dt} &= x_i f_i(x, y), & i &= 1, \dots, n, \\ \frac{dy_j}{dt} &= g_j(x, y), & j &= 1, \dots, m, \end{aligned}$$

with state space  $S := [0, \infty)^n \times K$ , and where  $x = (x_1, \dots, x_n) \in [0, \infty)^n$  is the vector of population densities. The *extinction set*  $S_0 := \{(x, y) \in S \mid \prod_{i=1}^n x_i = 0\}$  is the set which has at least one species extinct (zero density). Let  $z.t$  denote the solution to this model for initial condition  $z = (x, y) \in S$ , and let  $Z.T := \{z.t \mid z \in Z, t \in T\}$ . Assume  $x_i f_i$  and  $g_j$  are locally Lipschitz functions and that there is an invariant compact set  $Q \subset S$  such that  $Q.[0, \infty) \subset Q$  and  $z.t \in Q$  for  $t$  sufficiently large for all  $z \in S$ . Define the  $\omega$ -limit set of a set  $Z$  as  $\omega(Z) := \bigcap_{t \geq 0} \overline{Z.[t, \infty)}$ , and the  $\alpha$ -limit set of a set  $Z$  as  $\alpha(Z) := \bigcap_{t \leq 0} \overline{Z.(-\infty, t]}$ . The *global attractor* of this system  $\Lambda$  is defined as  $\Lambda := \omega(Q)$ .

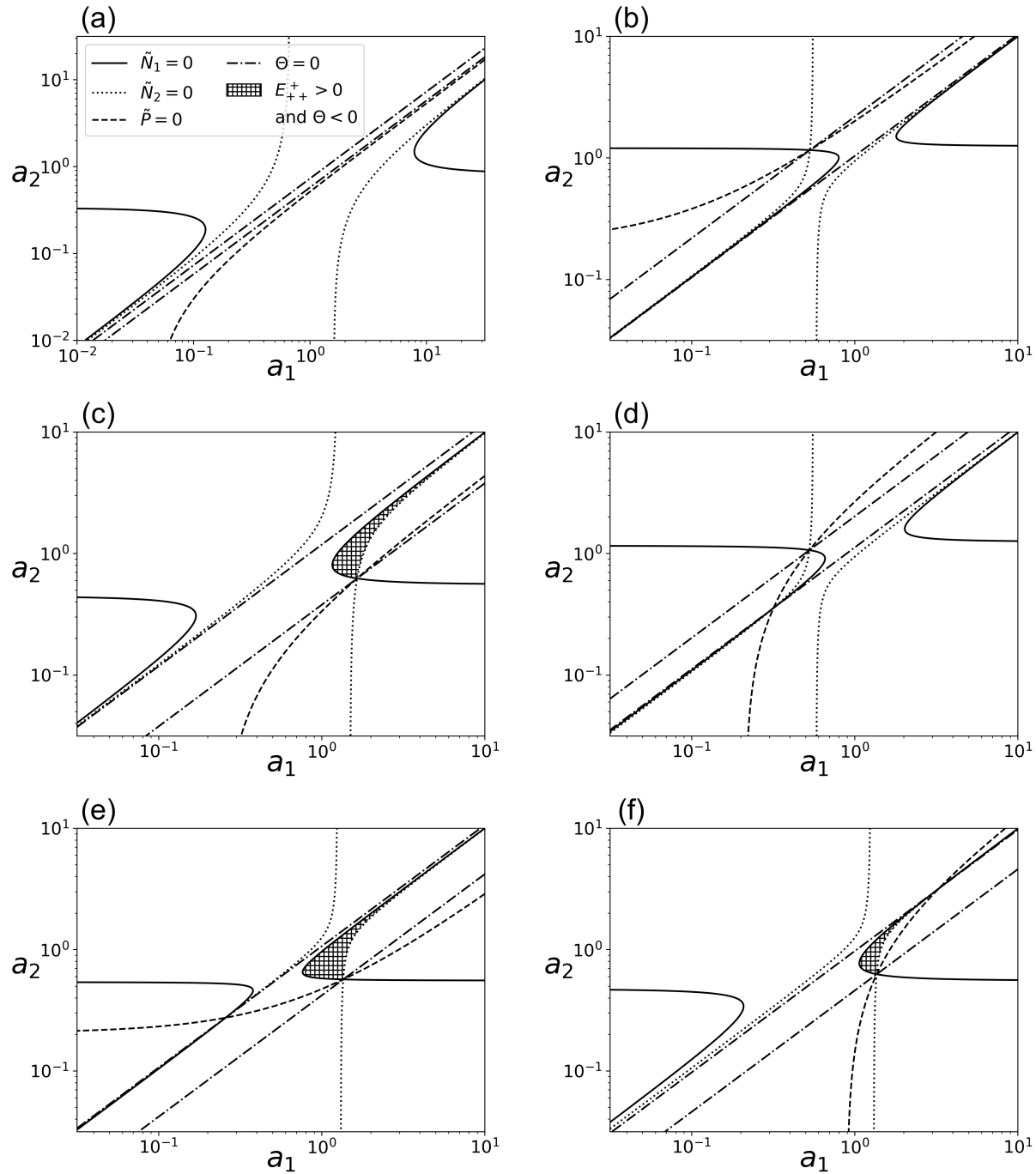


FIGURE C.2. Bifurcation diagrams of Model (3.1) in cases 3, 4, and 5 in the proof of Theorem 3.3. (a) Case 3.  $r_1 = 1.5$ ,  $r_2 = 0.5$ ,  $c_{12} = 1.2$ ,  $c_{21} = 0.8$ ,  $e_1 = 0.5$ ,  $e_2 = 1.2$ ,  $d = 0.5$ . In (b-f),  $r_1 = r_2 = 1$  and  $d = 0.5$ . In (b,d),  $e_1 = 0.9$  and  $e_2 = 0.4$ . In (c,e,f),  $e_1 = 0.4$  and  $e_2 = 0.9$ . (b) Case 4.1.  $c_{12} = 0.96$  and  $c_{21} = 1.05$ . (c) Case 4.1  $c_{12} = 0.8$  and  $c_{21} = 1.2$ . (d) Case 5.1.  $c_{12} = 0.925$  and  $c_{21} = 1.05$ . (e) Case 5.2.  $c_{12} = 0.97$  and  $c_{21} = 1.05$ . (f) Case 5.3.  $c_{12} = 0.85$  and  $c_{21} = 1.05$ .

DEFINITION 1 (Morse Decomposition). *A collection of sets  $\mathcal{M} = \{M_1, \dots, M_\ell\}$  is a Morse decomposition for a compact invariant set  $\Gamma$  if  $M_1, \dots, M_\ell$  are pairwise disjoint, isolated invariant compact sets, called Morse sets, such that for every  $z \in \Gamma \setminus \bigcup_{k=1}^\ell M_k$  there are integers  $i < j$  such that  $\omega(z) \subset M_i$  and  $\alpha(z) \subset M_j$ .*

THEOREM C.4 (Patel and Schreiber [2018], Theorem 2). *Let  $\mathcal{M} = \{M_1, \dots, M_\ell\}$  be a Morse decomposition for  $S_0 \cap \Gamma$ , where  $\Gamma$  is the global attractor for (C.10). If, for each  $M_k \in \mathcal{M}$ , there exists  $p_{k1}, \dots, p_{kn} > 0$  such that for every  $z \in M_k$ , there is a  $T_z$  such that*

$$\sum_{i=1}^n p_{ki} \int_0^{T_z} f_i(z.t) dt > 0,$$

*then (C.10) is robustly permanent.*

Recall Model (3.2) from the main text and its state space  $S := [0, \infty)^3 \times [\theta_1, \theta_2]$ .

THEOREM C.5. *Model (3.2) is dissipative.*

PROOF. If  $N_j = 0$  and  $P = 0$ , then  $\frac{dN_i}{dt} = N_i(r_i - N_i)$ , which is the well-known one-dimensional Logistic equation and is a dissipative system.

If  $N_j \neq 0$  or  $P \neq 0$ , then  $\frac{dN_i}{dt} < 0$  for all  $N_i \geq r_i$ . Thus there is some  $T > 0$  such that  $N_i(t) < 2r_i$  for all  $t > T$ . Let  $y := \sum_{i=1}^2 e_i N_i + P$ . Then

$$\begin{aligned} \dot{y} &= \sum_{i=1}^2 e_i N_i (r_i - N_i) - (e_1 c_{12} + e_2 c_{21}) N_1 N_2 - dP \\ &\leq \sum_{i=1}^2 e_i (2r_i)(r_i - N_i) - dP \\ &= 2 \sum_{i=1}^2 e_i r_i^2 - 2 \sum_{i=1}^2 e_i r_i N_i - dP. \end{aligned}$$

Let  $\alpha := 2 \sum_{i=1}^2 e_i r_i^2$  and  $\beta := \min \{2r_1, 2r_2, d\}$ . Thus,

$$\dot{y} \leq \alpha - \beta y,$$

and thus (3.2) is dissipative. All flow eventually enters the compact set

$$Q := \left\{ (N_1, N_2, P, \bar{x}) \mid y \leq \frac{2\alpha}{\beta} \right\} \subset S.$$

□

Since (3.2) is dissipative, there exists a compact global attractor  $\Lambda \subset S$  of (3.2). The next three theorems provide conditions for permanence of model (3.2) for each of three cases. Theorems C.6 and C.7 cover when  $(r_1, 0)$  is globally stable in the  $N_1$ - $N_2$  subsystem and Theorem C.8 covers when  $(r_1, 0)$  and  $(0, r_2)$  are bistable in the  $N_1$ - $N_2$  subsystem. In Theorem C.6, the predator must be able to subsist on either of the prey without the other, and in Theorem C.7, the predator must only subsist on the superior competitor. In Theorem C.8, the predator must have a positive per-capita growth rate when the prey are at any of the three nonzero equilibria of the  $N_1$ - $N_2$  subsystem.

**THEOREM C.6.** *Assume the following:*

- (i)  $c_{12} < \frac{r_1}{r_2}$  and  $c_{21} > \frac{r_2}{r_1}$ ,
- (ii)  $\bar{a}_1(\theta_1)e_1r_1 > d$ ,
- (iii)  $d(\bar{a}_2(\theta_1) - c_{21}\bar{a}_1(\theta_1)) > \bar{a}_1(\theta_1)e_1(\bar{a}_2(\theta_1)r_1 - \bar{a}_1(\theta_1)r_2)$ ,
- (iv)  $\bar{a}_2(\theta_2)e_2r_2 > d$ , and
- (v)  $d(\bar{a}_1(\theta_2) - c_{12}\bar{a}_2(\theta_2)) > \bar{a}_2(\theta_2)e_2(\bar{a}_1(\theta_2)r_2 - \bar{a}_2(\theta_2)r_1)$ .

*Then Model (3.2) is robustly permanent.*

**PROOF.** Denote  $M_1 = (E_{+0}^+) \times \{\theta_1\}$ ,  $M_2 = (E_{0+}^+) \times \{\theta_2\}$ ,  $M_3 = (E_{+0}^0) \times \{\theta_1\}$ ,  $M_4 = (E_{0+}^0) \times \{\theta_2\}$ , and  $M_5 = (E_{00}^0) \times [\theta_1, \theta_2]$ . Schreiber and Patel [2015, Proposition 1] proved that  $M_1$  and  $M_2$  are globally stable within the  $N_1$ - $P$ - $\bar{x}$  and  $N_2$ - $P$ - $\bar{x}$  subsystems, respectively. Similarly, in the  $N_1$ - $\bar{x}$  subsystem, if  $N_1(0) > 0$ , then since  $\frac{dN_1}{dt} = N_1(r_1 - N_1)$ , then  $N_1 \rightarrow r_1$  asymptotically. Since  $N_2 = 0$ , then  $\frac{d\bar{x}}{dt} = \sigma_G^2 \bar{a}'_1(\bar{x})e_1N_1 = -\sigma_G^2 e_1 \frac{\beta_1 r_1 (\bar{x} - \theta_1)}{(\sigma^2 + r_1^2)^{3/2}} \exp\left[-\frac{(\bar{x} - \theta_1)^2}{2A_1}\right] N_1$ . The only equilibrium is  $\bar{x} = \theta_1$ , and  $\frac{d\bar{x}}{dt} < 0$  for all  $\bar{x} > \theta_1$ . So  $\lim_{t \rightarrow \infty} \bar{x}(t) = \theta_1$  and thus  $M_3$  is globally stable within the  $N_1$ - $\bar{x}$  subsystem. Similarly,  $M_4$  is globally stable within the  $N_2$ - $\bar{x}$  subsystem.

Next we show  $\mathcal{M} = \{M_1, M_2, M_3, M_4, M_5\}$  is a Morse decomposition for  $\Lambda \cap S_0$ . Let  $z \in (\Lambda \cap S_0) \setminus \bigcup_{i=1}^5 M_i$ , where  $z = (N_1, N_2, P, \bar{x})$ . Then either

- (a)  $N_2 = P = 0$ ,  $N_1 > 0$ ,

- (b)  $N_2 = 0, N_1 > 0, P > 0,$
- (c)  $N_1 = P = 0, N_2 > 0,$
- (d)  $N_1 = 0, N_2 > 0, P > 0,$  or
- (e)  $P = 0, N_1 > 0, N_2 > 0.$

If (a) holds, then  $\alpha(z) \subset M_5$  and  $\omega(z) = M_3$ . If (b) holds, then  $\omega(z) = M_1$ , and by Mischaikow et al. [1995, Proposition 1.5], either  $\alpha(z) \subset M_5$ ,  $\alpha(z) = M_3$ , or  $\alpha(z) = M_1$ . Since  $M_1$  is globally stable within the  $N_1$ - $P$ - $\bar{x}$  subsystem, then  $\alpha(z) = \omega(z) = M_1$  implies  $z \in M_1$ , which contradicts our assumptions that  $z \in \bigcup_{i=1}^5 M_i$ . Thus  $\alpha(z) \subset M_5$  or  $\alpha(z) = M_3$ . Cases (c) and (d) follow similarly. If (e) holds, then (i) implies  $\omega(z) = M_3$  and either  $\alpha(z) = M_3$  or  $\alpha(z) = M_4$  or  $\alpha(z) \subset M_5$ . Again, if  $\alpha(z) = \omega(z) = M_3$ , then by Mischaikow et al. [1995, Proposition 1.5],  $z = M_3$ , which is a contradiction. Thus  $\alpha(z) = M_4$  or  $\alpha(z) \subset M_5$ . Thus  $\mathcal{M}$  forms a Morse decomposition for  $\Lambda \cap S_0$ .

To apply Theorem 2 in Patel and Schreiber [2018], then for each  $M_k \in \mathcal{M}$  we must find  $(n_1, n_2, p) \in \mathbb{R}_+^3$  such that  $n_1 \left( \frac{1}{N_1} \frac{dN_1}{dt} \right) + n_2 \left( \frac{1}{N_2} \frac{dN_2}{dt} \right) + p \left( \frac{1}{N_1} \frac{dP}{dt} \right) > 0$  for all  $(N_1, N_2, P) \in M_k$ . For  $M_5$ , choose  $(n_1, n_2, p) = \left( \frac{d}{r_1}, \frac{d}{r_2}, 1 \right)$ . For  $M_4$ , choose  $(n_1, n_2, p) = (1, 1, 1)$ . For  $M_3$ , choose  $\epsilon$  sufficiently small and  $(n_1, n_2, p) = (1, \epsilon, 1)$ . For  $M_2$  and  $M_1$ , choose  $(1, 1, 1)$ . Thus (3.2) is permanent.  $\square$

**THEOREM C.7.** *Assume the following:*

- (i)  $c_{12} < \frac{r_1}{r_2}$  and  $c_{21} > \frac{r_2}{r_1},$
- (ii)  $\bar{a}_1(\theta_1)e_1r_1 > d,$
- (iii)  $d(\bar{a}_2(\theta_1) - c_{21}\bar{a}_1(\theta_1)) > \bar{a}_1(\theta_1)e_1(\bar{a}_2(\theta_1)r_1 - \bar{a}_1(\theta_1)r_2),$  and
- (iv)  $\bar{a}_2(\theta_2)e_2r_2 < d.$

*Then Model (3.2) is robustly permanent.*

**PROOF.** Denote  $M_i, i = 1, 3, 4, 5$  as in the proof of Theorem C.6. If  $N_1(0) = 0$  and  $N_2(0)P(0) > 0$ , then  $\lim_{t \rightarrow \infty} (N_1(t), N_2(t), P(t), \bar{x}(t)) = M_4$  [Schreiber and Patel, 2015, Proposition 1]. We show  $\mathcal{M} = \{M_1, M_3, M_4, M_5\}$  is a Morse decomposition for  $\Lambda \cap S_0$ . Let  $z \in (\Lambda \cap S_0) \setminus \left( M_1 \cup \bigcup_{i=3}^5 M_i \right)$ , where  $z = (N_1, N_2, P, \bar{x})$ . The conclusions for (a), (b), (c), and (e) are identical to the proof of Theorem C.6. If (d) holds, then  $\alpha(z) \subset M_5$  and  $\omega(z) = M_4$ . Thus  $\mathcal{M}$  forms a Morse decomposition for  $\Lambda \cap S_0$ . For the application of Theorem 2 in Patel and Schreiber [2018], the choice of  $(n_1, n_2, p)$

for  $M_1$ ,  $M_3$ , and  $M_5$  from the proof of Theorem C.6 also work in this case. For  $M_4$ , choose  $\epsilon$  sufficiently small and  $(n_1, n_2, p) = (1, 1, \epsilon)$ . Thus (3.2) is permanent.  $\square$

**THEOREM C.8.** *Let  $W := \left\{ \bar{x} \in [\theta_1, \theta_2] \mid \frac{d}{d\bar{x}} \left( \frac{1}{P} \frac{dP}{dt} \right) \Big|_{(N_1, N_2, P, \bar{x}) = \left( \frac{r_1 - c_{12}r_2}{1 - c_{12}c_{21}}, \frac{r_2 - c_{21}r_1}{1 - c_{12}c_{21}}, 0, \bar{x} \right)} \right\}$  and assume the following:*

- (i)  $c_{12} > \frac{r_1}{r_2}$  and  $c_{21} > \frac{r_1}{r_2}$ ,
- (ii)  $\bar{a}_1(x^*)e_1 \frac{r_1 - c_{12}r_2}{1 - c_{12}c_{21}} + \bar{a}_2(x^*)e_2 \frac{r_2 - c_{21}r_1}{1 - c_{12}c_{21}} > d$  for all  $x^* \in W$ ,
- (iii)  $\bar{a}_1(\theta_1)e_1r_1 > d$ ,
- (iv)  $d(\bar{a}_2(\theta_1) - c_{21}\bar{a}_1(\theta_1)) > \bar{a}_1(\theta_1)e_1(\bar{a}_2(\theta_1)r_1 - \bar{a}_1(\theta_1)r_2)$ ,
- (v)  $\bar{a}_2(\theta_2)e_2r_2 > d$ , and
- (vi)  $d(\bar{a}_1(\theta_2) - c_{12}\bar{a}_2(\theta_2)) > \bar{a}_2(\theta_2)e_2(\bar{a}_1(\theta_2)r_2 - \bar{a}_2(\theta_2)r_1)$ .

Then Model (3.2) is robustly permanent.

**PROOF.** Denote  $M_i$ ,  $i = 1, 2, 3, 4$  as in the proof of Theorem C.6. Denote  $M_5 = (E_{++}^0) \times [y_1, y_2]$ , where  $y_1 = \min_{y \in W} y$  and  $y_2 = \max_{y \in W} y$  and  $M_6 = (E_{00}^0) \times [\theta_1, \theta_2]$ . The  $N_1$ - $N_2$  subsystem is bistable, with  $(E_{+0}) = (r_1, 0)$  and  $(E_{0+}) = (0, r_2)$  both locally stable and  $(E_{++}) = \left( \frac{r_1 - c_{12}r_2}{1 - c_{12}c_{21}}, \frac{r_2 - c_{21}r_1}{1 - c_{12}c_{21}} \right)$  a saddle. The two-dimensional stable manifold for  $(E_{++})$  is a surface separating the basins of attraction for  $(E_{+0})$  and  $(E_{0+})$ . If  $(N_1, N_2) \rightarrow (E_{+0})$  asymptotically, then  $\bar{x} \rightarrow \theta_1$  asymptotically (proof of Theorem C.6), and thus in the  $N_1$ - $N_2$ - $\bar{x}$  subsystem,  $(r_1, 0, \theta_1)$  is asymptotically stable. Similarly, if  $(N_1, N_2) \rightarrow (E_{0+})$  is asymptotically in the  $N_1$ - $N_2$  subsystem, then  $(0, r_2, \theta_2)$  is asymptotically stable in the  $N_1$ - $N_2$ - $\bar{x}$  subsystem. If  $(N_1, N_2) \rightarrow (E_{++})$ , then by Mischaikow et al. [1995, Proposition 1.5],  $\lim_{t \rightarrow \infty} \bar{x}(t) \in W$ .

Next we show  $\mathcal{M} = \{M_1, M_2, M_3, M_4, M_5, M_6\}$  is a Morse decomposition for  $\Lambda \cap S_0$ . Let  $z \in (\Lambda \cap S_0) \setminus \bigcup_{i=1}^6 M_i$ , where  $z = (N_1, N_2, P, \bar{x})$ . The conclusions for (a), (b), (c), and (d) from the proof of Theorem C.6 hold for this case. If (e) holds, then either:

- (I)  $z$  is in the two-dimensional stable manifold of  $(E_{++})$ ,
- (II)  $z$  is in the basin of attraction for  $(E_{+0})$ , or
- (III)  $z$  is in the basin of attraction for  $(E_{0+})$ .

In case (I),  $\alpha(z) = M_6$  and  $\omega(z) = M_5$ . In case (II),  $\alpha(z) \in M_5 \cup M_6$  and  $\omega(z) = M_3$ . In case (III),  $\alpha(z) \in M_5 \cup M_6$  and  $\omega(z) = M_4$ . Thus  $\mathcal{M}$  forms a Morse decomposition for  $\Lambda \cap S_0$ .

For the application of Theorem 2 in Patel and Schreiber [2018], the choice of  $(n_1, n_2, p)$  for  $M_1$ ,  $M_2$ ,  $M_3$ , and  $M_4$  from the above proof also work in this case. For  $M_5$ , choose  $(n_1, n_2, p) = (1, 1, 1)$  and for  $M_6$ , choose  $(n_1, n_2, p) = \left(\frac{d}{r_1}, \frac{d}{r_2}, 1\right)$ . Thus (3.2) is permanent.  $\square$

## Bibliography

- P. A. Abrams. The evolution of predator-prey interactions: Theory and evidence. *Annual Review of Ecology and Systematics*, 31:79–105, 2000. ISSN 00664162. URL <http://www.jstor.org/stable/221726>.
- P. A. Abrams and H. Matsuda. Prey adaptation as a cause of predator-prey cycles. *Society for the Study of Evolution*, 51:1742–1750, 1997a.
- P. A. Abrams and H. Matsuda. Fitness minimization and dynamic instability as a consequence of predator–prey coevolution. *Evolutionary Ecology*, 11(1):1–20, Jan 1997b. ISSN 1573-8477. doi: 10.1023/A:1018445517101. URL <https://doi.org/10.1023/A:1018445517101>.
- Peter A. Abrams. Effect of increased productivity on the abundances of trophic levels. *The American Naturalist*, 141(3):351–371, March 1993. doi: 10.1086/285478. URL <https://doi.org/10.1086/285478>.
- Peter A. Abrams. Adaptive change in the resource-exploitation traits of a generalist consumer: the evolution and coexistence of generalists and specialists. *Evolution*, 60(3):427–439, March 2006. doi: 10.1111/j.0014-3820.2006.tb01124.x. URL <https://doi.org/10.1111/j.0014-3820.2006.tb01124.x>.
- Priyanga Amarasekare. Spatial dynamics of keystone predation. *Journal of Animal Ecology*, 77(6): 1306–1315, November 2008. doi: 10.1111/j.1365-2656.2008.01439.x. URL <https://doi.org/10.1111/j.1365-2656.2008.01439.x>.
- T. K. Anderson and M. V. K. Sukhdeo. Host centrality in food web networks determines parasite diversity. *PLOS ONE*, 6(10):1–9, 10 2011.
- Francisco J. Ayala, Michael E. Gilpin, and Joan G. Ehrenfeld. Competition between species: Theoretical models and experimental tests. *Theoretical Population Biology*, 4(3):331–356, September 1973. doi: 10.1016/0040-5809(73)90014-2. URL [https://doi.org/10.1016/0040-5809\(73\)90014-2](https://doi.org/10.1016/0040-5809(73)90014-2).

- I Barber and J. P. Scharsack. The three-spined stickleback-schistocephalus solidus system: an experimental model for investigating host-parasite interactions in fish. *Parasitology*, 137(3):411–424, 2009.
- L. Becks, S. P. Ellner, L. E. Jones, and N. G. Hairston Jr. Reduction of adaptive genetic diversity radically alters eco-evolutionary community dynamics. *Ecology Letters*, 13(8):989–997, 2010. doi: 10.1111/j.1461-0248.2010.01490.x. URL <https://onlinelibrary.wiley.com/doi/abs/10.1111/j.1461-0248.2010.01490.x>.
- J. R. Beddington, C. A. Free, and J. H. Lawton. Dynamic complexity in predator-prey models framed in difference equations. *Nature*, 255:58, may 1975. URL <http://dx.doi.org/10.1038/255058a0><http://10.0.4.14/255058a0>.
- M. Bengfort, E. van Velzen, and U. Gaedke. Slight phenotypic variation in predators and prey causes complex predator-prey oscillations. *Ecological Complexity*, 31:115 – 124, 2017. ISSN 1476-945X. doi: <https://doi.org/10.1016/j.ecocom.2017.06.003>. URL <http://www.sciencedirect.com/science/article/pii/S1476945X1730048X>.
- R. J. Berry. The evolution of an island population of the house mouse. *Evolution*, 18(3):468, September 1964. doi: 10.2307/2406357. URL <https://doi.org/10.2307/2406357>.
- A. A. Berryman. The origins and evolution of predator-prey theory. *Ecology*, 73(5):1530–1535, 1992.
- M. D. Bertness and R. Callaway. The role of positive forces in natural communities: a post-cold war perspective. *Trends in Ecology and Evolution*, 9:191–193, 1994.
- D. I. Bolnick, P. Amarasekare, M. S. Araújo, R. Bürger, J. M. Levine, M. Novak, V. H. W. Rudolf, S. J. Schreiber, M. C. Urban, and D. A. Vasseur. Why intraspecific trait variation matters in community ecology. *Trends in Ecology and Evolution*, 26(4):183–192, 2011.
- Daniel I Bolnick, Richard Svanbäck, James A Fordyce, Louie H Yang, Jeremy M Davis, C Darrin Hulsey, and Matthew L Forister. The ecology of individuals: incidence and implications of individual specialization. *The American Naturalist*, 161(1):1–28, 2003.
- Daniel I. Bolnick, Lisa K. Snowberg, Philipp E. Hirsch, Christian L. Lauber, Rob Knight, J. Gregory Caporaso, and Richard Svanbäck. Individuals' diet diversity influences gut microbial diversity in two freshwater fish (threespine stickleback and eurasian perch). *Ecology Letters*, 17(8):979–987,

- may 2014. doi: 10.1111/ele.12301. URL <https://doi.org/10.1111/ele.12301>.
- D. I. Bolnick and O. L. Lau. Predictable patterns of disruptive selection in stickleback in postglacial lakes. *The American Naturalist*, 172(1):1–11, 2008. doi: 10.1086/587805. URL <https://doi.org/10.1086/587805>. PMID: 18452402.
- E. D. Brodie III. Correlational selection for color pattern and antipredator behavior in the garter snake *thamnophis ordinoides*. *Evolution*, 46(5):1284–1298, 1992.
- E. D. Brodie III and E. D. Brodie Jr. Predator-prey arms races. *Bioscience*, 49(7):557–568, 1999.
- Guy L. Bush. Sympatric host race formation and speciation in frugivorous flies of the genus *rhagoletis* (diptera, tephritidae). *Evolution*, 23(2):237, June 1969. doi: 10.2307/2406788. URL <https://doi.org/10.2307/2406788>.
- V. Calcagno, M. Dubosclard, and C. de Mazancourt. Rapid exploiter-victim coevolution: The race is not always to the swift. *The American Naturalist*, 176(2):198–211, 2010. ISSN 00030147, 15375323. URL <http://www.jstor.org/stable/10.1086/653665>.
- S. P. Carroll, A. P. Hendry, D. N. Reznick, and C. W. Fox. Evolution on ecological time-scales. *Functional Ecology*, 21(3):387–393, June 2007. doi: 10.1111/j.1365-2435.2007.01289.x. URL <https://doi.org/10.1111/j.1365-2435.2007.01289.x>.
- T. J. Case and J. Roughgarden. An illustrated guide to theoretical ecology. *Oxford University Press*, page 449, 2000.
- Jonathan M. Chase, Peter A. Abrams, James P. Grover, Sebastian Diehl, Peter Chesson, Robert D. Holt, Shane A. Richards, Roger M. Nisbet, and Ted J. Case. The interaction between predation and competition: a review and synthesis. *Ecology Letters*, 5(2):302–315, March 2002. doi: 10.1046/j.1461-0248.2002.00315.x. URL <https://doi.org/10.1046/j.1461-0248.2002.00315.x>.
- V. C. Clark, C. J. Raxworthy, V. Rakotomalala, P. Sierwald, and B. L. Fisher. Convergent evolution of chemical defense in poison frogs and arthropod prey between madagascar and the neotropics. *Proceedings of the National Academy of Sciences*, 102(33):11617–11622, August 2005. doi: 10.1073/pnas.0503502102. URL <https://doi.org/10.1073/pnas.0503502102>.
- C. Combes. *Parasitism: The Ecology and Evolution of Intimate Interactions*. University of Chicago Press, 2001. URL <https://press.uchicago.edu/ucp/books/book/chicago/P/bo3634576.html>.

- M. H. Cortez and S. P. Ellner. Understanding rapid evolution in predator-prey interactions using the theory of fast-slow dynamical systems. *The American Naturalist*, 176(5):E109–E127, 2010. ISSN 00030147, 15375323. URL <http://www.jstor.org/stable/10.1086/656485>.
- M. H. Cortez and J. S. Weitz. Coevolution can reverse predator-prey cycles. *Proceedings of the National Academy of Sciences*, 111(20):7486–7491, 2014. ISSN 0027-8424. doi: 10.1073/pnas.1317693111. URL <http://www.pnas.org/content/111/20/7486>.
- Michael H. Cortez and Swati Patel. The effects of predator evolution and genetic variation on predator-prey population-level dynamics. *Bulletin of Mathematical Biology*, 79(7):1510–1538, June 2017. doi: 10.1007/s11538-017-0297-y. URL <https://doi.org/10.1007/s11538-017-0297-y>.
- Michael H Cortez, Swati Patel, and Sebastian J Schreiber. Destabilizing evolutionary and eco-evolutionary feedbacks drive empirical eco-evolutionary cycles. *Proceedings of the Royal Society B*, 287(1919):20192298, 2020.
- Charles Darwin. *On the Origin of Species by Means of Natural Selection, or the Preservation of Favoured Races in the Struggle for Life*. J. Murray, London, UK, 1859.
- J. P. DeLong. Ecological pleiotropy suppresses the dynamic feedback generated by a rapidly changing trait. *The American Naturalist*, 189(5):592–597, 2017. doi: 10.1086/691100. URL <https://doi.org/10.1086/691100>. PMID: 28410029.
- J. P. DeLong and J. P. Gibert. Gillespie eco-evolutionary models (gems) reveal the role of heritable trait variation in eco-evolutionary dynamics. *Ecology and Evolution*, 6(4):935–945, 2016. doi: 10.1002/ece3.1959. URL <https://onlinelibrary.wiley.com/doi/abs/10.1002/ece3.1959>.
- J. P. DeLong, V. E. Forbes, N. Galic, J. P. Gibert, R. G. Laport, J. S. Phillips, and J. M. Vavra. How fast is fast? eco-evolutionary dynamics and rates of change in populations and phenotypes. *Ecology and Evolution*, 6(2):573–581, 2016. doi: 10.1002/ece3.1899. URL <https://onlinelibrary.wiley.com/doi/abs/10.1002/ece3.1899>.
- C. Eizaguirre, T. L. Lenz, M. Kalbe, and M. Milinski. Divergent selection on locally adapted major histocompatibility complex immune genes experimentally proven in the field. *Ecology Letters*, 15(7):723–731, may 2012. doi: 10.1111/j.1461-0248.2012.01791.x. URL <https://doi.org/10.1111/j.1461-0248.2012.01791.x>.

- J. A. Endler. Variation in the appearance of guppy color patterns to guppies and their predators under different visual conditions. *Vision Research*, 31(3):587–608, 1991.
- C. Englund, A. E. Uv, R. Cantera, L. D. Mathies, M. A. Krasnow, and C. Samakovlis. *adrift*, a novel bnl-induced drosophila gene, required for tracheal pathfinding into the CNS. *The Company of Biologists Ltd*, 126:1505–1514, 1999.
- J. A. Estes, M. L. Riedman, M. M. Staedler, M. T. Tinker, and B. E. Lyon. Individual variation in prey selection by sea otters: patterns, causes and implications. *Journal of Animal Ecology*, 72(1):144–155, Jan 2003. doi: 10.1046/j.1365-2656.2003.00690.x. URL <https://doi.org/10.1046/j.1365-2656.2003.00690.x>.
- V. O. Ezenwa, R. S. Etienne, G. Luikart, A. Beja-Pereira, and A. E. Jolles. Hidden consequences of living in a wormy world: Nematode-induced immune suppression facilitates tuberculosis invasion in African buffalo. *The American Naturalist*, 176(5):613–624, Nov 2010. doi: 10.1086/656496. URL <https://doi.org/10.1086/656496>.
- S. R. Fleischer, C. P. terHorst, and J. Li. Pick your trade-offs wisely: Predator-prey eco-evo dynamics are qualitatively different under different trade-offs. *Journal of Theoretical Biology*, 456:201–212, 2018. URL <https://doi.org/10.1016/j.jtbi.2018.08.013>.
- Samuel R. Fleischer, Daniel I. Bolnick, and Sebastian J. Schreiber. Sick of eating: eco-evo-immuno dynamics of predators and their trophically acquired parasites. May 2020. doi: 10.1101/2020.05.26.117622. URL <https://doi.org/10.1101/2020.05.26.117622>.
- K. Fujii. Overview of S. Utida’s research. *Researches on Population Ecology*, 41:11–13, 1999.
- Simpson George Gaylord. The Baldwin effect. *Evolution*, 7(2):110–117, 1953. doi: 10.1111/j.1558-5646.1953.tb00069.x. URL <https://onlinelibrary.wiley.com/doi/abs/10.1111/j.1558-5646.1953.tb00069.x>.
- Stefan A.H. Geritz, Éva Kisdi, and Ping Yan. Evolutionary branching and long-term coexistence of cycling predators: Critical function analysis. *Theoretical Population Biology*, 71(4):424–435, June 2007. doi: 10.1016/j.tpb.2007.03.006. URL <https://doi.org/10.1016/j.tpb.2007.03.006>.
- Z. Maciej Gliwicz and Dariusz Wrzosek. Predation-mediated coexistence of large- and small-bodied daphnia at different food levels. *The American Naturalist*, 172(3):358–374, September 2008. doi: 10.1086/589890. URL <https://doi.org/10.1086/589890>.

- Richard Gomulkiewicz and Robert D. Holt. When does evolution by natural selection prevent extinction? *Evolution*, 49(1):201, February 1995. doi: 10.2307/2410305. URL <https://doi.org/10.2307/2410305>.
- P. R. Grant and B. R. Grant. Unpredictable evolution in a 30-year study of darwin's finches. *Science*, 296(5568):707–711, April 2002. doi: 10.1126/science.1070315. URL <https://doi.org/10.1126/science.1070315>.
- N. Gross, G. Kunstler, P. Liancourt, F. de Bello, K. N. Suding, and S. Lavorel. Linking individual response to biotic interactions with community structure: a trait-based framework. *Functional Ecology*, 23:1167–1178, 2009.
- J. Gurevitch, J. A. Morrison, and L. V. Hedges. The interaction between competition and predation: A meta-analysis of field experiments. *The American Naturalist*, 155(4):435–453, 2000a.
- Jessica Gurevitch, Janet A. Morrison, and Larry V. Hedges. The interaction between competition and predation: A meta-analysis of field experiments. *The American Naturalist*, 155(4):435–453, April 2000b. doi: 10.1086/303337. URL <https://doi.org/10.1086/303337>.
- N. G. Hairston Jr., S. P. Ellner, M. A. Geber, T. Yoshida, and J. A. Fox. Rapid evolution and the convergence of ecological and evolutionary time. *Ecology Letters*, 8:1114–1127, 2005.
- J. Hale and H. Koçak. *Dynamics and Bifurcations*. Springer-Verlag, 1st edition, 1991.
- A. Hayward, M. Tsuboi, C. Owusu, A. Kotrschal, S. D. Buechel, J. Zidar, C. K. Cornwallis, H. Løvlie, and N. Kolm. Evolutionary associations between host traits and parasite load: insights from lake tanganyika cichlids. *Journal of Evolutionary Biology*, 30(6):1056–1067, mar 2017. doi: 10.1111/jeb.13053. URL <https://doi.org/10.1111/jeb.13053>.
- Geertje Hek. Geometric singular perturbation theory in biological practice. *Journal of Mathematical Biology*, 60(3):347–386, April 2009. doi: 10.1007/s00285-009-0266-7. URL <https://doi.org/10.1007/s00285-009-0266-7>.
- A. P. Hendry. *Eco-evolutionary dynamics*. Princeton University Press, Princeton, 2017. ISBN 9780691145433.
- Andrew P. Hendry and Michael T. Kinnison. PERSPECTIVE: THE PACE OF MODERN LIFE: MEASURING RATES OF CONTEMPORARY MICROEVOLUTION. *Evolution*, 53(6):1637–1653, December 1999. doi: 10.1111/j.1558-5646.1999.tb04550.x. URL <https://doi.org/10.1111/j.1558-5646.1999.tb04550.x>.

1111/j.1558-5646.1999.tb04550.x.

- Alexandru Hening, Dang H. Nguyen, and Sebastian J. Schreiber. A classification of the dynamics of three-dimensional stochastic ecological systems, 2020.
- T. Hiltunen, N. G. Hairston, G. Hooker, Jones L. E., S. P. Ellner, and F. Adler. A newly discovered role of evolution in previously published consumer–resource dynamics. *Ecology Letters*, 17(8): 915–923, 2014. doi: 10.1111/ele.12291. URL <https://onlinelibrary.wiley.com/doi/abs/10.1111/ele.12291>.
- Vincent Hin, Tim Schellekens, Lennart Persson, and André M. de Roos. Coexistence of predator and prey in intraguild predation systems with ontogenetic niche shifts. *The American Naturalist*, 178(6):701–714, December 2011. doi: 10.1086/662676. URL <https://doi.org/10.1086/662676>.
- J. Hofbauer and K. Sigmund. *Evolutionary games and population dynamics*. Cambridge university press, 1998.
- R. D. Holt and J. H. Lawton. The ecological consequences of shared natural enemies. *Annual Review of Ecology and Systematics*, 25(1):495–520, 1994. doi: 10.1146/annurev.es.25.110194.002431. URL <https://doi.org/10.1146/annurev.es.25.110194.002431>.
- Robert D. Holt. Predation, apparent competition, and the structure of prey communities. *Theoretical Population Biology*, 12(2):197–229, October 1977. doi: 10.1016/0040-5809(77)90042-9. URL [https://doi.org/10.1016/0040-5809\(77\)90042-9](https://doi.org/10.1016/0040-5809(77)90042-9).
- C. B. Huffaker. Experimental studies on predation: dispersion factors and predator-prey oscillations. *University of California*, 1958.
- V. Hutson and G.T. Vickers. A criterion for permanent coexistence of species, with an application to a two-prey one-predator system. *Mathematical Biosciences*, 63(2):253–269, April 1983. doi: 10.1016/0025-5564(82)90042-6. URL [https://doi.org/10.1016/0025-5564\(82\)90042-6](https://doi.org/10.1016/0025-5564(82)90042-6).
- Vivian Hutson and Klaus Schmitt. Permanence and the dynamics of biological systems. *Mathematical Biosciences*, 111(1):1–71, September 1992. doi: 10.1016/0025-5564(92)90078-b. URL [https://doi.org/10.1016/0025-5564\(92\)90078-b](https://doi.org/10.1016/0025-5564(92)90078-b).
- R. Iritani and T. Sato. Host-manipulation by trophically transmitted parasites: The switcher-paradigm. *Trends in Parasitology*, 34(11):934–944, nov 2018. doi: 10.1016/j.pt.2018.08.005. URL <https://doi.org/10.1016/j.pt.2018.08.005>.

- Y. Iwasa, A. Pomiankowski, and S. Nee. The evolution of costly mate preferences ii. the "handicap" principle. *Evolution*, 45(6):1431–1442, 1991.
- Vincent AA Jansen and Karl Sigmund. Shaken, not stirred: On permanence in ecological communities. 1998.
- C. K. Johnson, M. T. Tinker, J. A. Estes, P. A. Conrad, M. Staedler, M. A. Miller, D. A. Jessup, and J. A. K. Mazet. Prey choice and habitat use drive sea otter pathogen exposure in a resource-limited coastal system. *Proceedings of the National Academy of Sciences*, 106(7):2242–2247, jan 2009. doi: 10.1073/pnas.0806449106. URL <https://doi.org/10.1073/pnas.0806449106>.
- E. Jones, T. Oliphant, P. Peterson, et al. SciPy: Open source scientific tools for Python, 2001–. URL <http://www.scipy.org/>. [Online; accessed 20 May 2019].
- M. Kalbe and J. Kurtz. Local differences in immunocompetence reflect resistance of sticklebacks against the eye fluke diplostomum pseudospathaceum. *Parasitology*, 132(01):105–116, sep 2005. doi: 10.1017/s0031182005008681. URL <https://doi.org/10.1017/s0031182005008681>.
- A. I. Khibnik and A. S. Kondrashov. Three mechanisms of red queen dynamics. *Proceedings of the Royal Society of London*, 264:1049–1056, 1997.
- Gabriela Kirlinger. Permanence in lotka-volterra equations: linked prey-predator systems. *Mathematical Biosciences*, 82(2):165–191, December 1986. doi: 10.1016/0025-5564(86)90136-7. URL [https://doi.org/10.1016/0025-5564\(86\)90136-7](https://doi.org/10.1016/0025-5564(86)90136-7).
- T. Klauschies, D. A. Vasseur, and U. Gaedke. Trait adaptation promotes species coexistence in diverse predator and prey communities. *Ecology and Evolution*, 6(12):4141–4159, 2016. doi: 10.1002/ece3.2172. URL <https://onlinelibrary.wiley.com/doi/abs/10.1002/ece3.2172>.
- C. J. Krebs, R. Boonstra, S. Boutin, and A. R. E. Sinclair. What drives the 10-year cycle of snowshoe hares? *Bioscience*, 51(1):25–35, 2001.
- K. D. Lafferty, A. P. Dobson, and A. M. Kuris. Parasites dominate food web links. *Proceedings of the National Academy of Sciences*, 103(30):11211–11216, 2006.
- R. Lande. Natural selection and random genetic drift in phenotypic evolution. *Society for the Study of Evolution*, 30(2):314–334, 1976.
- P. Lavin and J. D. McPhail. The evolution of freshwater diversity in the threespine stickleback (*Gasterosteus aculeatus*): site-specific differentiation of trophic morphology. *Canadian Journal*

- of Zoology*, 83:2632–2638, 1985.
- P. Lavin and J. D. McPhail. Adaptive divergence of trophic phenotype among freshwater populations of the threespine stickleback (*Gasterosteus aculeatus*). *Canadian Journal of Fisheries and Aquatic Sciences*, 43:2455–2463, 1986.
- J. T. Lill. Selection on herbivore life-history traits by the first and third trophic levels: the devil and the deep blue sea revisited. *Evolution*, 55(11):2236–2247, 2001.
- E. Litchman and C. A. Klausmeier. Trait-based community ecology of phytoplankton. *Annual Review of Ecology, Evolution, and Systematics*, 39:615–639, 2008.
- A. J. Lotka. Elements of physical biology. *Williams & Wilkins Company*, 1925.
- A. D. C. MacColl. Parasite burdens differ between sympatric three-spined stickleback species. *Ecography*, 32(1):153–160, apr 2009. doi: 10.1111/j.1600-0587.2008.05486.x. URL <https://doi.org/10.1111/j.1600-0587.2008.05486.x>.
- A. D. C. MacColl and S. M. Chapman. Parasites can cause selection against migrants following dispersal between environments. *Functional Ecology*, 24(4):847–856, feb 2010. doi: 10.1111/j.1365-2435.2010.01691.x. URL <https://doi.org/10.1111/j.1365-2435.2010.01691.x>.
- B. Matthews, K. B. Marchinko, D. I. Bolnick, and A. Mazumder. Specialization of trophic position and habitat use by sticklebacks in an adaptive radiation. *Ecology*, 91:1025–1034, 2010.
- Konstantin Mischaikow, Hal Smith, and Horst R. Thieme. Asymptotically autonomous semiflows: chain recurrence and lyapunov functions. *Transactions of the American Mathematical Society*, 347(5):1669–1685, May 1995. doi: 10.1090/s0002-9947-1995-1290727-7. URL <https://doi.org/10.1090/s0002-9947-1995-1290727-7>.
- J. E. Motychak, E. D. Brodie Jr., and E. D. Brodie III. Evolutionary response of predators to dangerous prey: Preadaptation and the evolution of tetrodotoxin resistance in garter snakes. *Evolution*, 53(5):1528–1535, 1999.
- A. Mougi. Predator-prey coevolution driven by size selective predation can cause anti-synchronized and cryptic population dynamics. *Theoretical Population Biology*, 81(2):113 – 118, 2012. ISSN 0040-5809. doi: <https://doi.org/10.1016/j.tpb.2011.12.005>. URL <http://www.sciencedirect.com/science/article/pii/S0040580911001158>.

- A. Mougi and Y. Iwasa. Evolution towards oscillation or stability in a predator-prey system. *Proceedings of the Royal Society of London B: Biological Sciences*, 277(1697):3163–3171, 2010. ISSN 0962-8452. doi: 10.1098/rspb.2010.0691. URL <http://rspb.royalsocietypublishing.org/content/277/1697/3163>.
- A. Mougi and Y. Iwasa. Unique coevolutionary dynamics in a predator-prey system. *Journal of Theoretical Biology*, 277(1):83 – 89, 2011. ISSN 0022-5193. doi: <https://doi.org/10.1016/j.jtbi.2011.02.015>. URL <http://www.sciencedirect.com/science/article/pii/S0022519311001093>.
- A. E. Nagar and A. D. C. MacColl. Parasites contribute to ecologically dependent postmating isolation in the adaptive radiation of three-spined stickleback. *Proceedings of the Royal Society B: Biological Sciences*, 283(1836):20160691, aug 2016. doi: 10.1098/rspb.2016.0691. URL <https://doi.org/10.1098/rspb.2016.0691>.
- S. L. Nuismer, M. Doebeli, and D. Browning. The coevolutionary dynamics of antagonistic interactions mediated by quantitative traits with evolving variances. *Evolution*, 59(10):2073–2082, 2005. ISSN 00143820, 15585646. URL <http://www.jstor.org/stable/3449093>.
- Swati Patel and Reinhard Bürger. Eco-evolutionary feedbacks between prey densities and linkage disequilibrium in the predator maintain diversity. *Evolution*, 73(8):1533–1548, June 2019. doi: 10.1111/evo.13785. URL <https://doi.org/10.1111/evo.13785>.
- Swati Patel and Sebastian J. Schreiber. Evolutionarily driven shifts in communities with intraguild predation. *The American Naturalist*, 186(5):E98–E110, nov 2015. doi: 10.1086/683170. URL <https://doi.org/10.1086/683170>.
- Swati Patel and Sebastian J. Schreiber. Robust permanence for ecological equations with internal and external feedbacks. *Journal of Mathematical Biology*, 77(1):79–105, 2018. doi: 10.1007/s00285-017-1187-5. URL <https://doi.org/10.1007/s00285-017-1187-5>.
- Swati Patel, Michael H. Cortez, and Sebastian J. Schreiber. Partitioning the effects of eco-evolutionary feedbacks on community stability. *The American Naturalist*, 191(3):381–394, March 2018. doi: 10.1086/695834. URL <https://doi.org/10.1086/695834>.
- Loïc Prosnier, Vincent Médoc, and Nicolas Loeuille. Evolution of predator foraging in response to prey infection favors species coexistence. *bioRxiv*, 2020. doi: 10.1101/2020.04.18.047811. URL <https://www.biorxiv.org/content/early/2020/04/18/2020.04.18.047811>.

- T. E. Reimchen. Spine deficiency and polymorphism in a population of *Gasterosteus aculeatus*: an adaptation to predators? *Canadian Journal of Zoology*, 58(7):1232–1244, 1980.
- T. E. Reimchen and P. Nosil. Dietary differences between phenotypes with symmetrical and asymmetrical pelvis in the stickleback *Gasterosteus aculeatus*. *Canadian Journal of Zoology*, 79(3): 533–539, 2001.
- David N. Reznick and Cameron K. Ghalambor. The population ecology of contemporary adaptations: What empirical studies reveal about the conditions that promote adaptive evolution. In *Microevolution Rate, Pattern, Process*, pages 183–198. Springer Netherlands, 2001.
- S. Rinaldi and S. Muratori. Slow-fast limit cycles in predator-prey models. *Ecological Modelling*, 61(3-4):287–308, June 1992. doi: 10.1016/0304-3800(92)90023-8. URL [https://doi.org/10.1016/0304-3800\(92\)90023-8](https://doi.org/10.1016/0304-3800(92)90023-8).
- B. Robinson. Trade offs in habitat-specific foraging efficiency and the nascent adaptive divergence of sticklebacks in lakes. *Behaviour*, 137(7-8):865–888, 2000. doi: 10.1163/156853900502501. URL <https://doi.org/10.1163/156853900502501>.
- A. Rogawa, S. Ogata, and A. Mougi. Parasite transmission between trophic levels stabilizes predator-prey interaction. *Scientific Reports*, 8(1), aug 2018. doi: 10.1038/s41598-018-30818-7. URL <https://doi.org/10.1038/s41598-018-30818-7>.
- Gregory Roth and Sebastian J. Schreiber. Persistence in fluctuating environments for interacting structured populations. *Journal of Mathematical Biology*, 69(5):1267–1317, December 2013. doi: 10.1007/s00285-013-0739-6. URL <https://doi.org/10.1007/s00285-013-0739-6>.
- Jonathan Roughgarden and Marcus Feldman. Species packing and predation pressure. *Ecology*, 56(2):489–492, March 1975. doi: 10.2307/1934982. URL <https://doi.org/10.2307/1934982>.
- I. Saloniemi. A coevolutionary predator-prey model with quantitative characters. *The American Naturalist*, 141:880–896, 1993.
- D. Schluter and J. D. McPhail. Ecological character displacement and speciation in sticklebacks. *The American Naturalist*, 140:85–108, 1992.
- D. W. Schmid, M. D. McGee, R. J. Best, O. Seehausen, and B. Matthews. Rapid divergence of predator functional traits affects prey composition in aquatic communities. *The American Naturalist*, 193(3):331–345, mar 2019. doi: 10.1086/701784. URL <https://doi.org/10.1086/701784>.

701784.

- O. J. Schmitz, P. A. Hambäck, and A. P. Beckerman. Trophic cascades in terrestrial systems: A review of the effects of carnivore removals on plants. *The American Naturalist*, 155(2):141–153, 2000.
- T. W. Schoener. The newest synthesis: Understanding the interplay of evolutionary and ecological dynamics. *Science*, 331(6016):426–429, 2011.
- Thomas W. Schoener. Alternatives to lotka-volterra competition: Models of intermediate complexity. *Theoretical Population Biology*, 10(3):309–333, December 1976. doi: 10.1016/0040-5809(76)90022-8. URL [https://doi.org/10.1016/0040-5809\(76\)90022-8](https://doi.org/10.1016/0040-5809(76)90022-8).
- S. J. Schreiber and S. Patel. Evolutionarily induced alternative states and coexistence in systems with apparent competition. *Natural Resource Modeling*, 28(4):475–496, 2015.
- S. J. Schreiber, R. Bürger, and D. I. Bolnick. The community effects of phenotypic and genetic variation within a predator population. *Ecology*, 92(8):1582–1593, 2011.
- Sebastian J. Schreiber. Generalist and specialist predators that mediate permanence in ecological communities. *Journal of Mathematical Biology*, 36(2):133–148, November 1997. doi: 10.1007/s002850050094. URL <https://doi.org/10.1007/s002850050094>.
- Sebastian J Schreiber. Criteria for cr robust permanence. *Journal of Differential Equations*, 162(2):400–426, 2000.
- Sebastian J. Schreiber. Persistence despite perturbations for interacting populations. *Journal of Theoretical Biology*, 242(4):844–852, October 2006. doi: 10.1016/j.jtbi.2006.04.024. URL <https://doi.org/10.1016/j.jtbi.2006.04.024>.
- Sebastian J. Schreiber and Timothy P. Killingback. Spatial heterogeneity promotes coexistence of rock-paper-scissors metacommunities. *Theoretical Population Biology*, 86:1–11, June 2013. doi: 10.1016/j.tpb.2013.02.004. URL <https://doi.org/10.1016/j.tpb.2013.02.004>.
- J. B. Shurin, E. T. Borer, E. W. Seabloom, K. Anderson, C. A. Blanchette, B. Broitman, S. D. Cooper, and B. S. Halpern. A cross-ecosystem comparison of the strength of trophic cascades. *Ecology Letters*, 5:785–791, 2002.
- F. A. Sibbing, L. A. J. Nagelkerke, R. J. M. Stet, and J. W. M. Osse. *Aquatic Ecology*, 32(3):217–227, 1998. doi: 10.1023/a:1009920522235. URL <https://doi.org/10.1023/a:1009920522235>.

- Andrew Sih, Philip Crowley, Mark McPeck, James Petranka, and Kevin Strohmeier. Predation, competition, and prey communities: A review of field experiments. *Annual Review of Ecology and Systematics*, 16(1):269–311, 1985. doi: 10.1146/annurev.es.16.110185.001413. URL <https://doi.org/10.1146/annurev.es.16.110185.001413>.
- L. K. Snowberg, K. M. Hendrix, and D. I. Bolnick. Covarying variances: more morphologically variable populations also exhibit more diet variation. *Oecologia*, 178(1):89–101, 2015.
- J. C. Sprott. *Chaos and time-series analysis*, volume 69. Citeseer, 2003.
- S. Y. Strauss, J. A. Lau, and S. P. Carroll. Evolutionary responses of natives to introduced species: what do introductions tell us about natural communities? *Ecology Letters*, 9(3):357–374, 2006.
- W. E. Stutz and D. I. Bolnick. Natural selection on MHC II $\beta$  in parapatric lake and stream stickleback: Balancing, divergent, both or neither? *Molecular Ecology*, 26(18):4772–4786, may 2017. doi: 10.1111/mec.14158. URL <https://doi.org/10.1111/mec.14158>.
- W. E. Stutz, O. L. Lau, and D. I. Bolnick. Contrasting patterns of phenotype-dependent parasitism within and among populations of threespine stickleback. *The American Naturalist*, 183(6):810–825, 2014.
- M. V. K. Sukhdeo. Where are the parasites in food webs? *Parasites & Vectors*, 5(1):239, 2012. doi: 10.1186/1756-3305-5-239. URL <https://doi.org/10.1186/1756-3305-5-239>.
- Y. Takeuchi and N. Adachi. Existence and bifurcation of stable equilibrium in two-prey, one-predator communities. *Bulletin of Mathematical Biology*, 45(6):877 – 900, 1983.
- J. N. Thompson. Specific hypotheses on the geographic mosaic of coevolution. *The American Naturalist*, 153(S5):S1–S14, 1999.
- R. J. Tien and S. P. Ellner. Variable cost of prey defense and coevolution in predator–prey systems. *Ecological Monographs*, 82(4):491–504, 2012. doi: 10.1890/11-2168.1. URL <https://esajournals.onlinelibrary.wiley.com/doi/abs/10.1890/11-2168.1>.
- M. T. Tinker, Bentall G., and J. A. Estes. Food limitation leads to behavioral diversification and dietary specialization in sea otters. *Proceedings of the National Academy of Sciences*, 105(2):560–565, jan 2008. doi: 10.1073/pnas.0709263105. URL <https://doi.org/10.1073/pnas.0709263105>.

- K. Tirok, B. Bauer, K. Wirtz, and U. Gaedke. Predator-prey dynamics driven by feedback between functionally diverse trophic levels. *PLOS ONE*, 6(11):1–13, 11 2011. doi: 10.1371/journal.pone.0027357. URL <https://doi.org/10.1371/journal.pone.0027357>.
- Minus van Baalen, Vlastimil Křivan, Paul C. J. van Rijn, and Maurice W. Sabelis. Alternative food, switching predators, and the persistence of predator-prey systems. *The American Naturalist*, 157(5):512–524, May 2001. doi: 10.1086/319933. URL <https://doi.org/10.1086/319933>.
- L. Van Valen. Variation genetics of extinct animals. *The American Naturalist*, 103(931):193–224, 1969. doi: 10.1086/282596. URL <https://doi.org/10.1086/282596>.
- L. Van Valen. A new evolutionary law. *Evolutionary Theory*, 1:1–30, 1973.
- E. van Velzen and U. Gaedke. Disentangling eco-evolutionary dynamics of predator-prey coevolution: the case of antiphase cycles. *Scientific Reports*, 7(1):17125, 2017. ISSN 2045-2322. doi: 10.1038/s41598-017-17019-4. URL <https://doi.org/10.1038/s41598-017-17019-4>.
- David A. Vasseur and Jeremy W. Fox. Adaptive dynamics of competition for nutritionally complementary resources: Character convergence, displacement, and parallelism. *The American Naturalist*, 178(4):501–514, 2011. doi: 10.1086/661896. URL <https://doi.org/10.1086/661896>. PMID: 21956028.
- David A. Vasseur, Priyanga Amarasekare, Volker H. W. Rudolf, and Jonathan M. Levine. Eco-evolutionary dynamics enable coexistence via neighbor-dependent selection. *The American Naturalist*, 178(5):E96–E109, November 2011. doi: 10.1086/662161. URL <https://doi.org/10.1086/662161>.
- V. Volterra and M. Brelot. Lecons sur la theorie mathematique de la lutte pour la vie. *Gauthier-Villars*, 6:214, 1931.
- M. R. Walsh and D. N. Reznick. Interactions between the direct and indirect effects of predators determine life history evolution in a killifish. *PNAS*, 105(2):594–599, 2008.
- J. N. Weber, M Kalbe, K. C. Shim, N. I. Erin, N. C. Steinel, L. Ma, and D. I. Bolnick. Resist globally, infect locally: A transcontinental test of adaptation by stickleback and their tapeworm parasite. *The American Naturalist*, 189(1):43–57, jan 2017a. doi: 10.1086/689597. URL <https://doi.org/10.1086/689597>.

- J. N. Weber, N. C. Steinel, K. C. Shim, and D. I. Bolnick. Recent evolution of extreme cestode growth suppression by a vertebrate host. *Proceedings of the National Academy of Sciences*, 114(25):6575–6580, jun 2017b. doi: 10.1073/pnas.1620095114. URL <https://doi.org/10.1073/pnas.1620095114>.
- E E Werner, , and J F Gilliam. The ontogenetic niche and species interactions in size-structured populations. *Annual Review of Ecology and Systematics*, 15(1):393–425, 1984. doi: 10.1146/annurev.es.15.110184.002141. URL <https://doi.org/10.1146/annurev.es.15.110184.002141>.
- K. West, A. Cohen, and M. Baron. Morphology and behavior of crabs and gastropods from lake tanganyika, africa: Implications for lacustrine predator-prey coevolution. *Ecology*, 45(3):589–607, 1991.
- Sabine Wollrab, André M. de Roos, and Sebastian Diehl. Ontogenetic diet shifts promote predator-mediated coexistence. *Ecology*, 94(12):2886–2897, December 2013. doi: 10.1890/12-1490.1. URL <https://doi.org/10.1890/12-1490.1>.
- C. L. Wood and P. T. J. Johnson. A world without parasites: exploring the hidden ecology of infection. *Frontiers in Ecology and the Environment*, 13(8):425–434, 2015. doi: 10.1890/140368. URL <https://esajournals.onlinelibrary.wiley.com/doi/abs/10.1890/140368>.
- T. Yoshida, L. E. Jones, S. P. Ellner, G. F. Fussmann, and N. G. Hairston Jr. Rapid evolution drives ecological dynamics in a predator–prey system. *Nature*, 424:303–306, 2003.
- T. Yoshida, S. P. Ellner, L. E. Jones, B. J. M. Bohannan, R. E. Lenski, and N. G. Hairston Jr. Cryptic population dynamics: Rapid evolution masks trophic interactions. *PLOS Biology*, 5(9):1868–1879, 2007.